ELECTRON TOMOGRAPHY

Part I

David Stokes

Adapted from Carmen Mannella
Resource for the Visualization of Biological Complexity
Wadsworth Center, Albany, NY

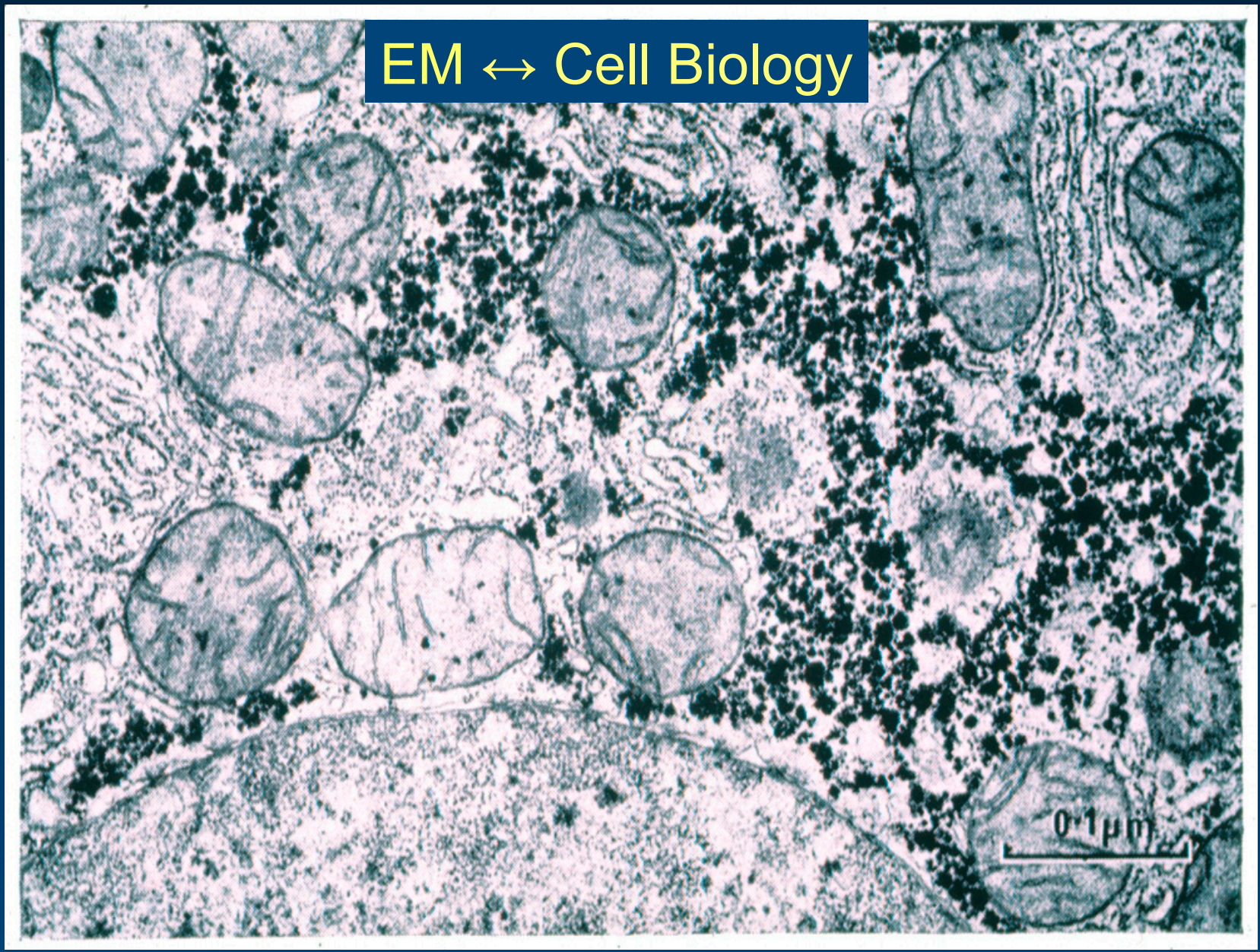

E.A. Munn 1974 *The Structure of Mitochondria*

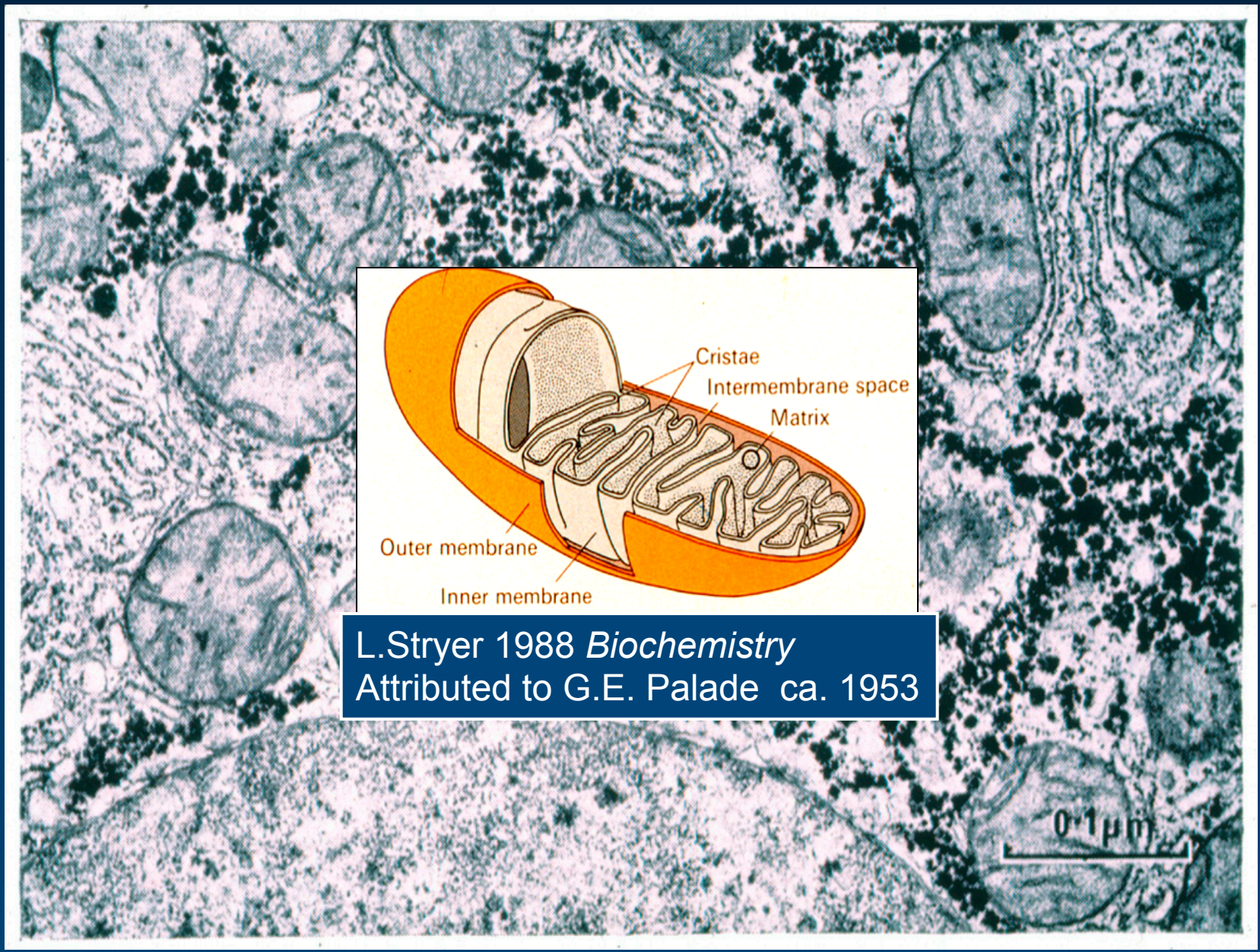

L.Stryer 1988 *Biochemistry*
Attributed to G.E. Palade ca. 1953

E.A. Munn 1974 *The Structure of Mitochondria*

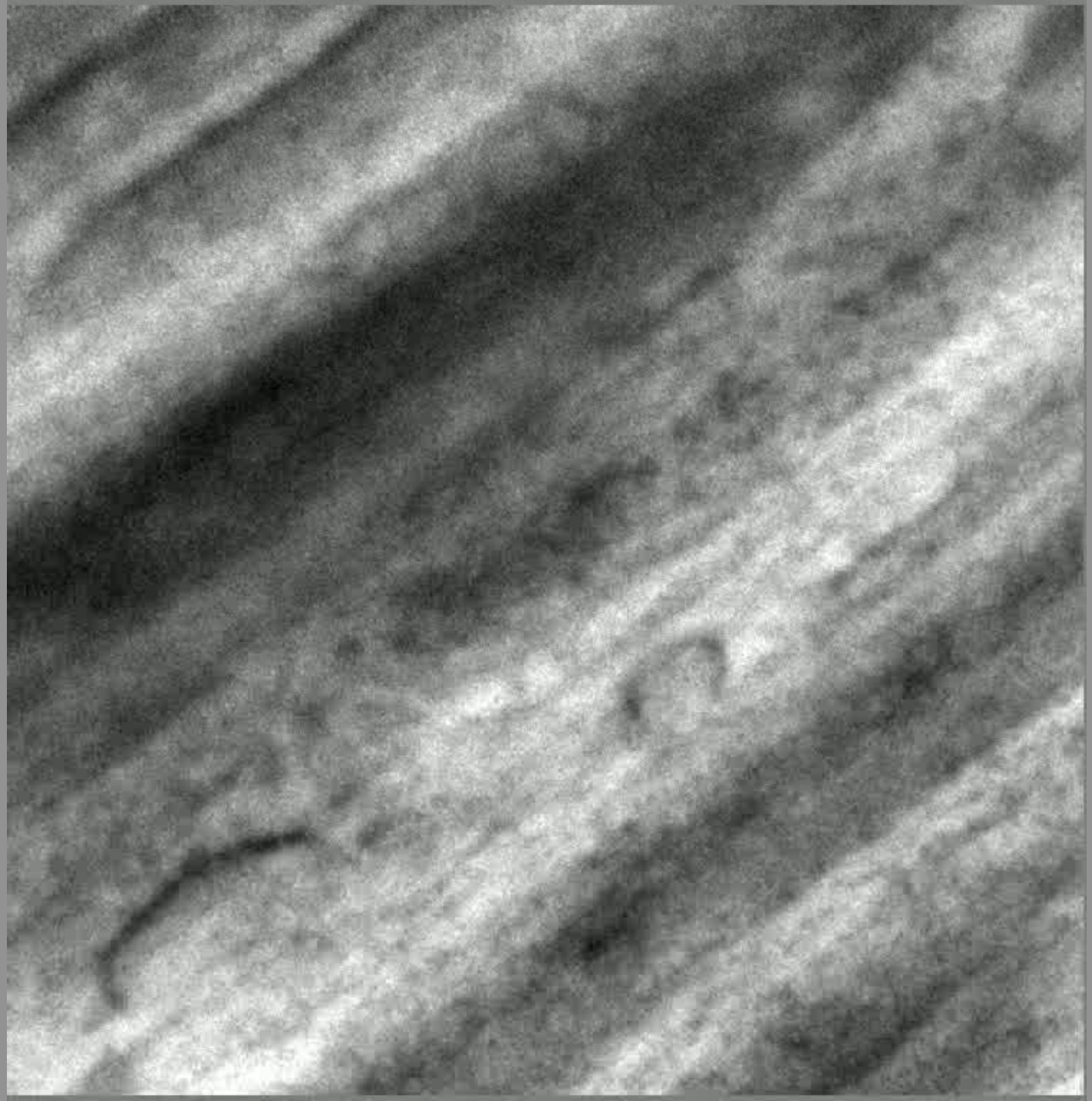

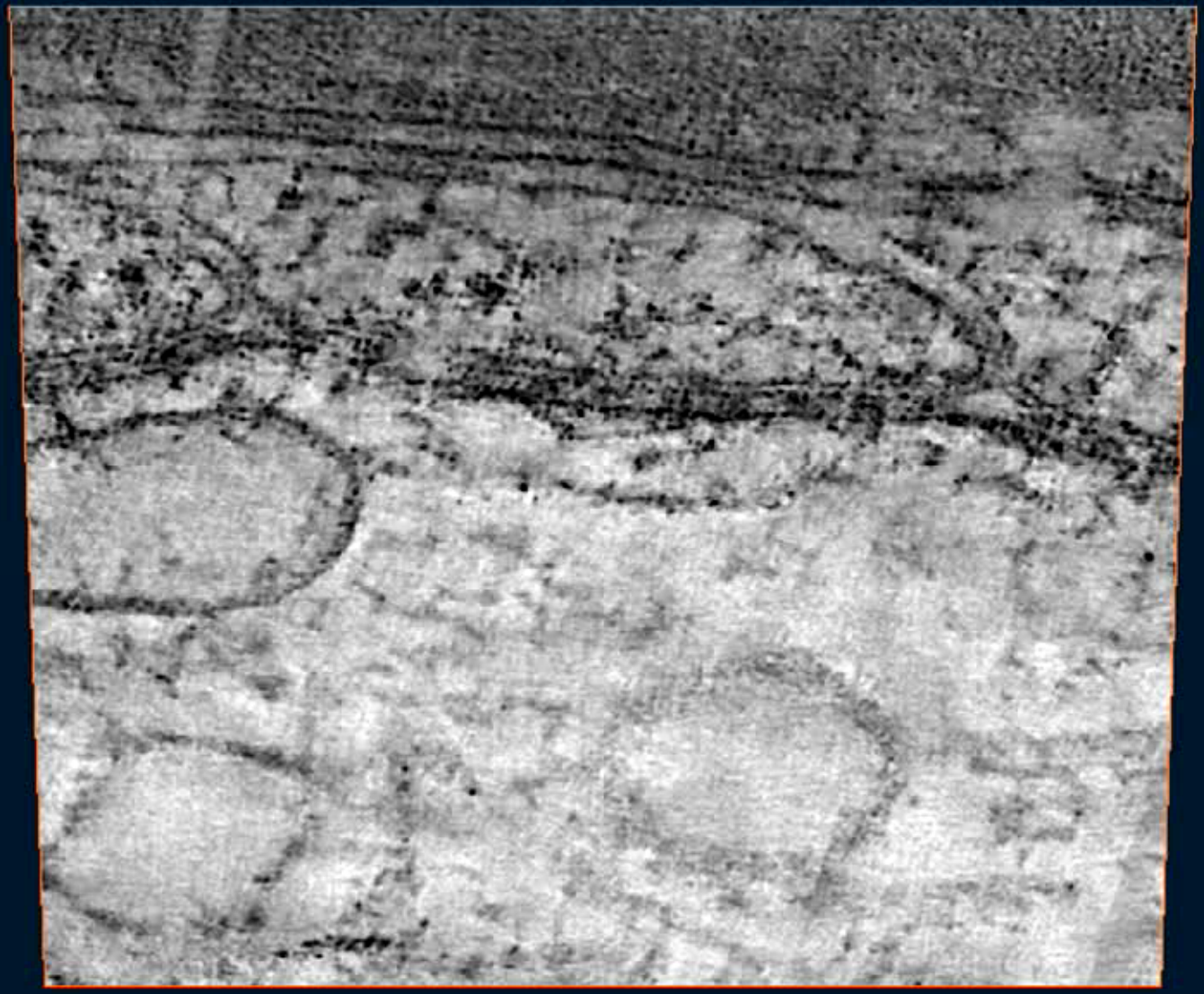

ELECTRON TOMOGRAPHY

Collect systematic set of projections

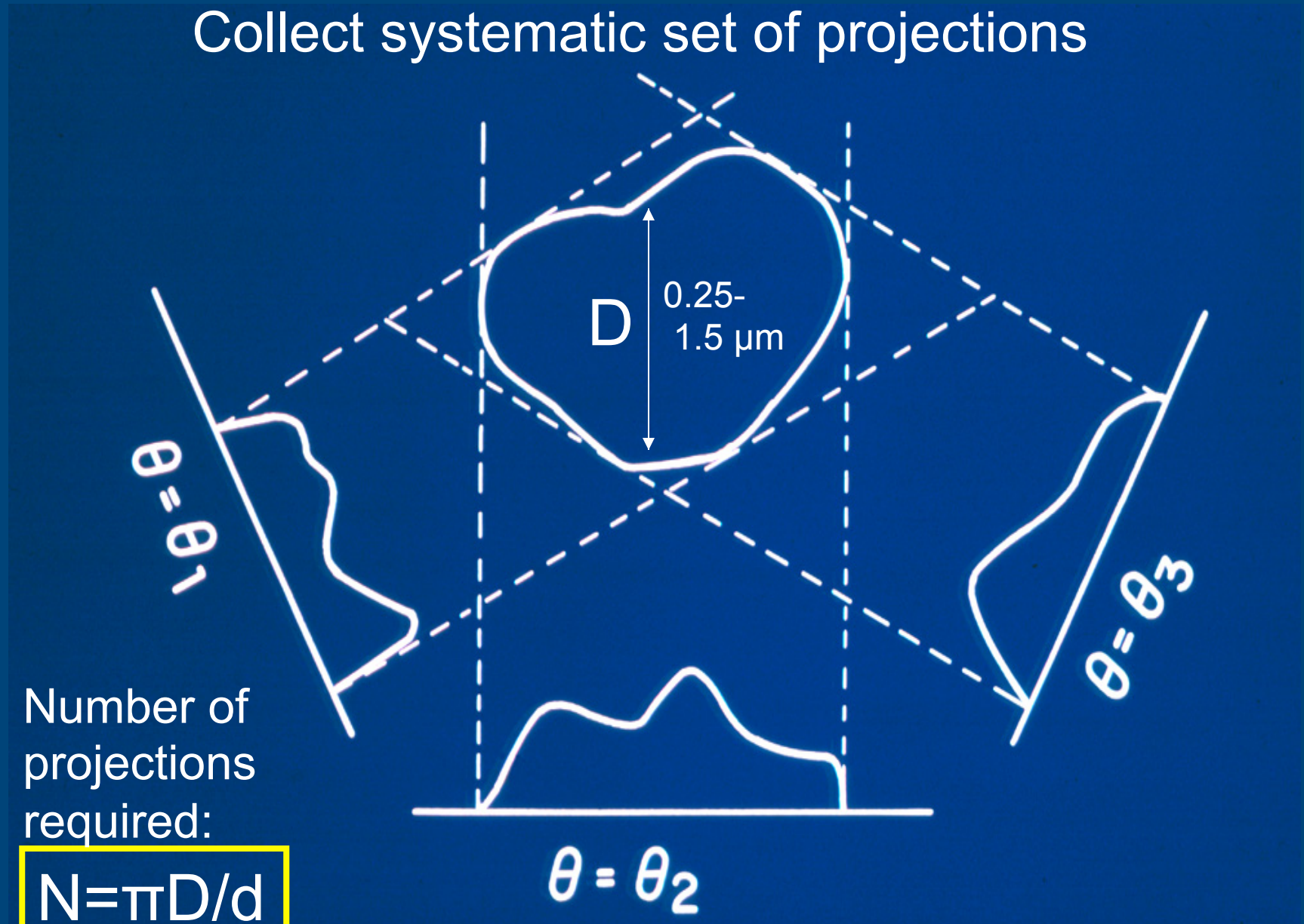

Number of projections required:

$N=\pi D/d$

Back projection or Fourier synthesis

Back projection

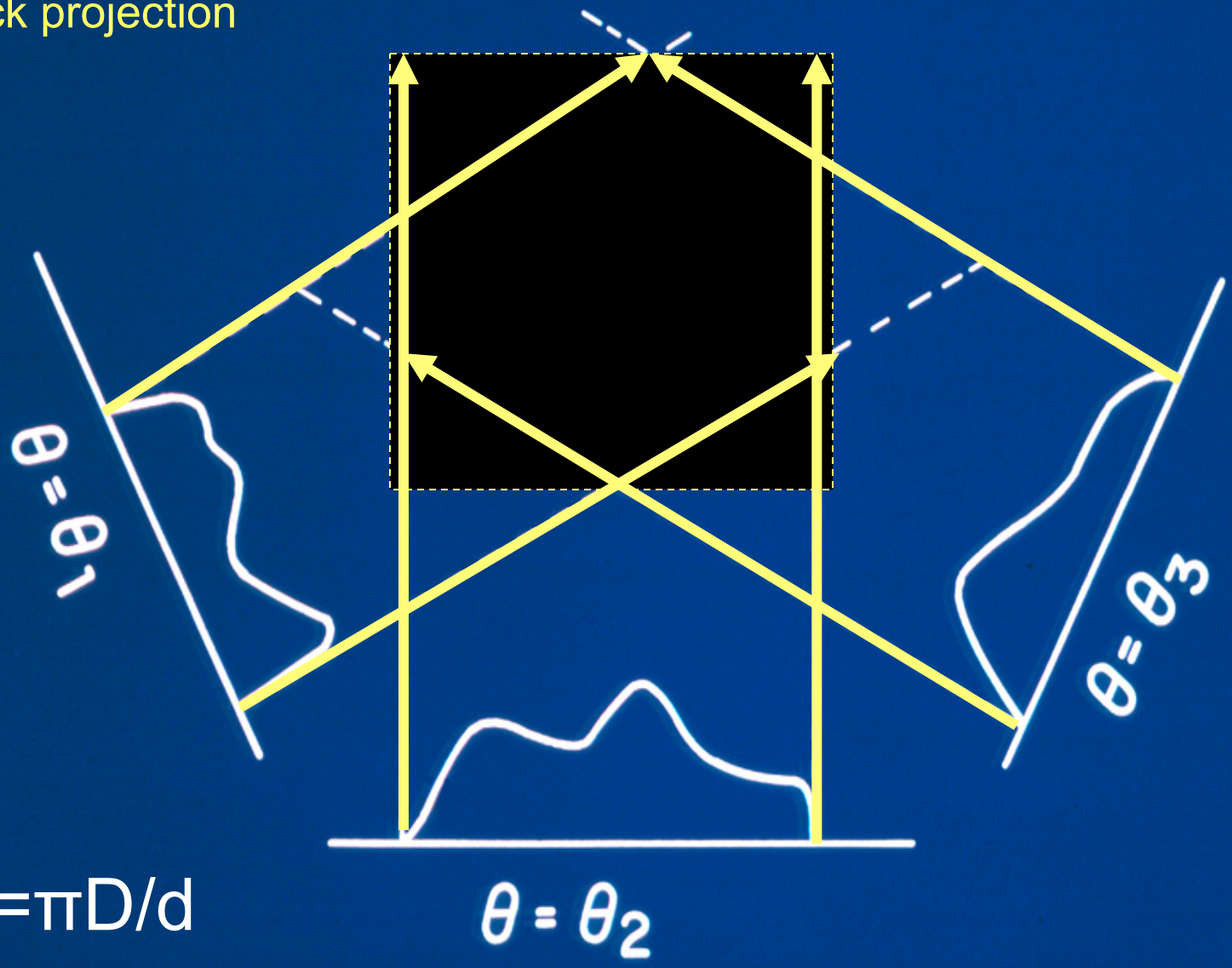

$N=\pi D/d$

1. Specimen Preparation

2. Data Collection

3. Computation

1. Specimen Preparation

Plastic sections
- Conventional fixation
- Freeze substitution

Freezing of cells and tissue

Grids

Holders

1. Preparation of Plastic Sections

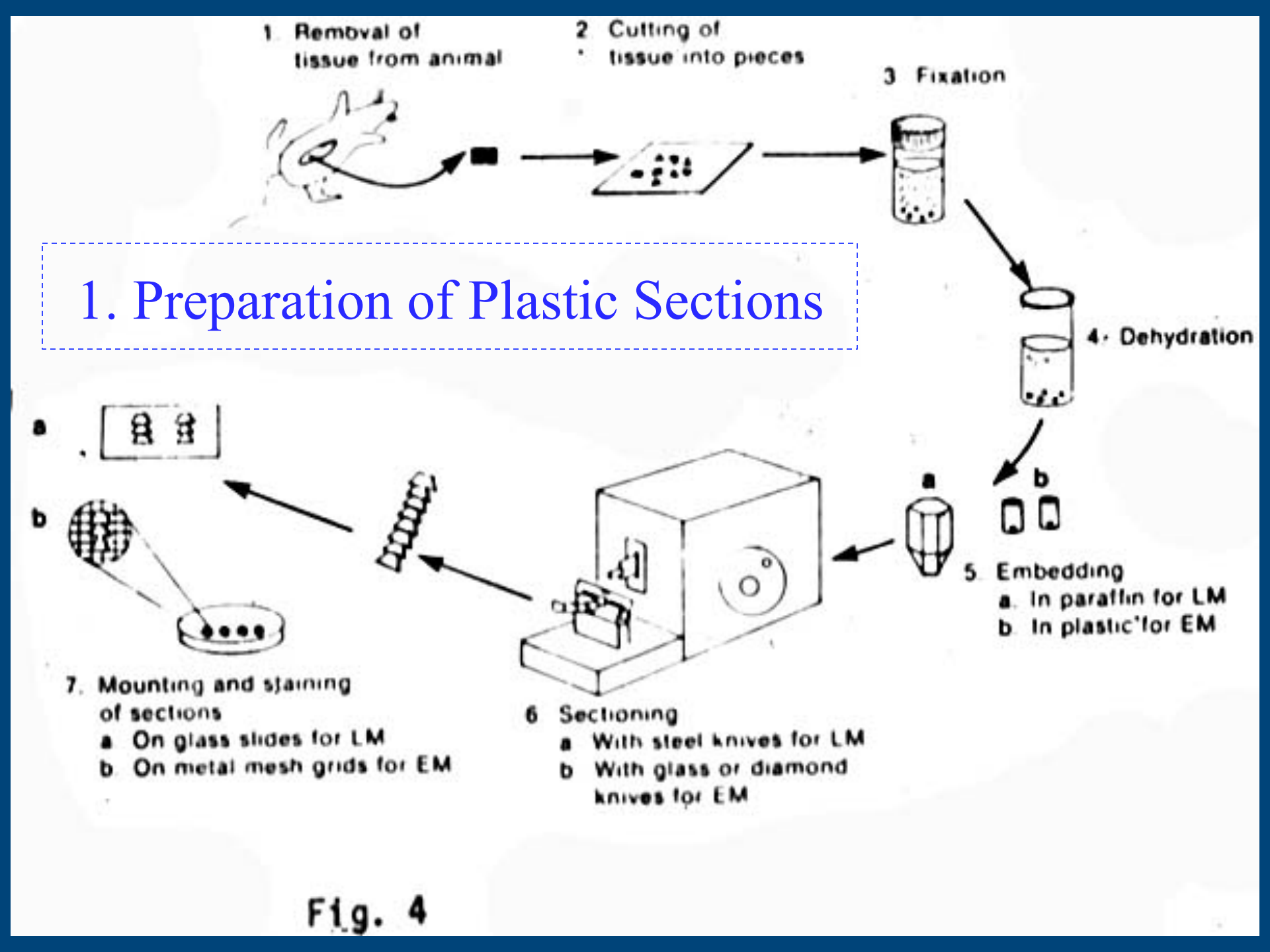

Fig. 4

Methods of Freezing:

- plunge freezing (5 um)
- freeze slamming (10 um)
- propane jet freezing (40 um)
- high pressure freezing (100-200 um)

High Pressure delays ice crystal nucleation

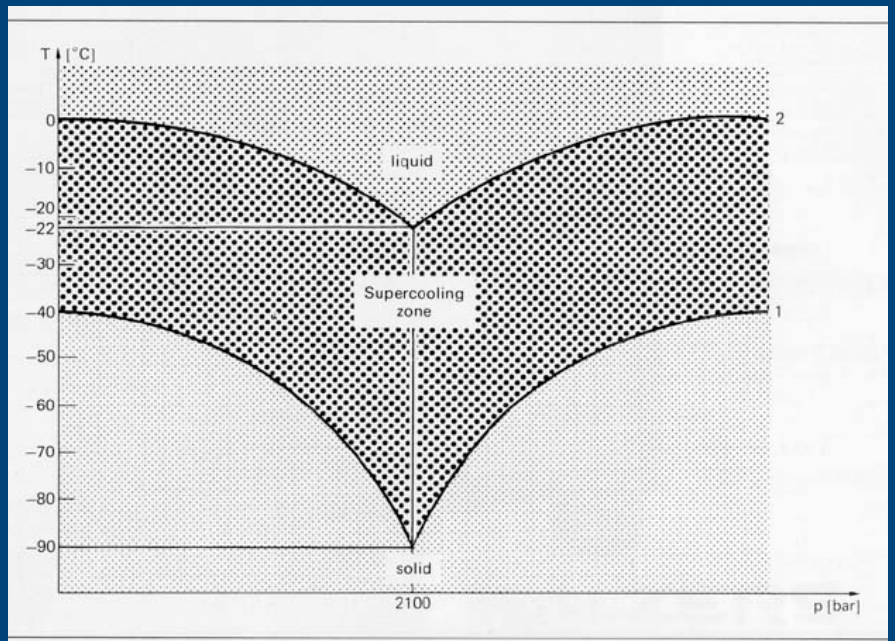

H_2O Phase Diagram

1 Superocooling capability curve
2 Melting point curve

Plunge-freezing

Rapid freezing (a few msec) prevents formation of ice crystals
Plunge freezing good for 5-10 μm thickness

Place drop of sample on grid

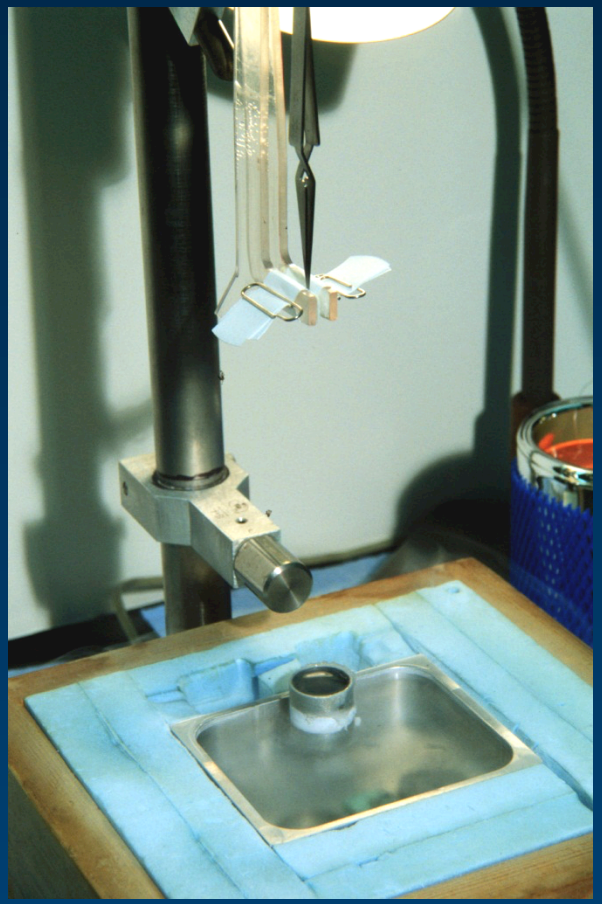

Blot excess fluid to form thin layer

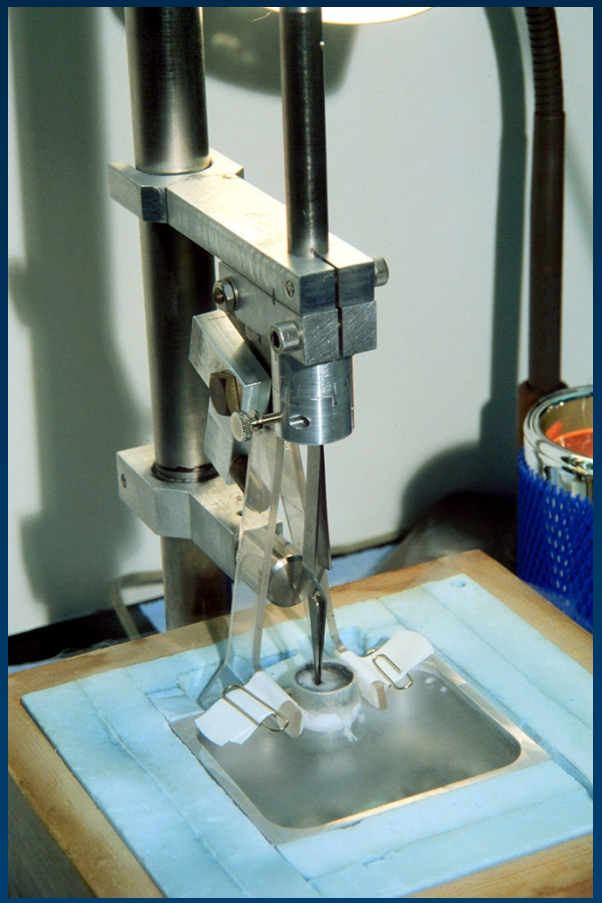

Plunge in liquid ethane

EM grids

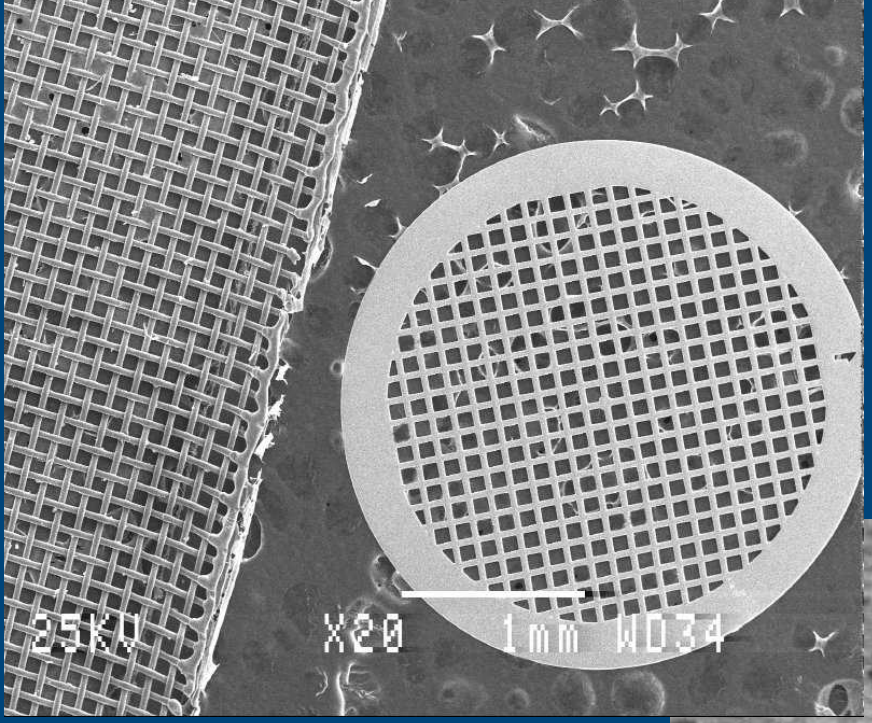

200 mesh grid

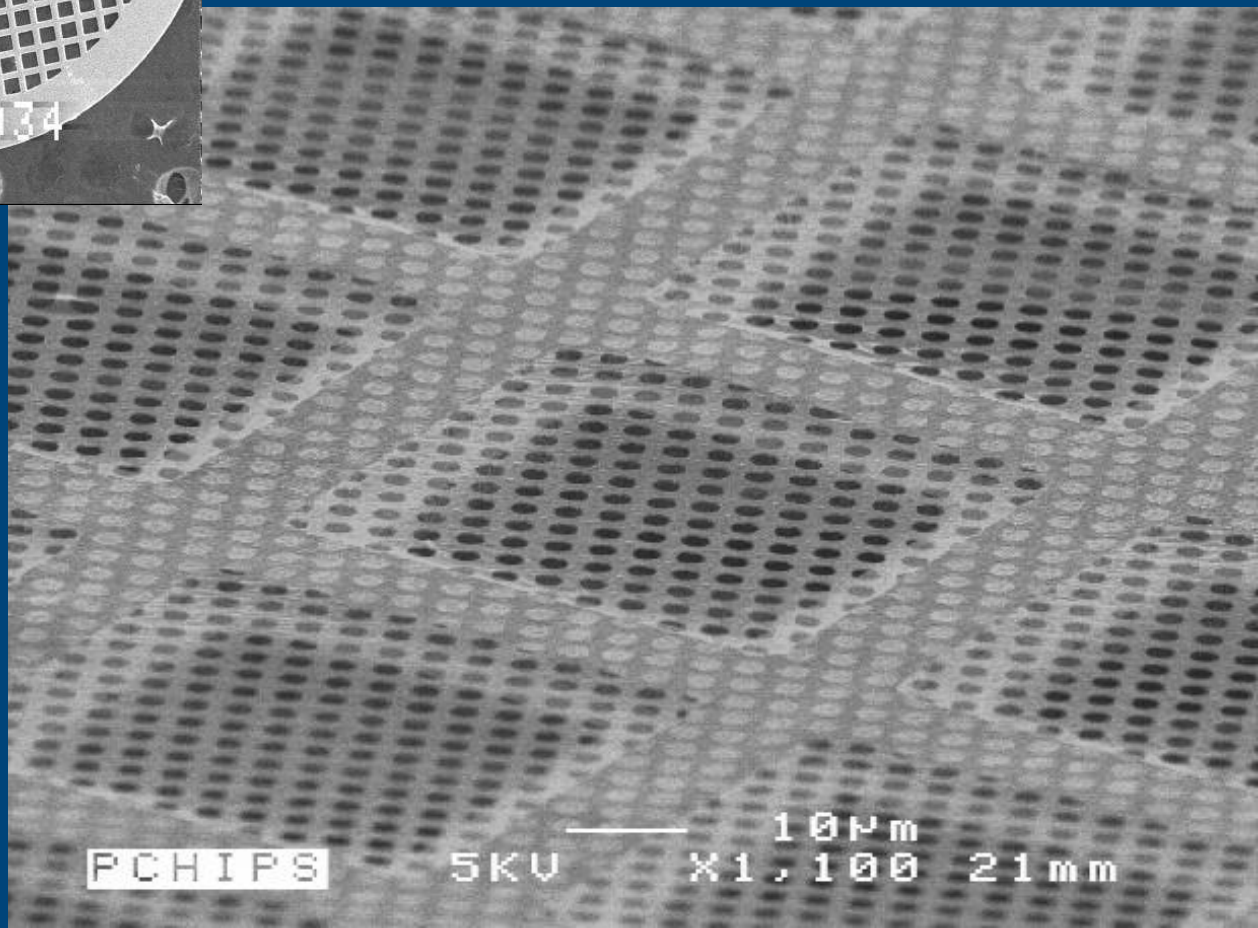

EM grids

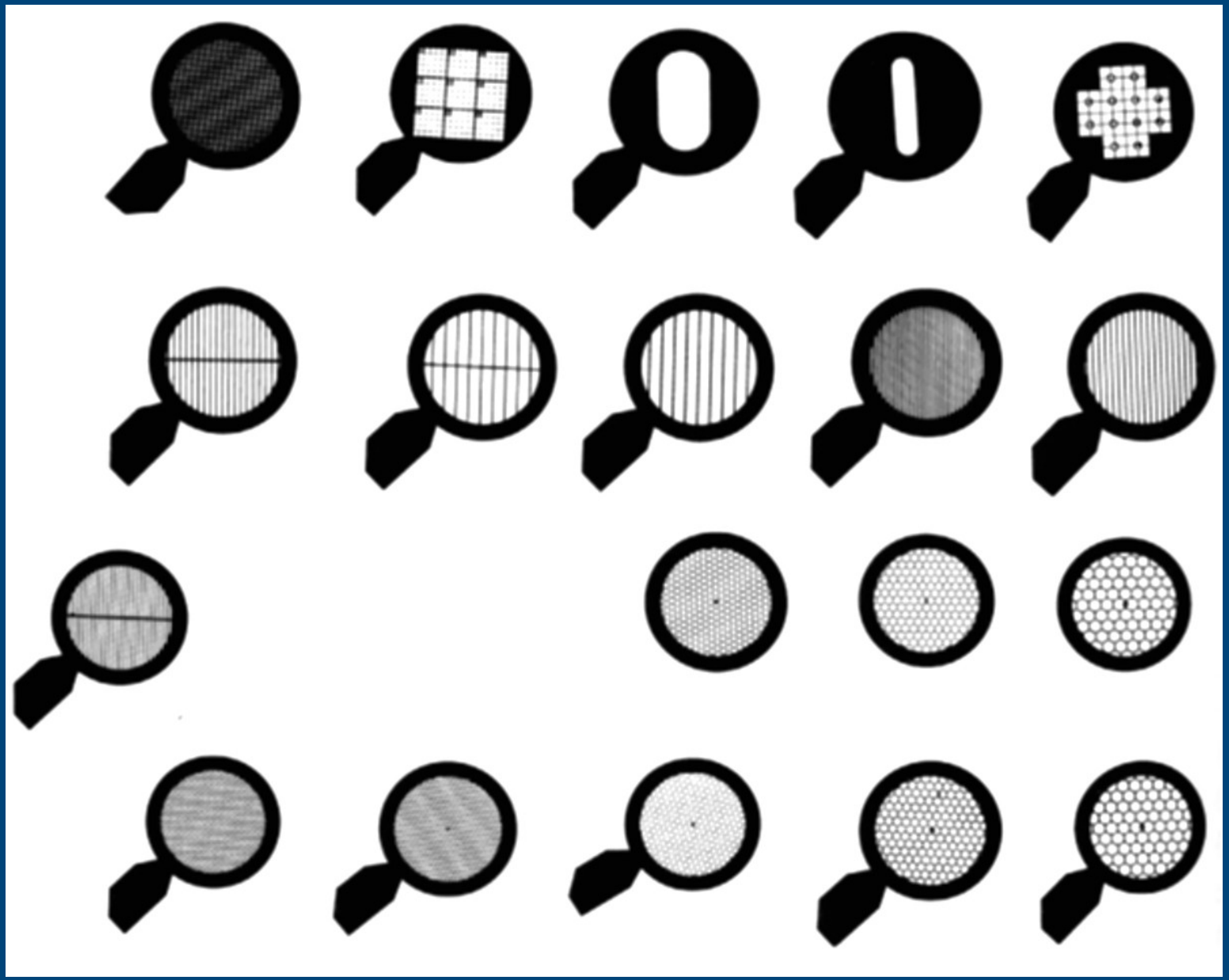

Plastic sections

- Often use thick sections (0.25 – 1.5 μm)
  For these, need to stain longer (penetration)

- Wide mesh, hexagonal or slot grids
  To reduce obstruction by bars during tilting

- Gold particles on the carbon support film
  10-20 nm colloidal gold as alignment markers

- Behavior of plastic sections during irradiation
  They all shrink, some warp, resin-dependent

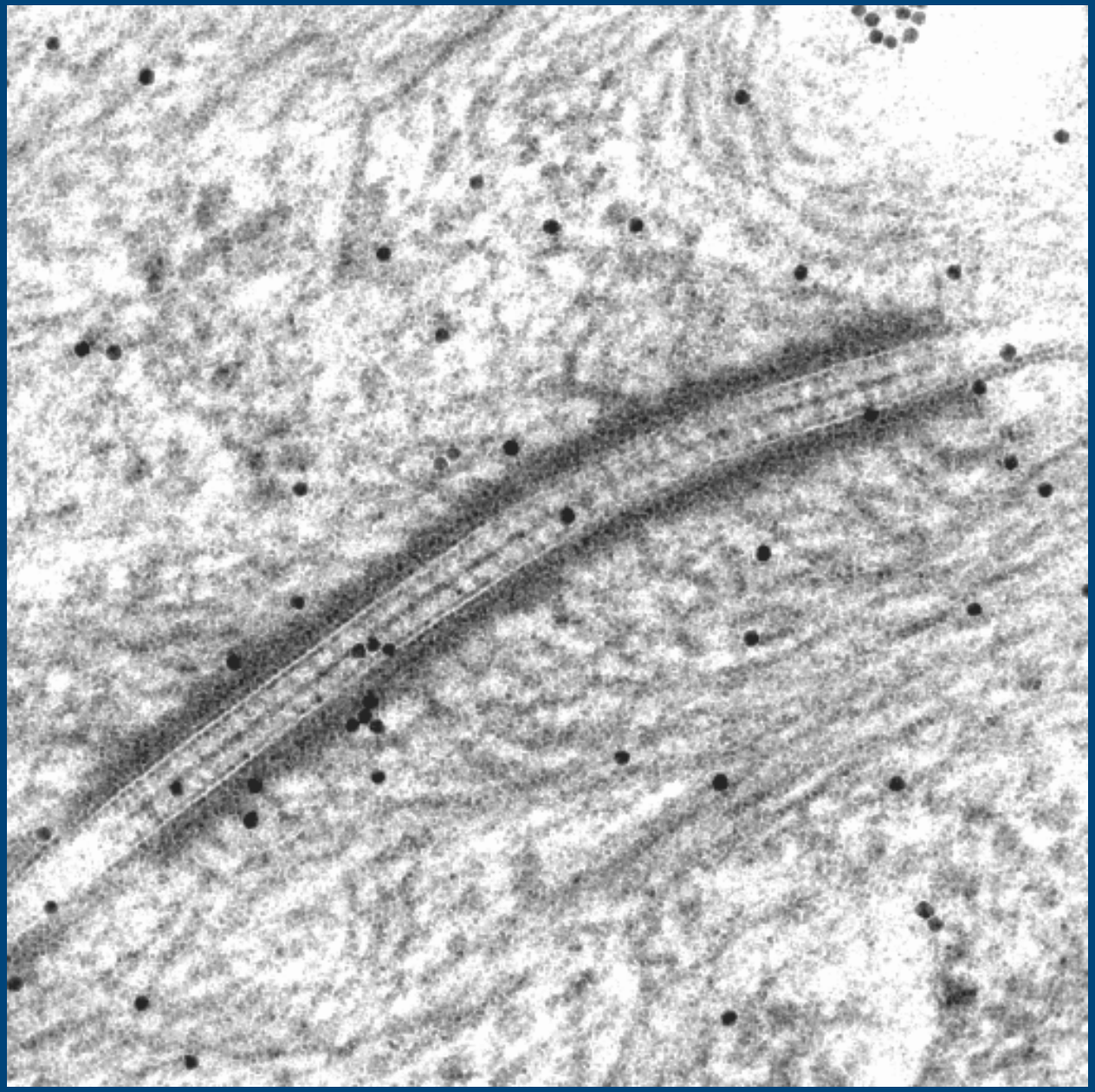

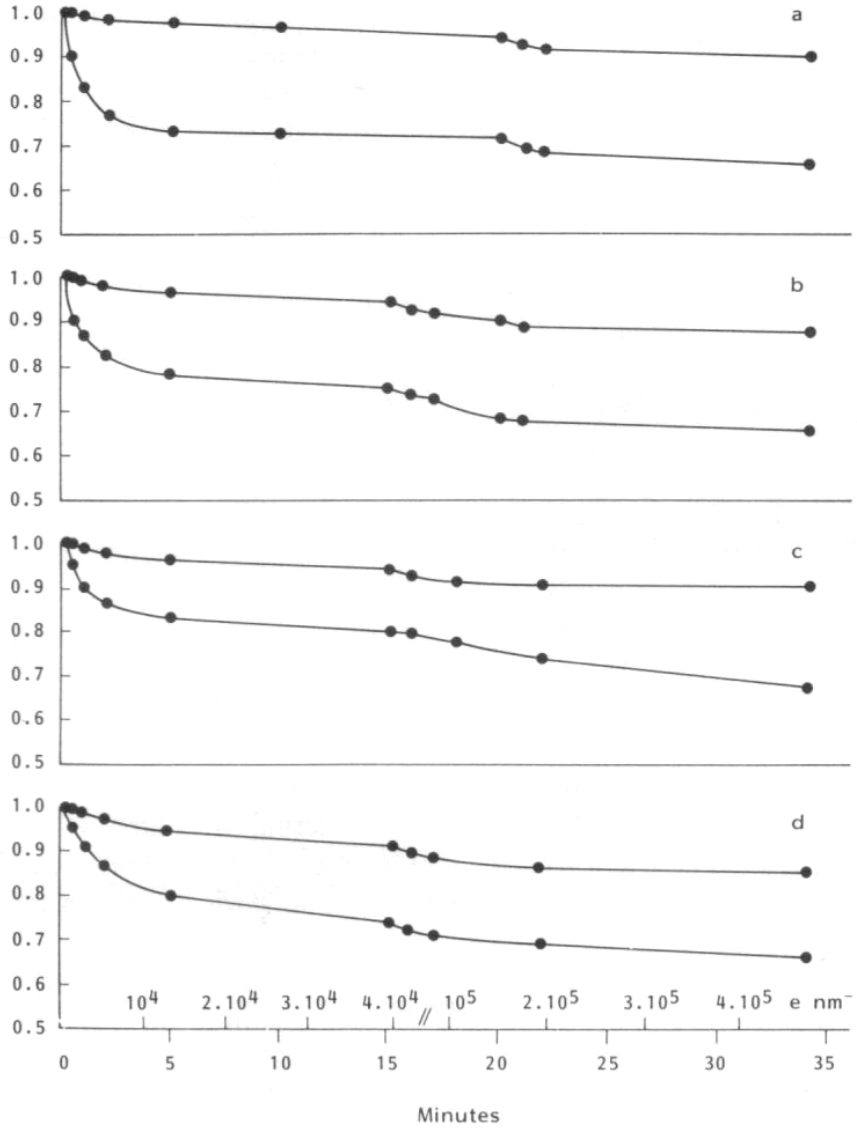

FIGURE 8. Measurement of section collapse (lower trace) and planar shrinkage (upper trace) as a function of electron dose. Panels (a, b, c) are from gold particles over resin only (Araldite), and panel (d) is from gold particles over a paracrystal. The dose rate, initially 0.5 (e/Å^2)/s, was increased to 4 (e/Å^2)/s after 20 min for (a) and after 15 min for (b, c, d). (From Luther *et al.*, 1988.)

In-plane

Axial

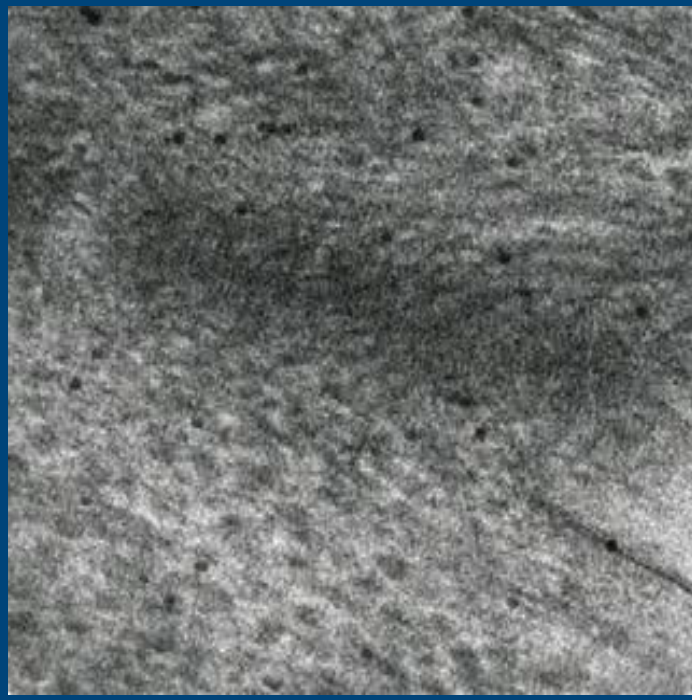

Strategy: Pre-shrink plastic sections

Pre-irradiate with ~ 10^5 e^- / Å^2

Cryo-Electron Tomography

Usual limit to specimen thickness is < 1 μm

Limited to organelles, viruses, bacteria, edges of eukaryotic cells

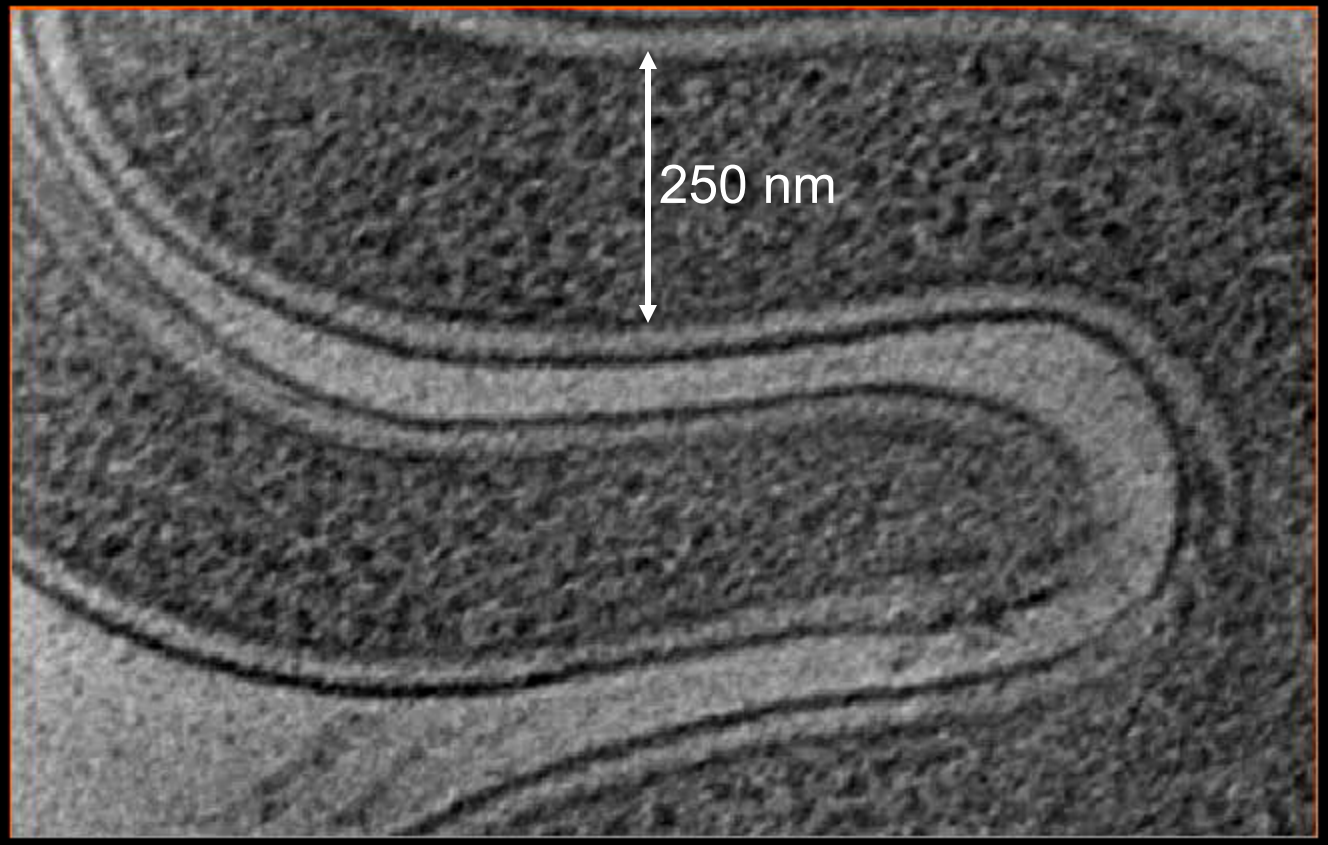

Spirochete
T. denticola
Jaques Izard
(Forsyth Inst)

Izard et al. (2009) J. Struct. Biol.

Cryo-Electron Tomography

Usual limit to specimen thickness is < 1 μm

Limited to organelles, viruses, bacteria, edges of eukaryotic cells

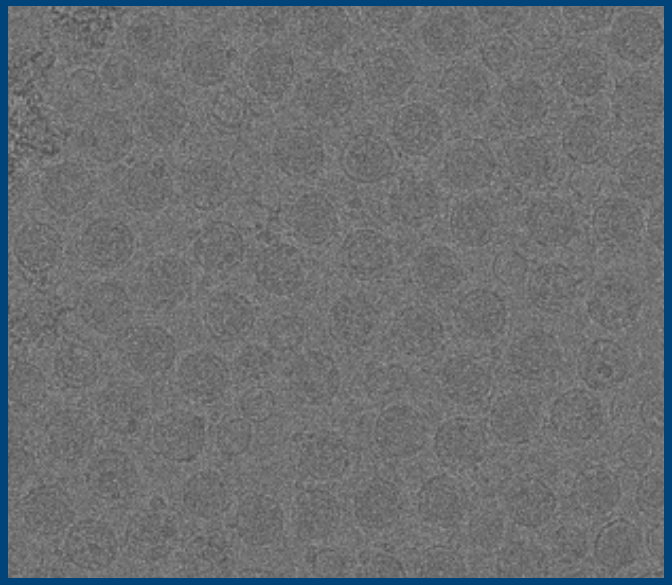

50 nm

Bacteriophage (ϕ12)

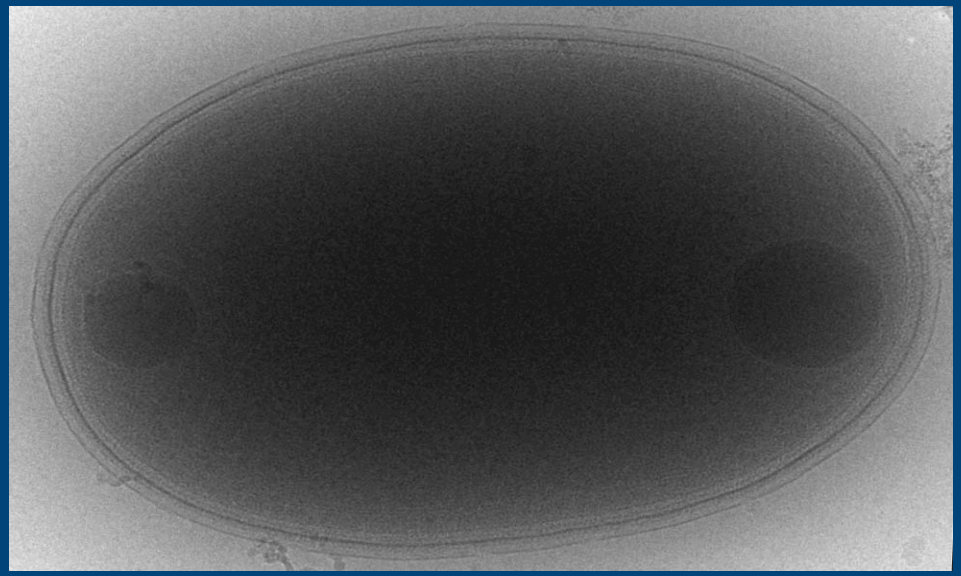

E. coli, Salmonella, Cyanobacteria

Cryo-Electron Tomography

Usual limit to specimen thickness is < 1 μm

Limited to organelles, viruses, bacteria, edges of eukaryotic cells

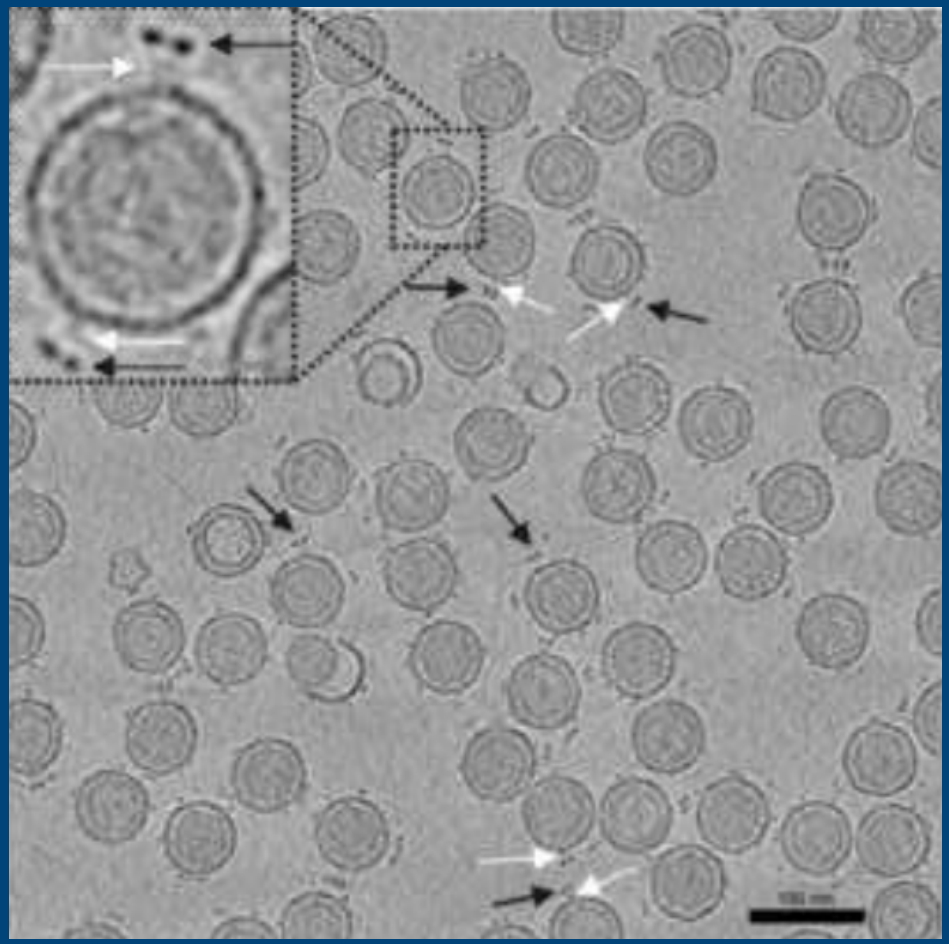

Bacteriophage ϕ12

Leo-Macias et al. Virology (2011) 414:103

Cryo-Electron Tomography

Usual limit to specimen thickness is < 1 μm

Limited to organelles, viruses, bacteria, edges of eukaryotic cells

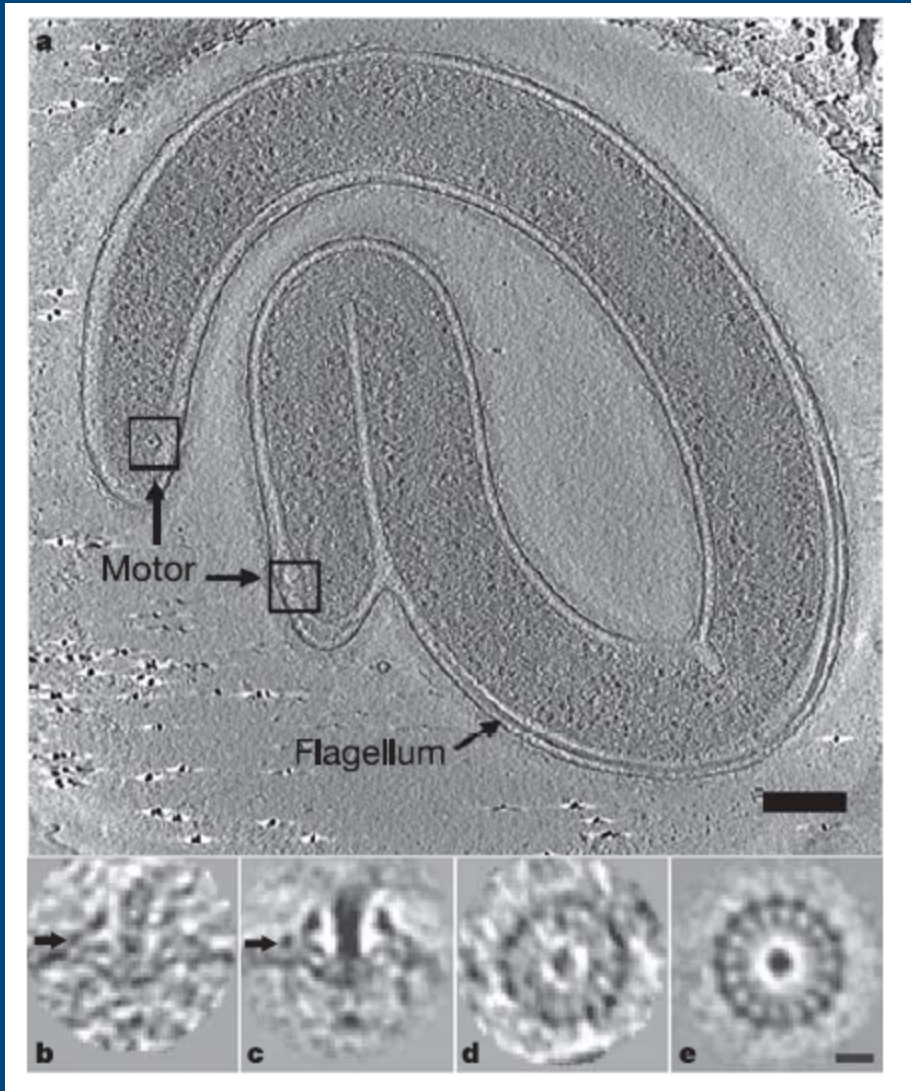

Intact spirochete: ***Treponema primitia***

Murphy et al. 2006, Nature 442:1062

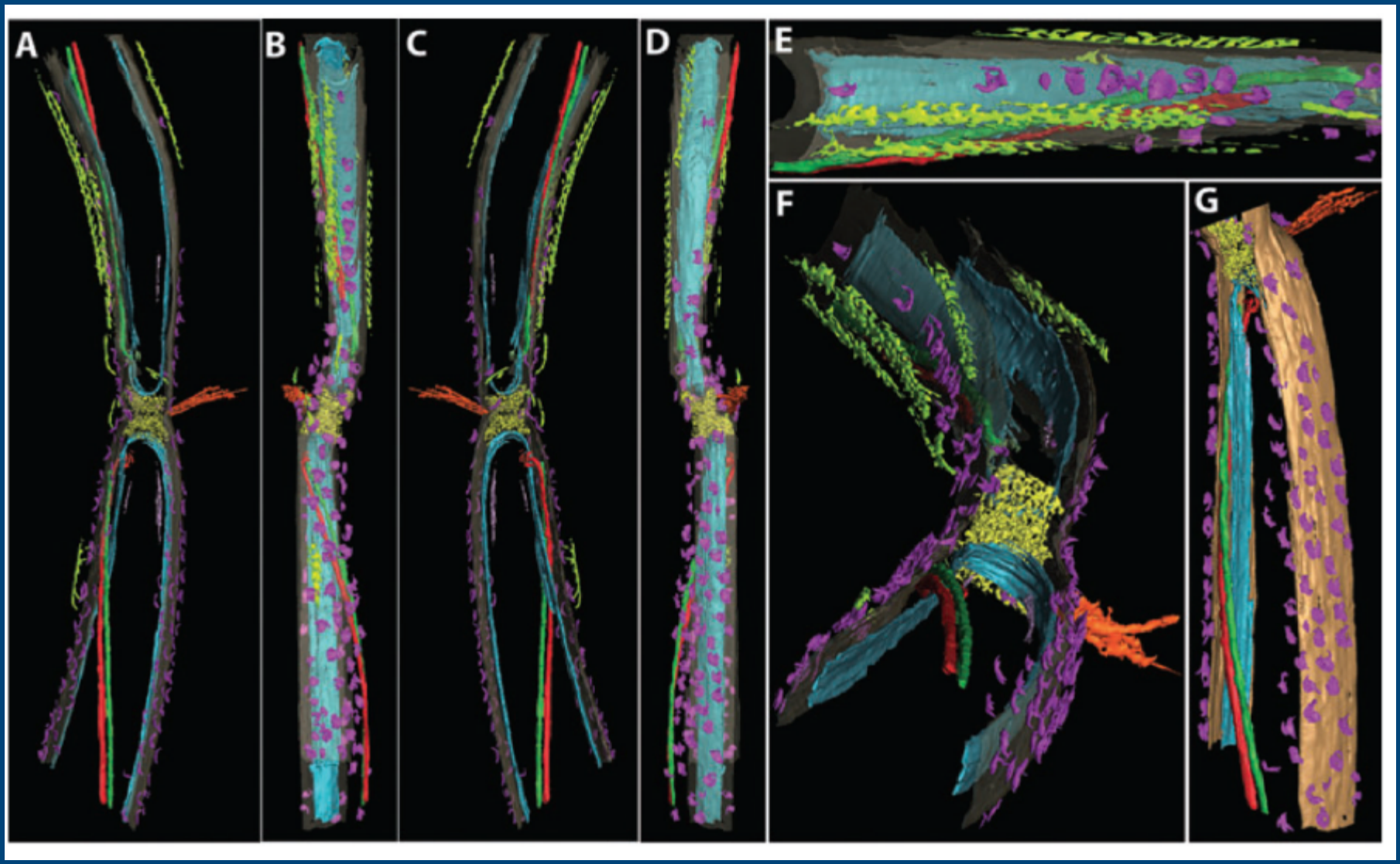

Murphy et al, 2008 Mol. Microbiol. 67:1184

Cryo-Electron Tomography

Usual limit to specimen thickness is < 1 μm

Limited to organelles, viruses, bacteria, edges of eukaryotic cells

Dictyostelium (slime mold)

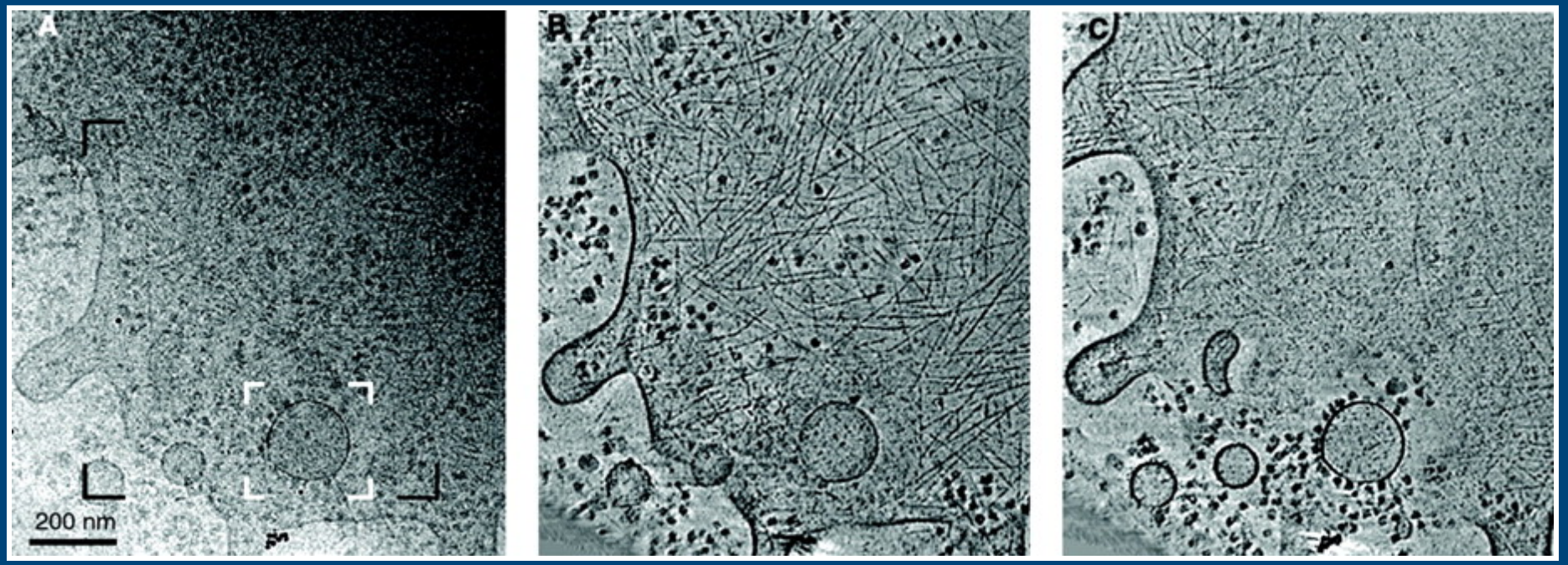

Medalia et al. Science 2002

Desmosome in cultured keratinocyte
Guobin Hu, unpublished

Cryo-Electron Tomography

Usual limit to specimen thickness is < 1 μm

Limited to organelles, viruses, bacteria, edges of eukaryotic cells

Want to expand cryo-electron tomography to:

thicker starting material (large cells, bulk tissue)

thinned appropriately for desired resolution

High-pressure freezing and

1) Cryo-ultramicrotomy (Hsieh et al, 2002, 2006) or
2) FIB-milling (Marko et al, 2006, 2007)

Cryo-Ultramicrotome

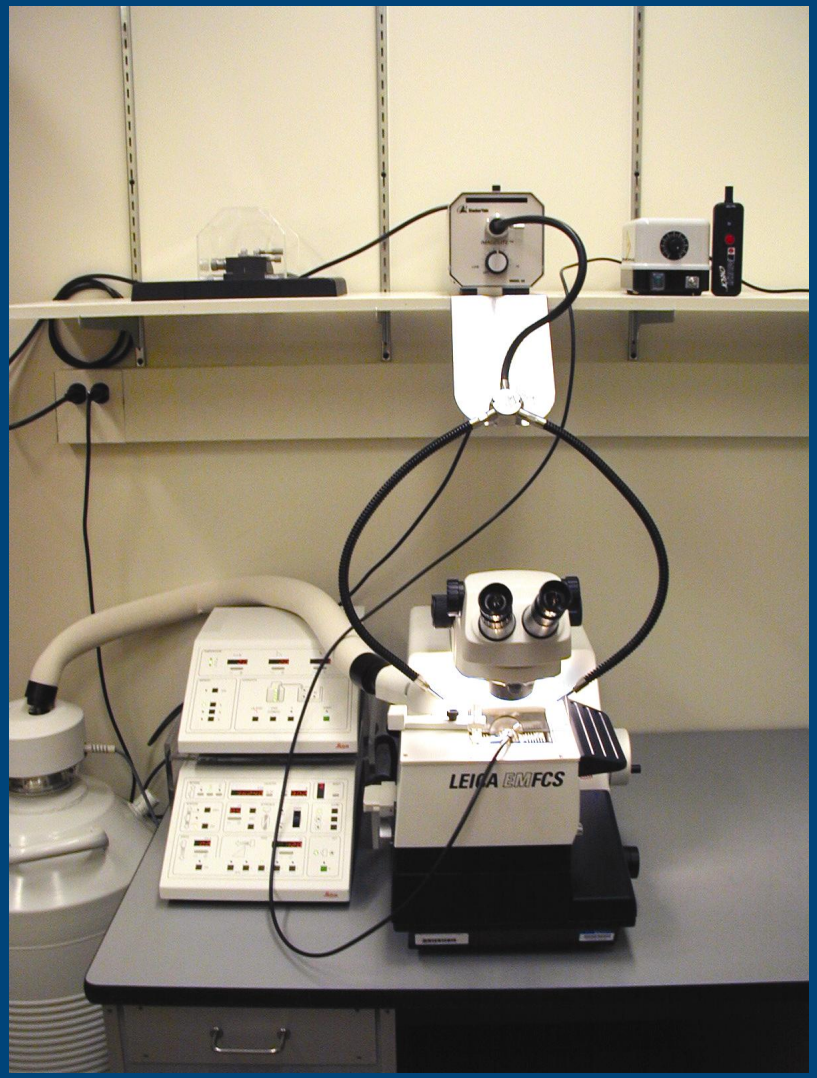

Leica Ultracut EM-FCS

Trimming high-pressure frozen specimens

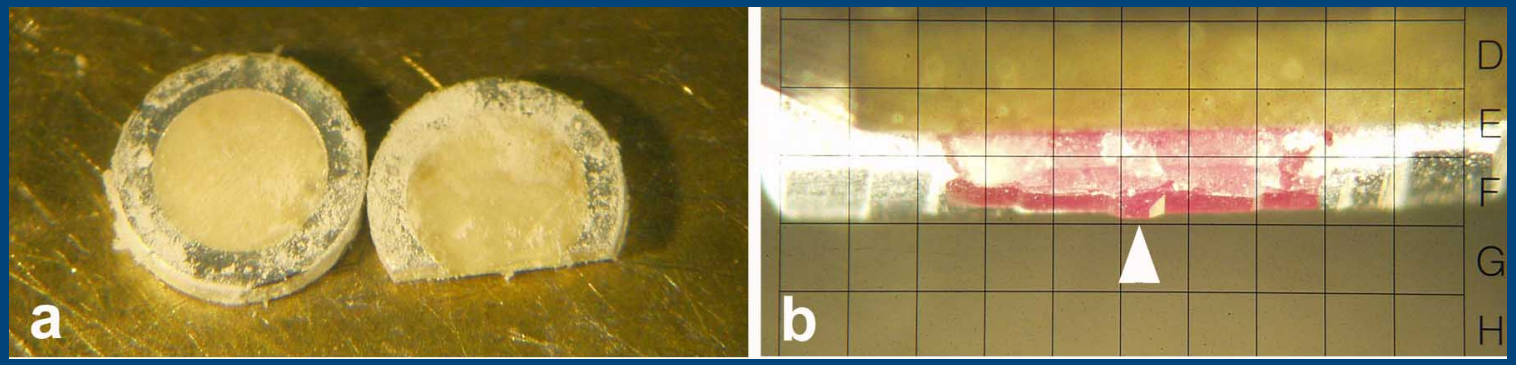

(a) A 3-mm-diameter aluminum specimen carrier before and after trimming. The upper portion of the carrier has been removed, revealing the specimen and allowing inspection for air bubbles and suitable areas for microtomy.
(b) Top view of the trimmed specimen carrier shows the trimmed block face, which is shaped like a low mesa (arrowhead), 100-µm square, as seen within a 250-µm graticle square of the stereomicroscope.

(Red: Cyanobacteria)

Knife edge→

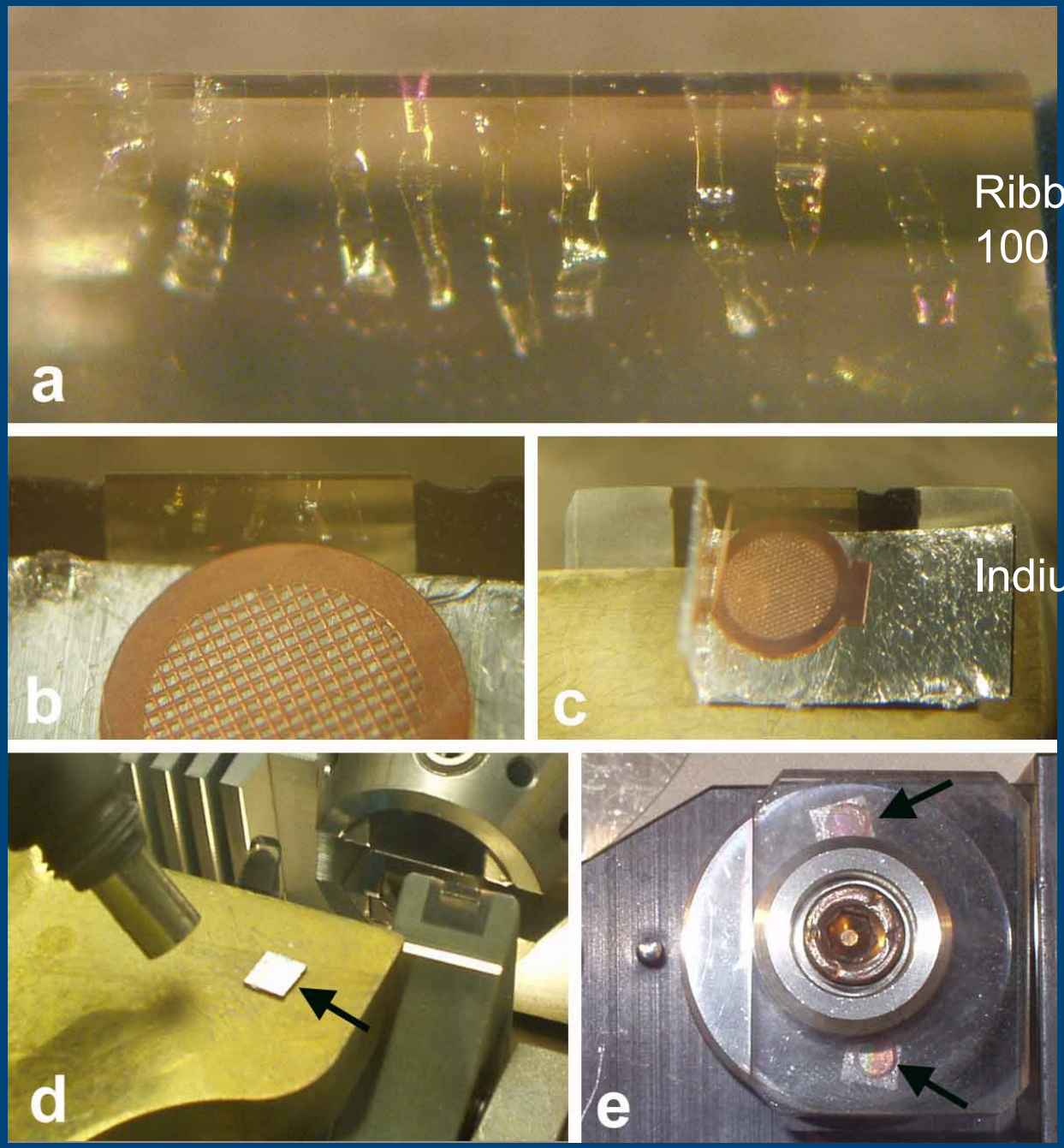

Ribbon width
100 μm or less

Indium foil

Frozen-hydrated section of rat liver

(200-nm thick)

No chemical fixation or metal stain

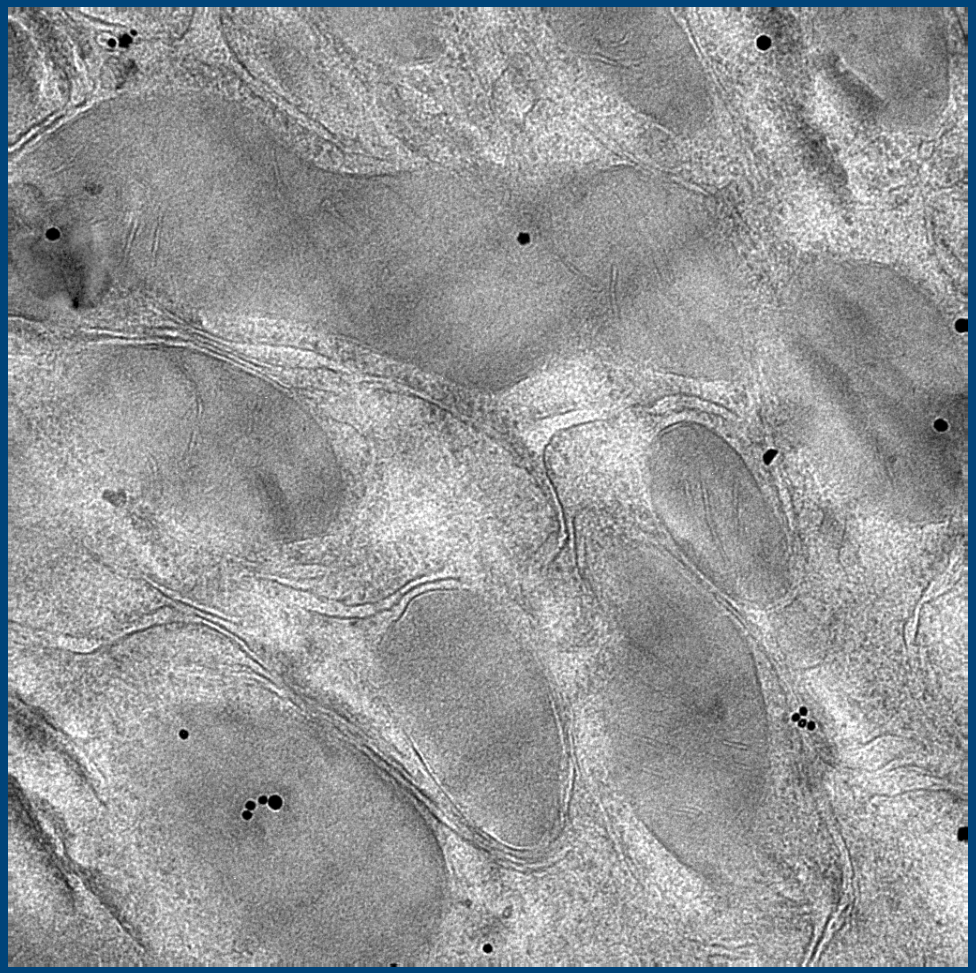

NIH / NCRR
RVBC

Hsieh et al. (2002) J. Struct. Biol. 138:63-73

Thin section (100 nm) of frozen-hydrated rat liver

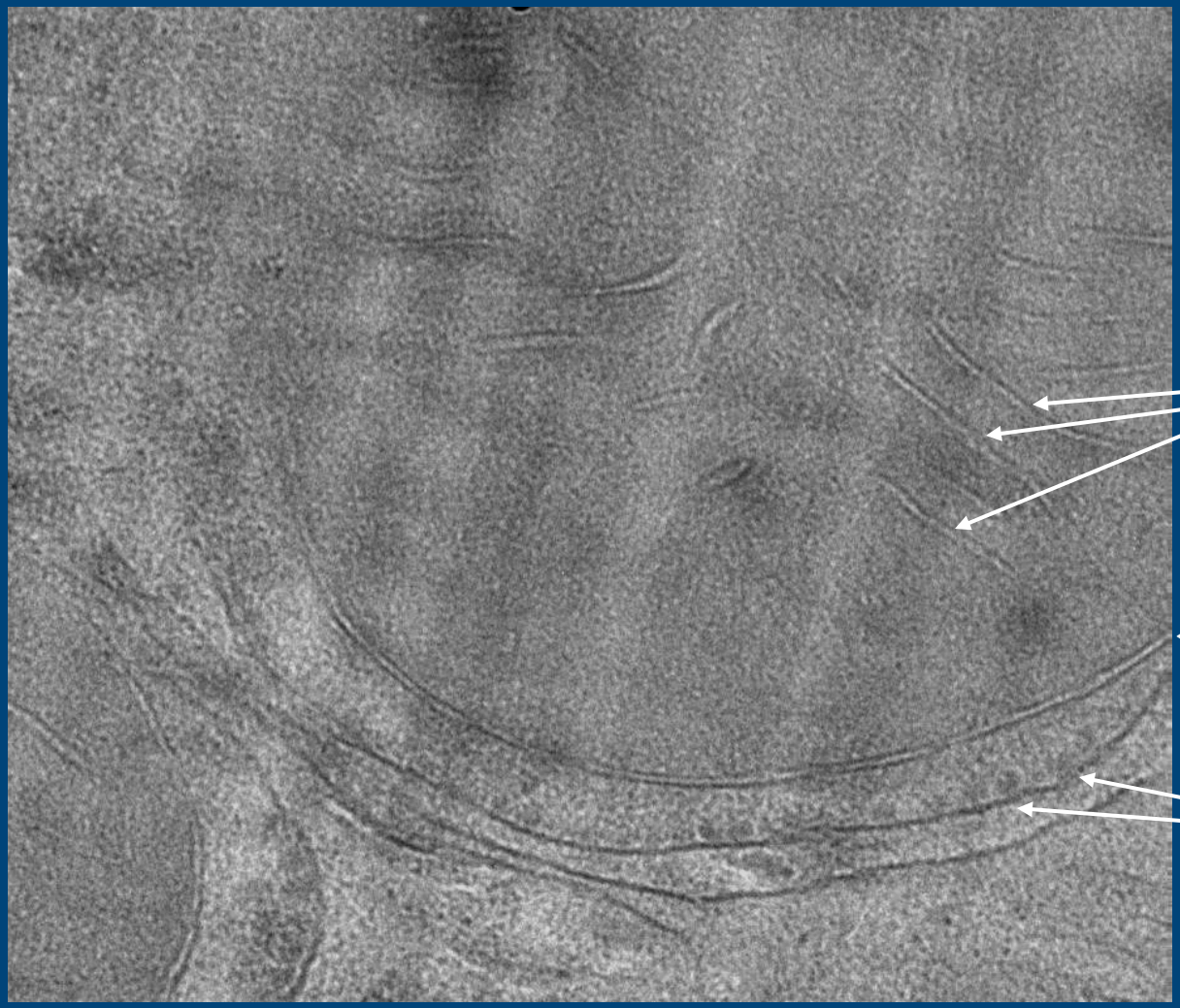

NIH / NCRR
RVBC

The Adhesion Problem

Side views of liver sections from tomograms

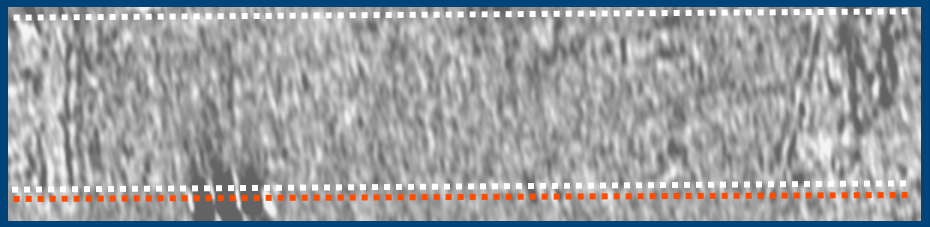

180 nm thick section attached to support film

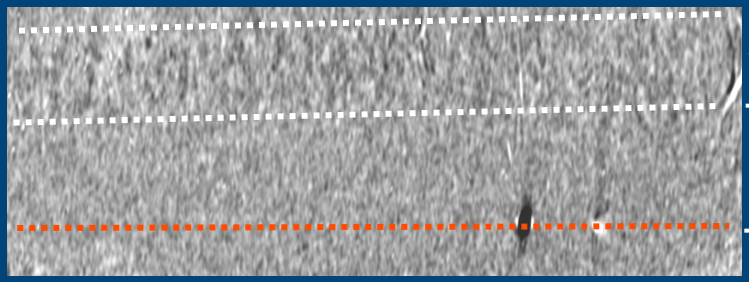

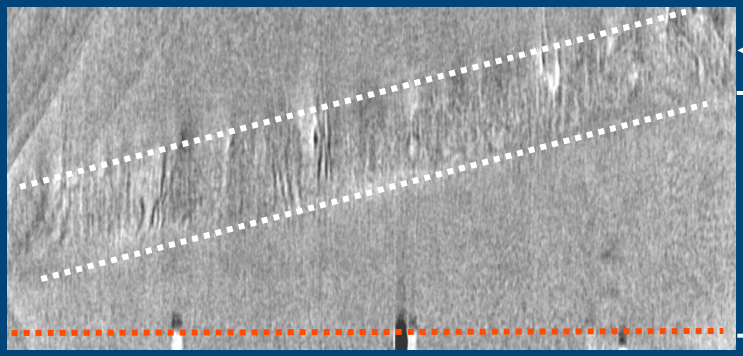

Focused Ion Beam (FIB) Milling

Dual beam FIB

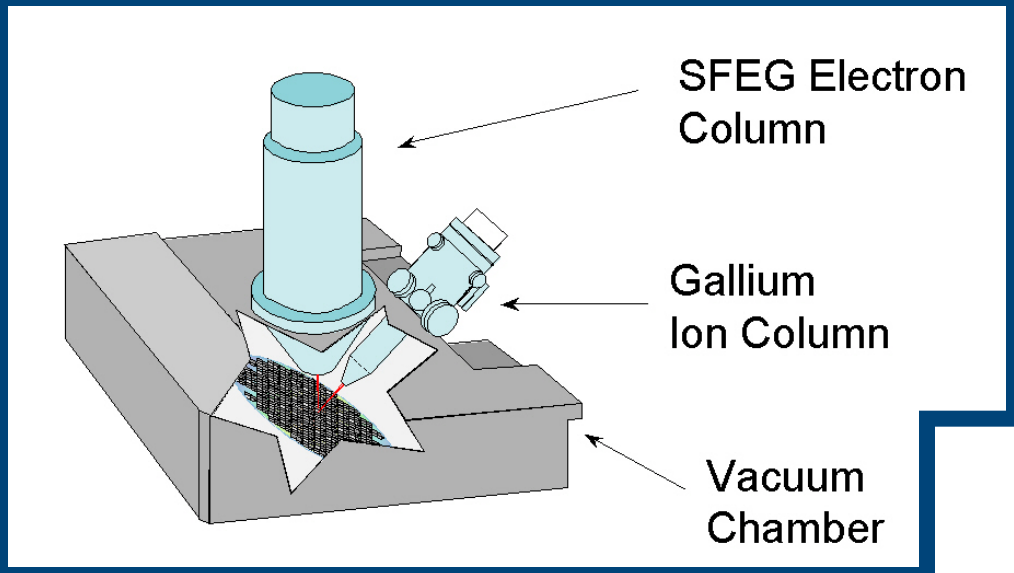

“Sputtering”

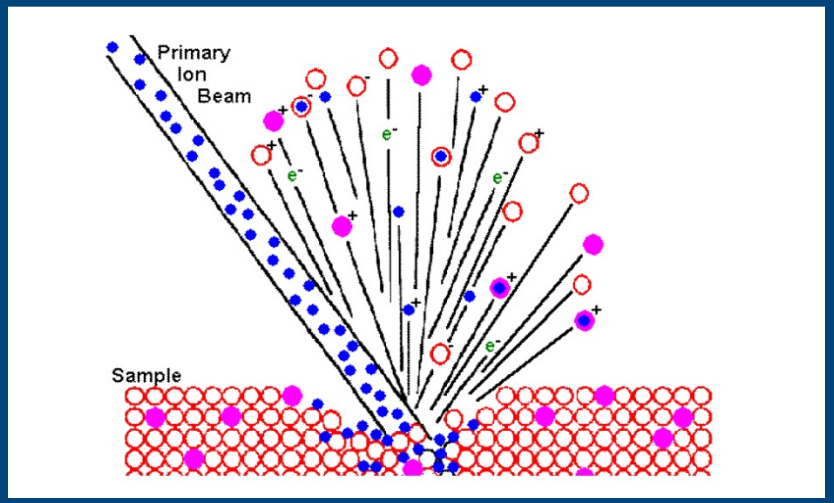

Grid shuttle for ion milling in dual-beam SEM

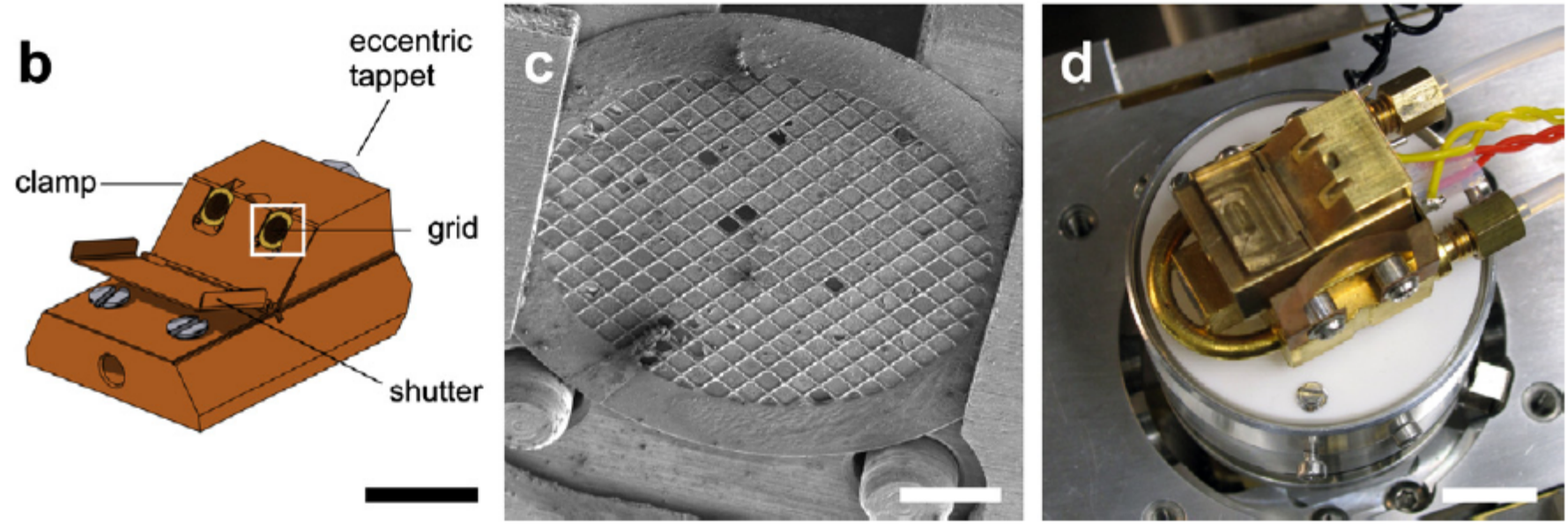

Rigort et al., 2010, J. Struct. Biol. 172:169

Strategies for milling

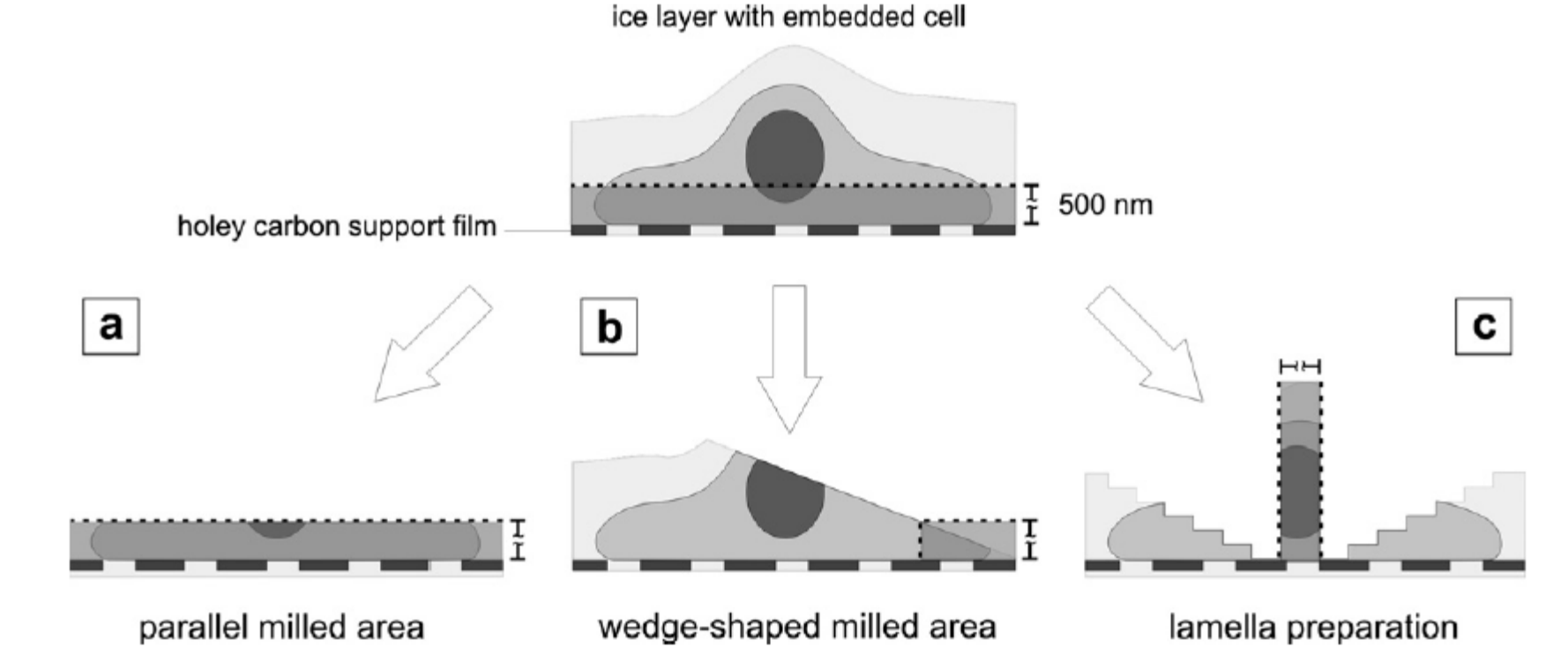

FIB-milling of bacteria

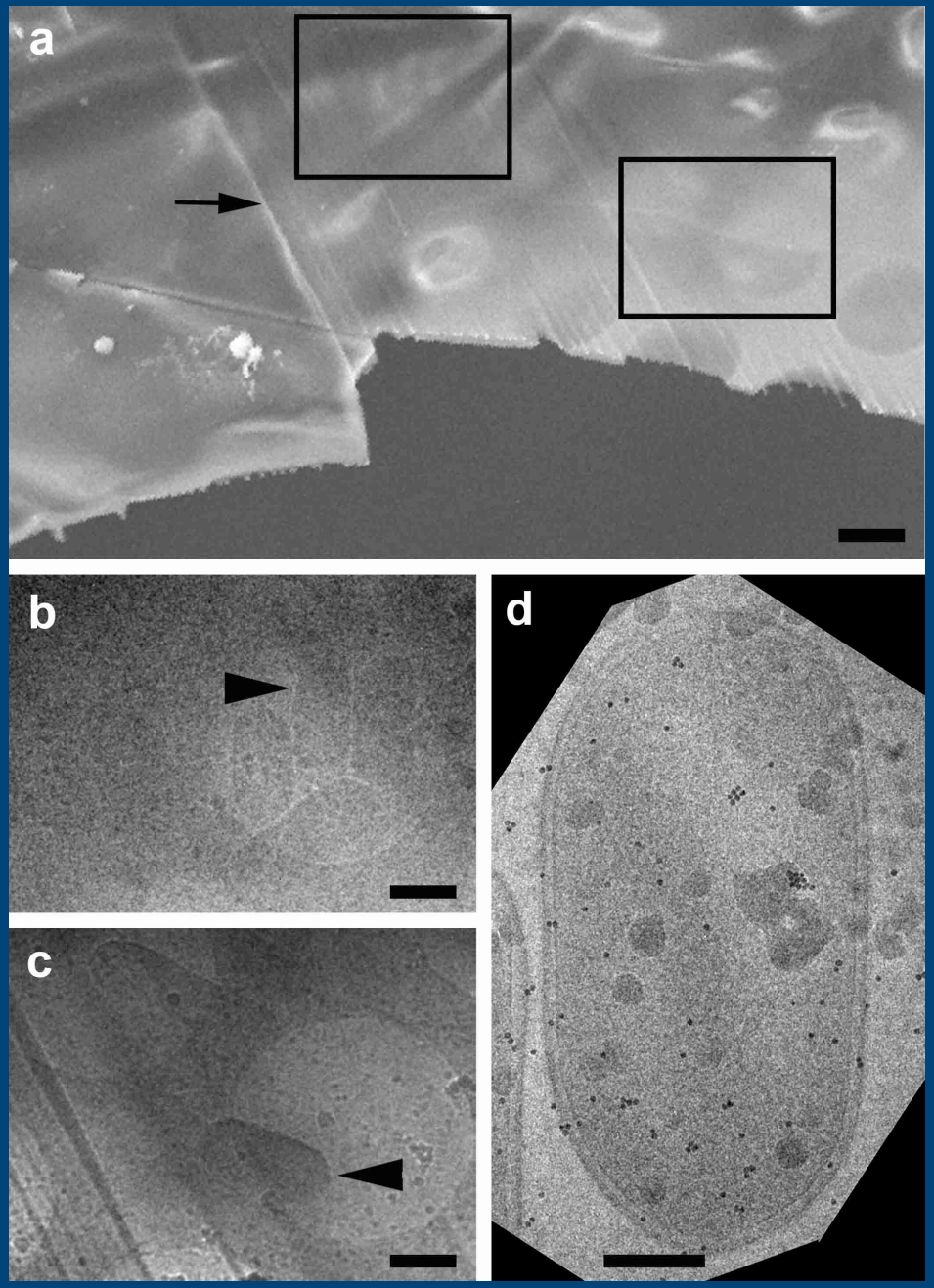

Marko et al (2007)
Nature Methods

NIH / NCRR
RVBC

FIB-milling of bacteria

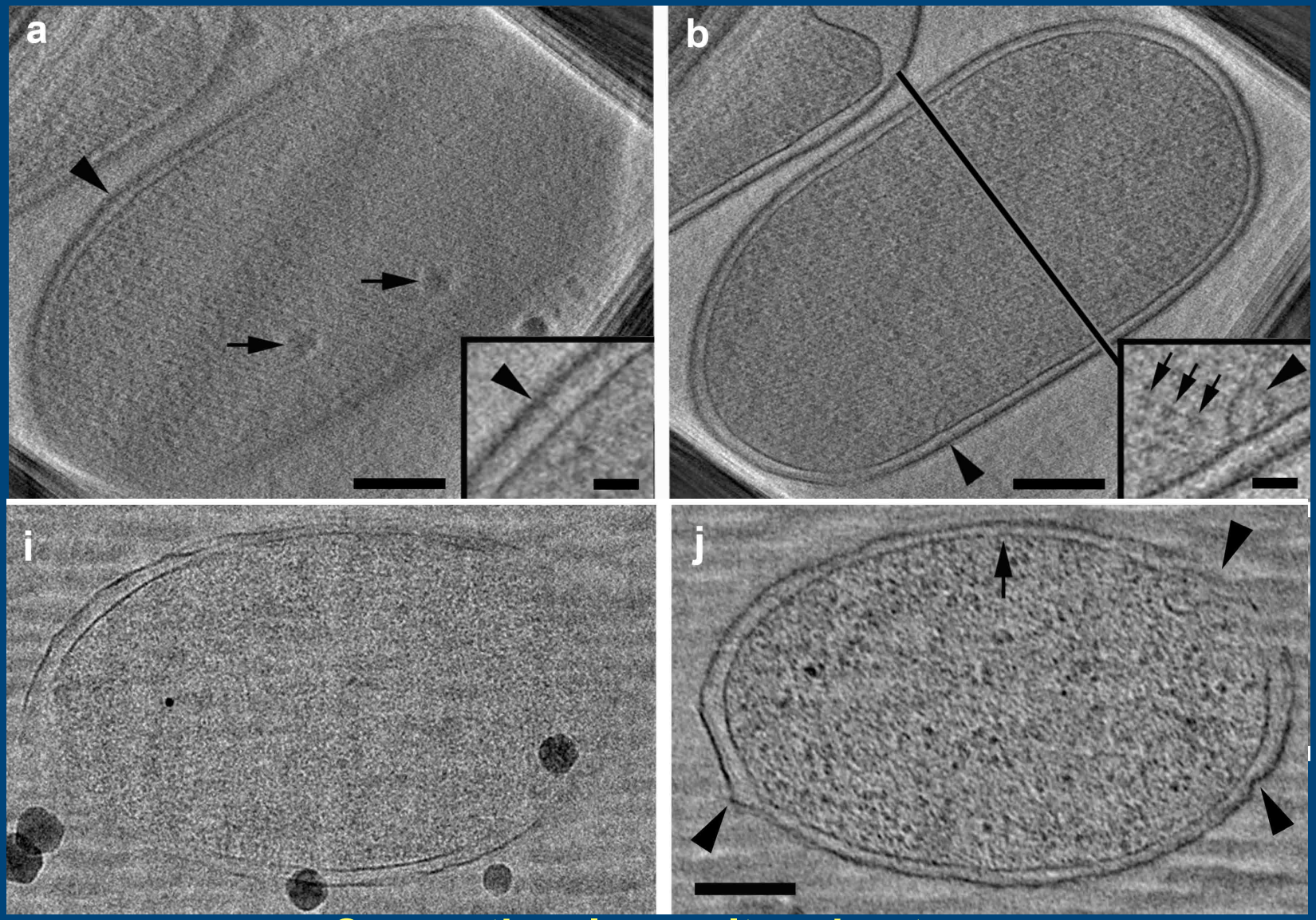

Conventional cryoultramicrotomy

FIB of cell lamellae

(Rigort & Plitzko, 2012, PNAS)

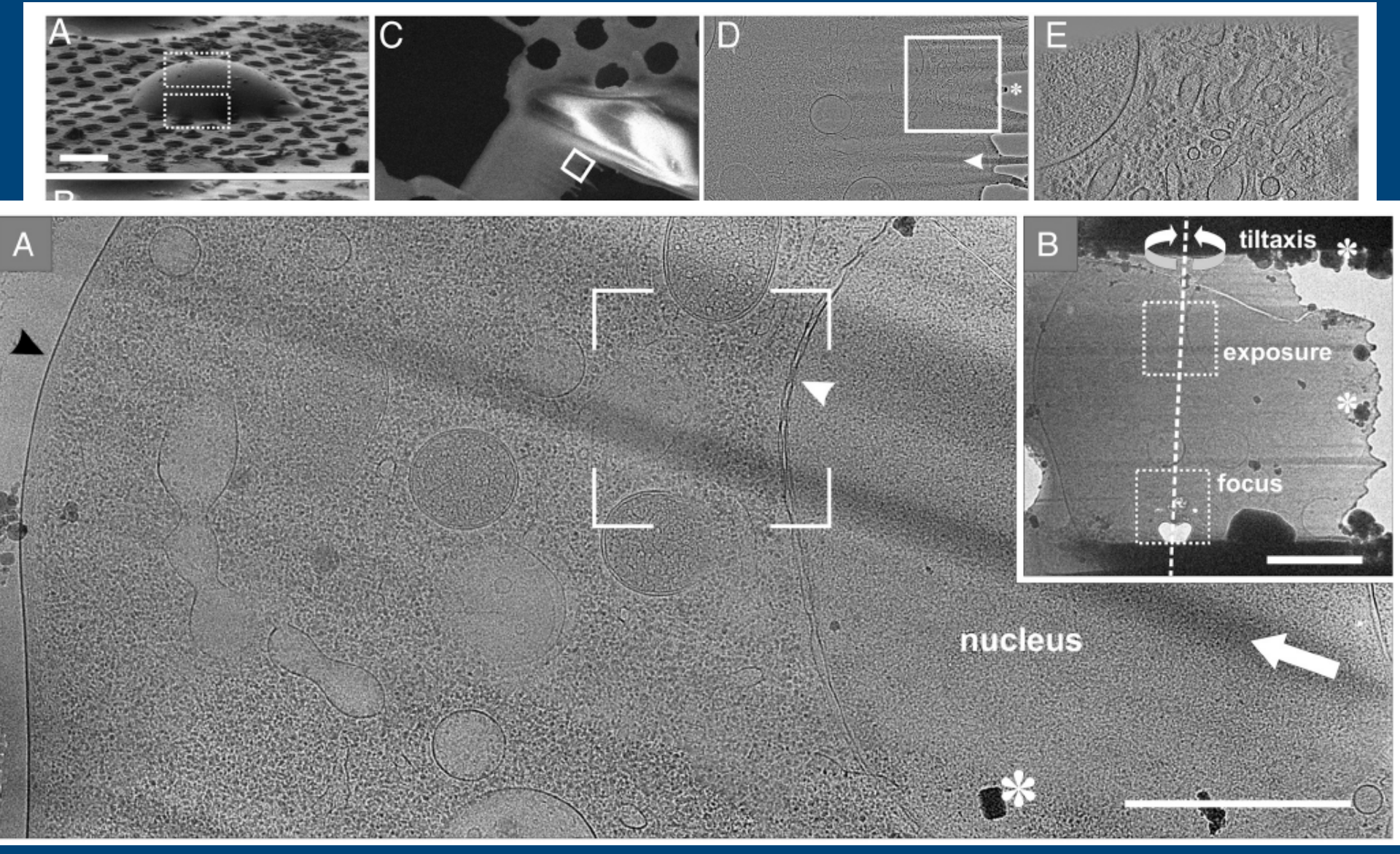

2. Data collection

- Automation
- Resolution/ number of tilts
- Dual Axis tilt series
- 1/cos tilt series
- Energy filtration

2. Data Collection: Computer control allows automation of EM operation and Image acquisition

Data collection

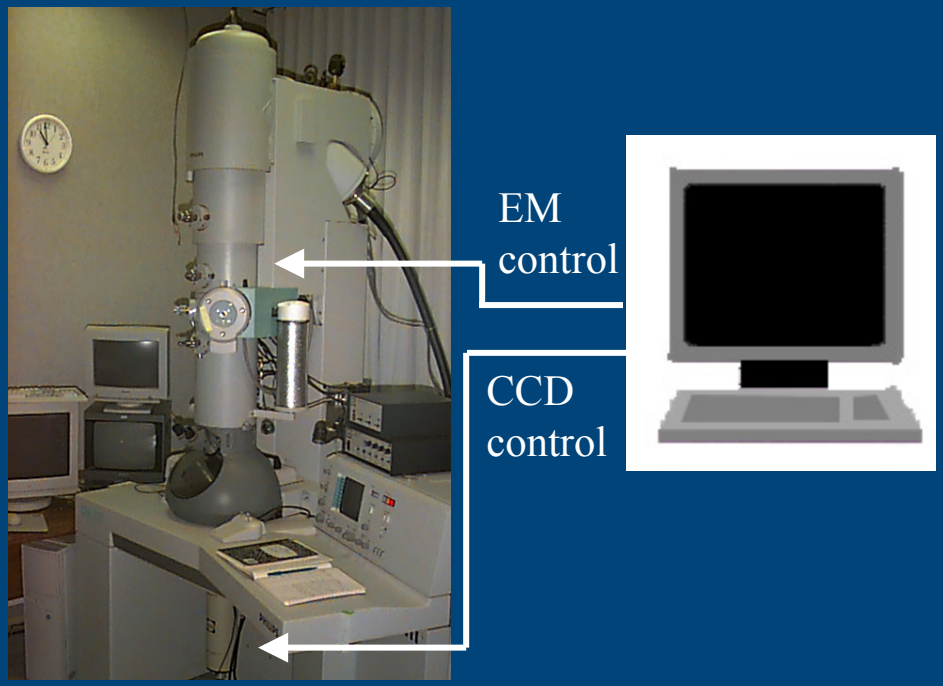

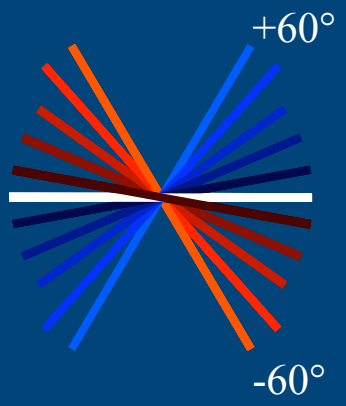

General scheme for automated tomographic data collection

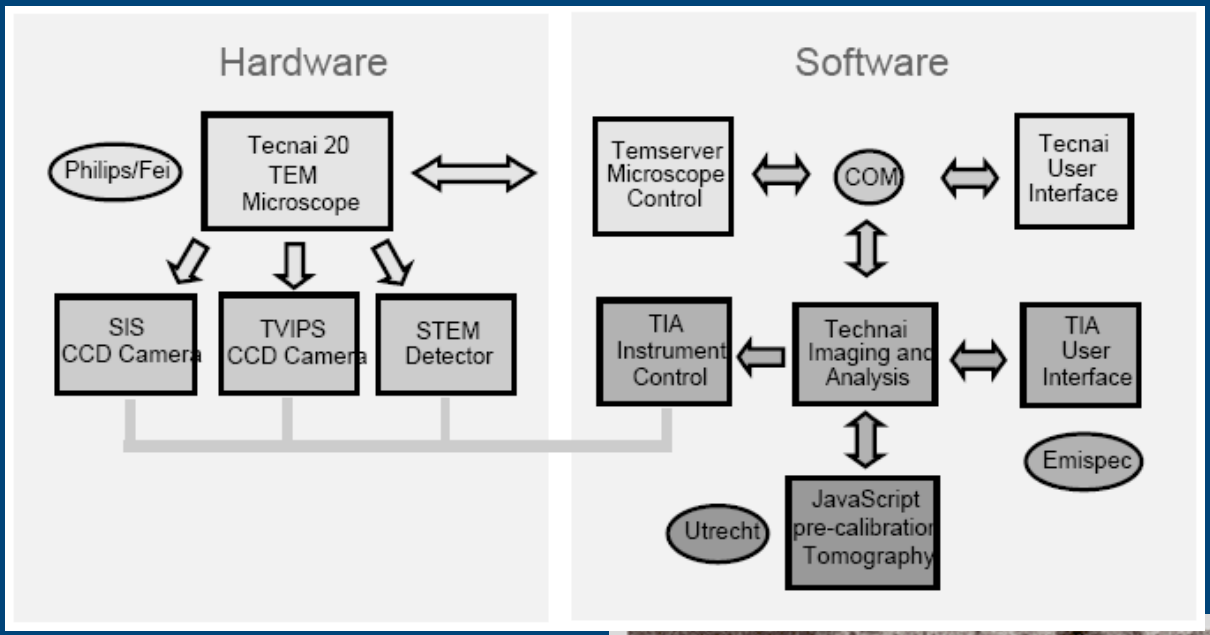

Tietz TVIPS website

Zeise et al (2002)
J Microsc 205:187

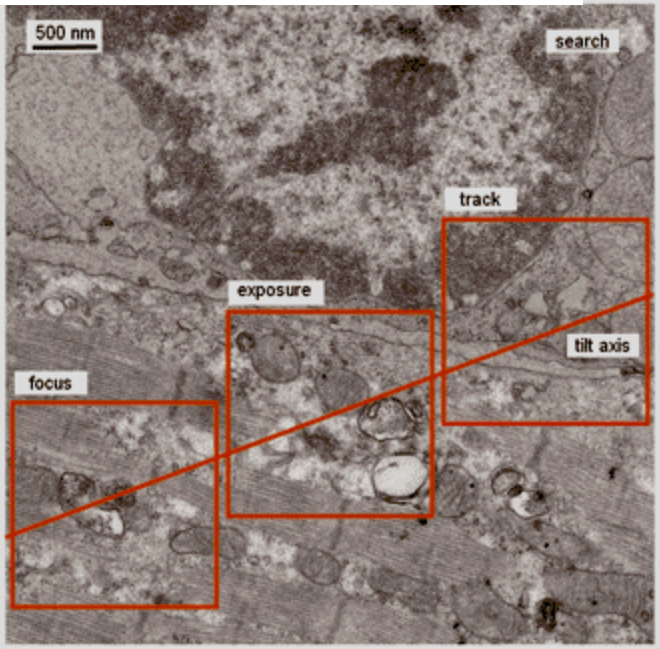

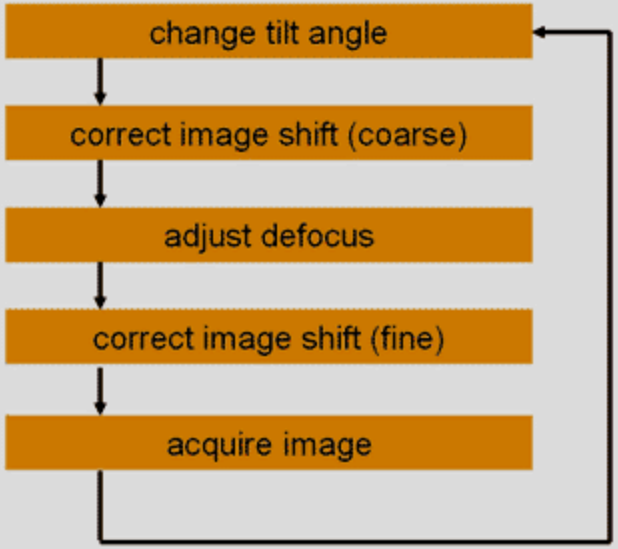

How many projections, N, do you need to achieve a specific "resolution" d?

Cylindrical geometry: $N = \pi D/d$

"Crowther criterion"

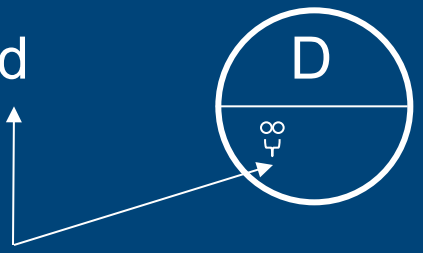

size of smallest feature
or detail of interest

Crowther, DeRosier and Klug (1970)
Proc Royal Soc London A 317: 319-340

How many projections, N, do you need to achieve a specific "resolution" d?

Cylindrical geometry: $N = \pi D/d$

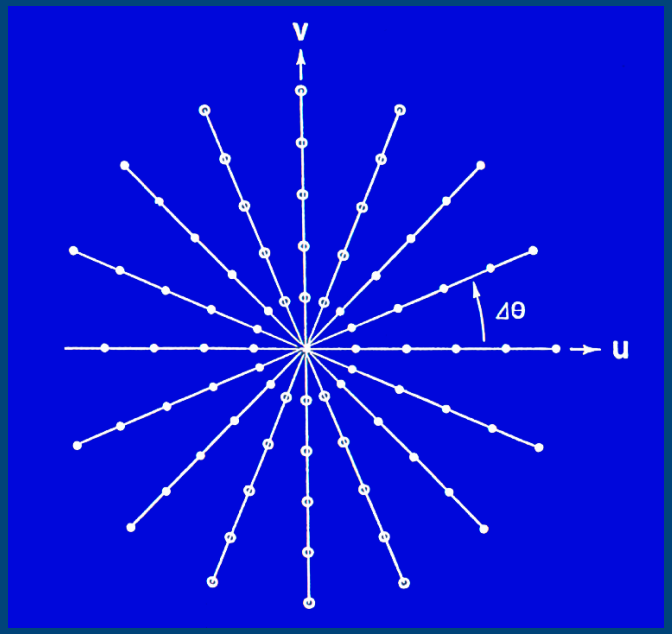

Assumes complete angular sampling

$\Delta\theta = 180^o/N = 180^o d/\pi D$

← Recall "central slice" theorem

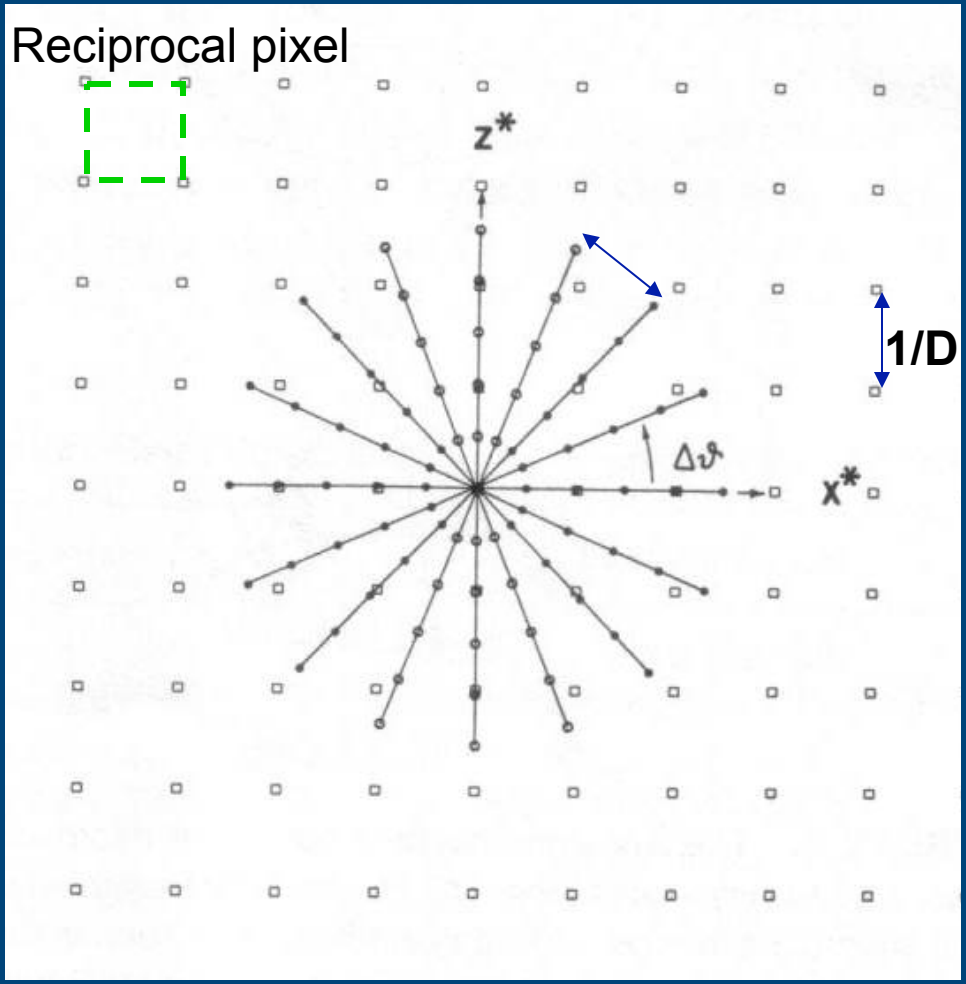

J. Frank (1992) Electron Tomography

Meaning of the criterion:

1/d = the spatial frequency at which each reciprocal pixel has at least one data point

Note: Fourier space at high spatial frequencies is increasingly sparsely populated

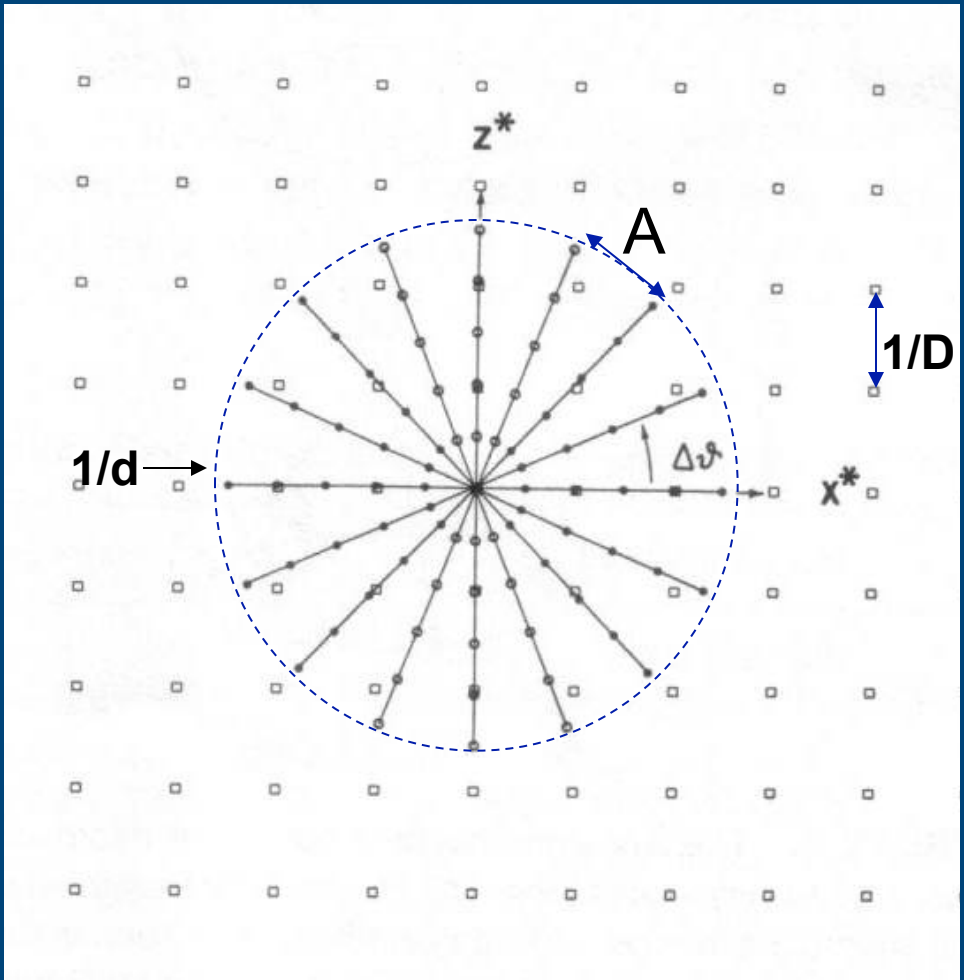

Meaning of the criterion:

1/d = the spatial frequency at which each reciprocal pixel has at least one data point

$C = \pi \text{ diam} = \pi \cdot 2(1/d)$
$C \sim 2N \cdot A = 2N\,(1/D)$

$2N/D = 2\pi/d$

$d = \pi D/N$

Electron Tomography

2. Data collection

Question: How many projections, N, do you need to achieve a specific “resolution” d?

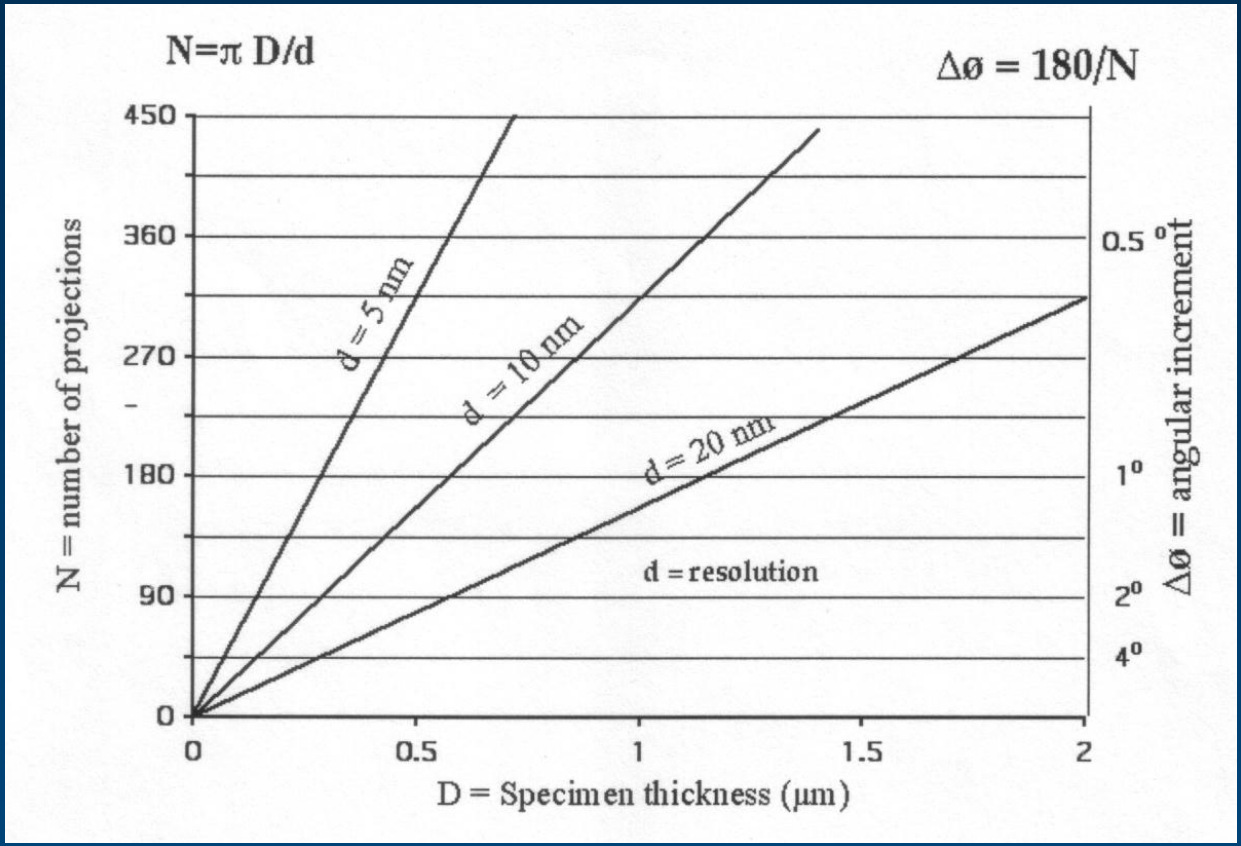

Electron Tomography

2. Data collection

Recall N = πD/d applies to complete, isotropic sampling of a cylindrical object

Is true cylindrical data collection possible?

1980s tomograms at 1 MeV:

Spore at end of milled glass capillary electrode

Membrane patch *inside* capillary

2010 tomograms:

Mill needle from plastic block and use special holder

TEM Sample lift out with Omniprobe after FIB

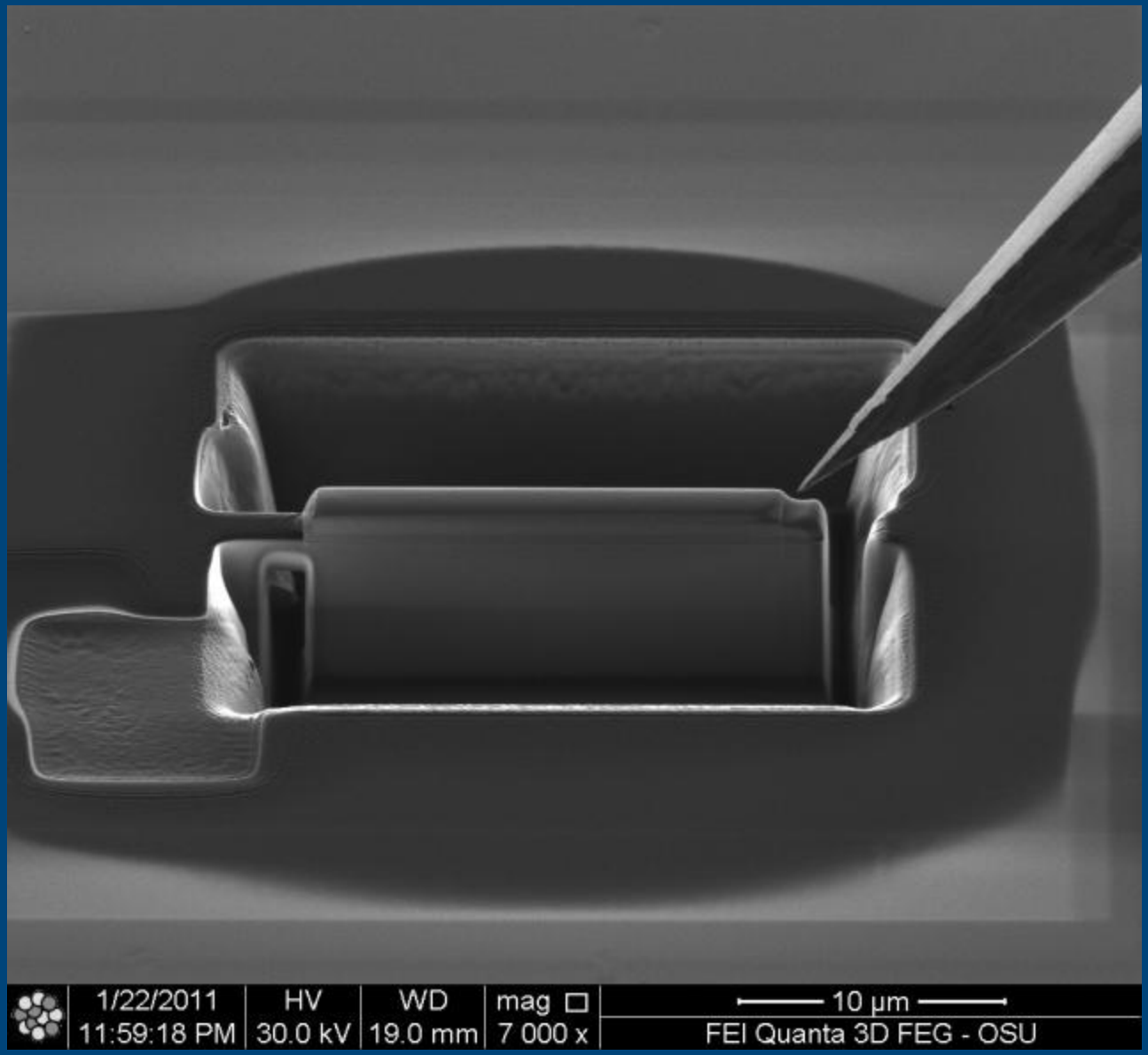

Electron Tomography

2. Data collection

More typical case: EM grid with slab geometry

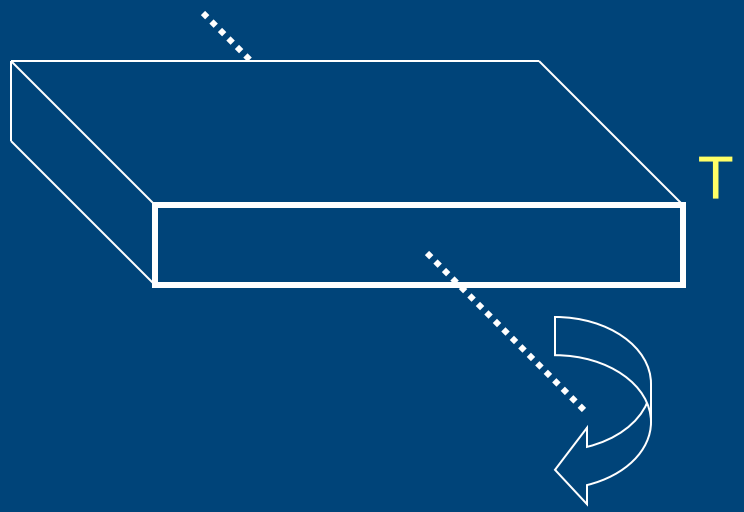

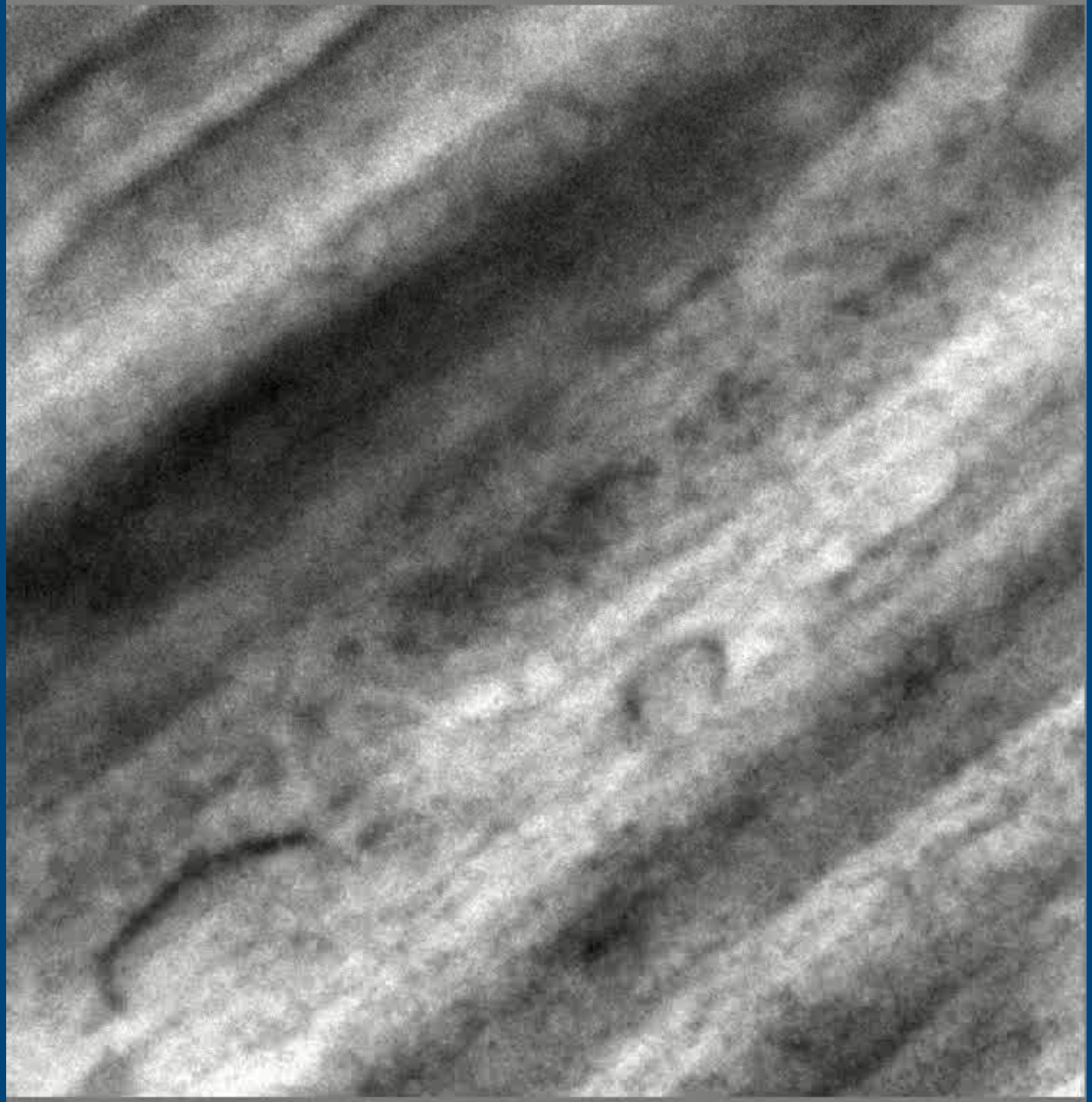

Limited tilting range → Anisotropic resolution

Tilted sample is thicker: t/cos(θ)

1/cos(60) = 2.0

1/cos(70) = 2.9

If y = tilt axis, max tilt angle = θ_{max}

$d_x = \pi D / N$ resolution in x direction

d_y = resolution of projections

$d_z \sim 2d_x$ for single tilt axis, $\theta_{max} = 60°$

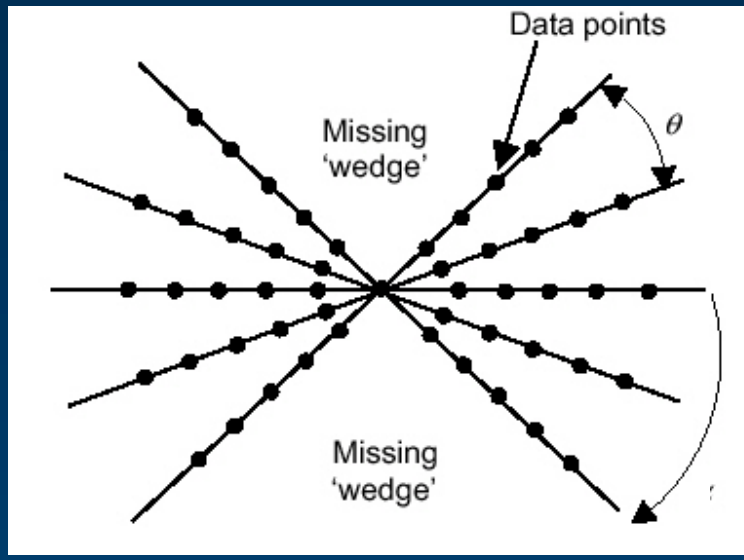

Midgley and Weyland (2003)
Ultramicroscopy 96:413

M. Radermacher in Electron Tomography (1992) J. Frank (ed.)

Quality of the Reconstruction

Missing Wedge: Directional resolution Loss

N too small: Artifacts obscure detail

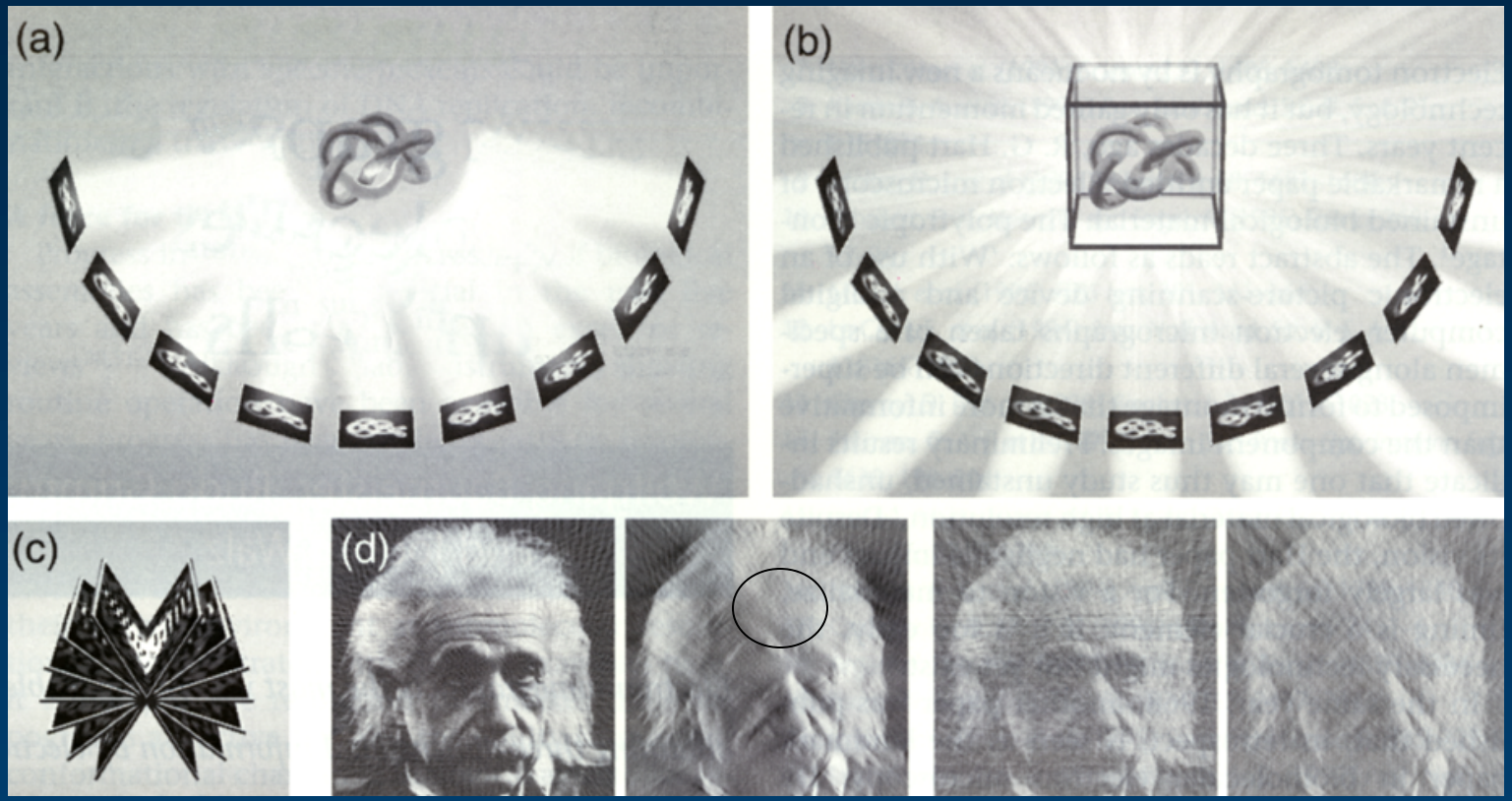

$\Delta\theta=2^o$ $\theta_{max}=90^o$ $\theta_{max}=60^o$

$\Delta\theta=5^o$ $\theta_{max}=90^o$ $\theta_{max}=60^o$

Baumeister et al. (1999) Trends Cell Biol. 9:81

Electron Tomography

2. Data collection

Single axis | Dual axis | Conical

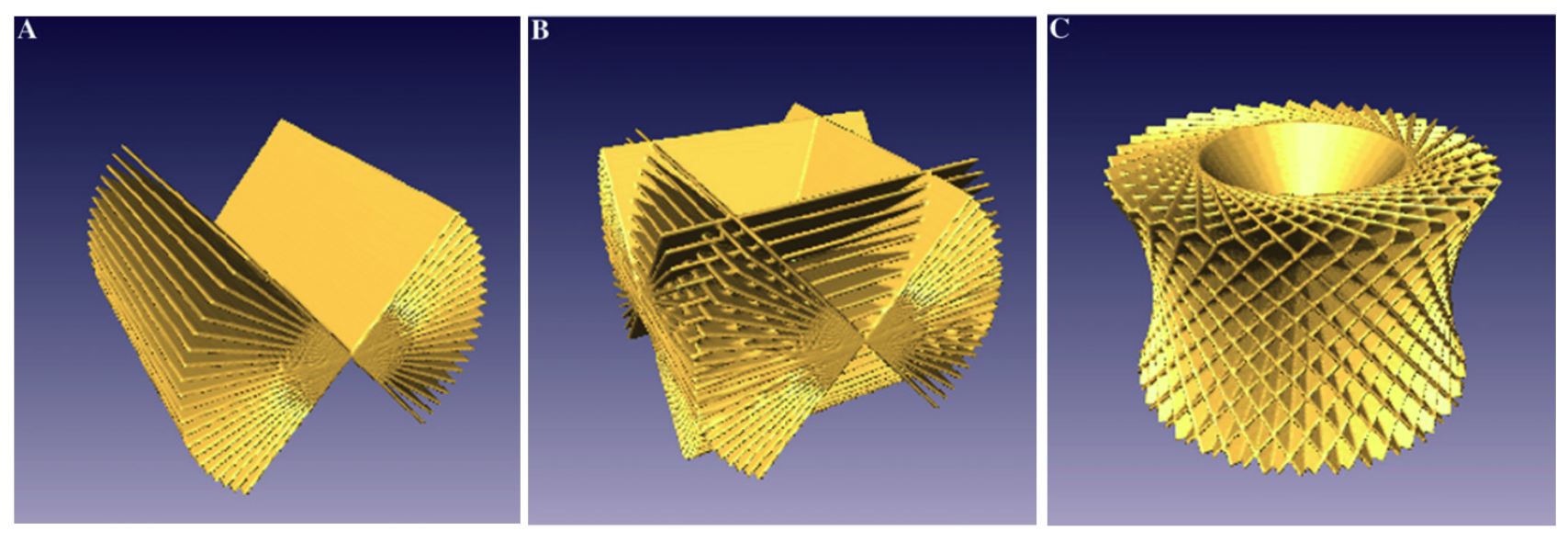

Missing wedge | Missing pyramid | Missing cone

S. Lanzavecchia

Electron Tomography

2. Data collection

Dual-axis tomography

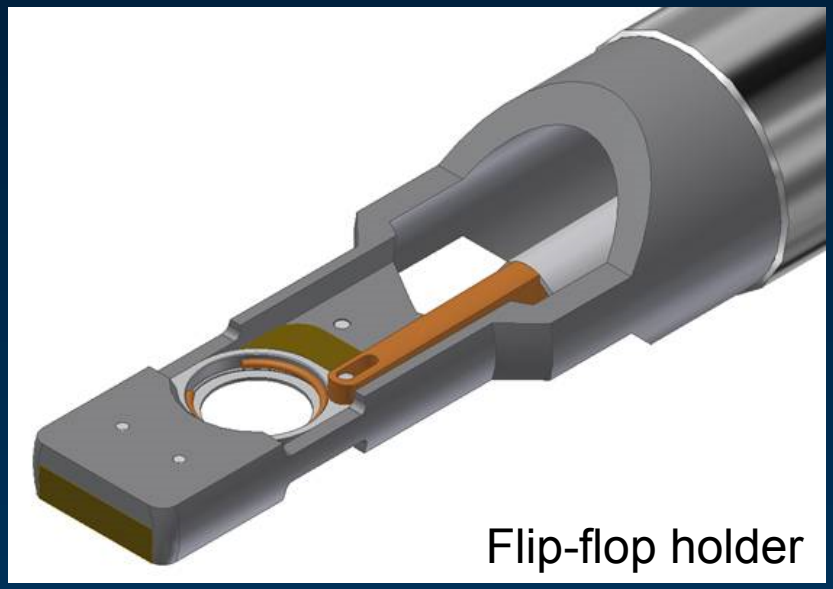

If y = tilt axis, max tilt angle = θ_{max}

$d_y = d_x = \pi D / N$ resolution in x direction

$d_z \sim 2d_x$ for single tilt axis, $\theta_{max} = 60°$

$\sim 1.5d_x$ for dual axis data " "

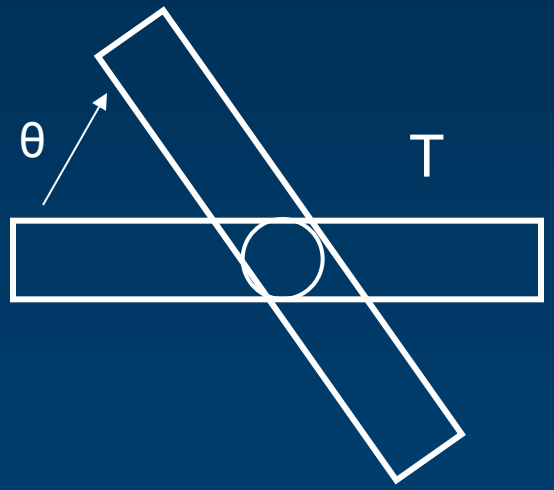

M. Radermacher in Electron Tomography (1992) J. Frank (ed.)

Dual axis tomogram

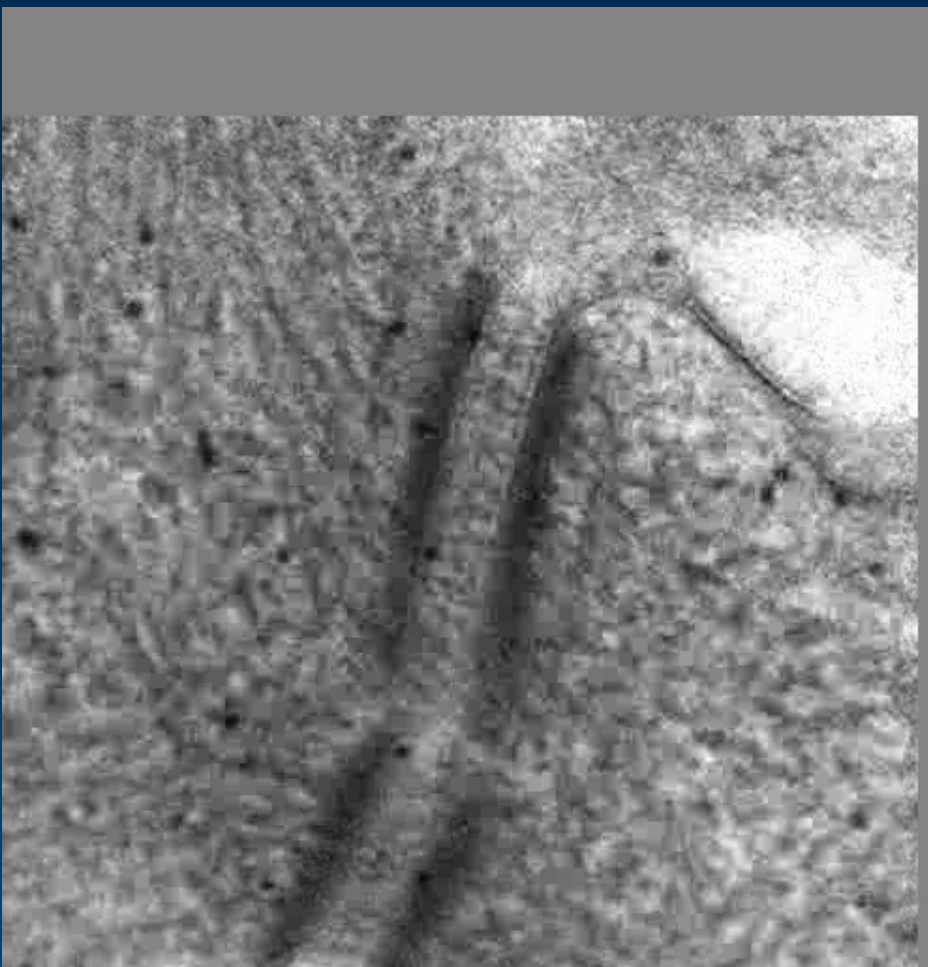

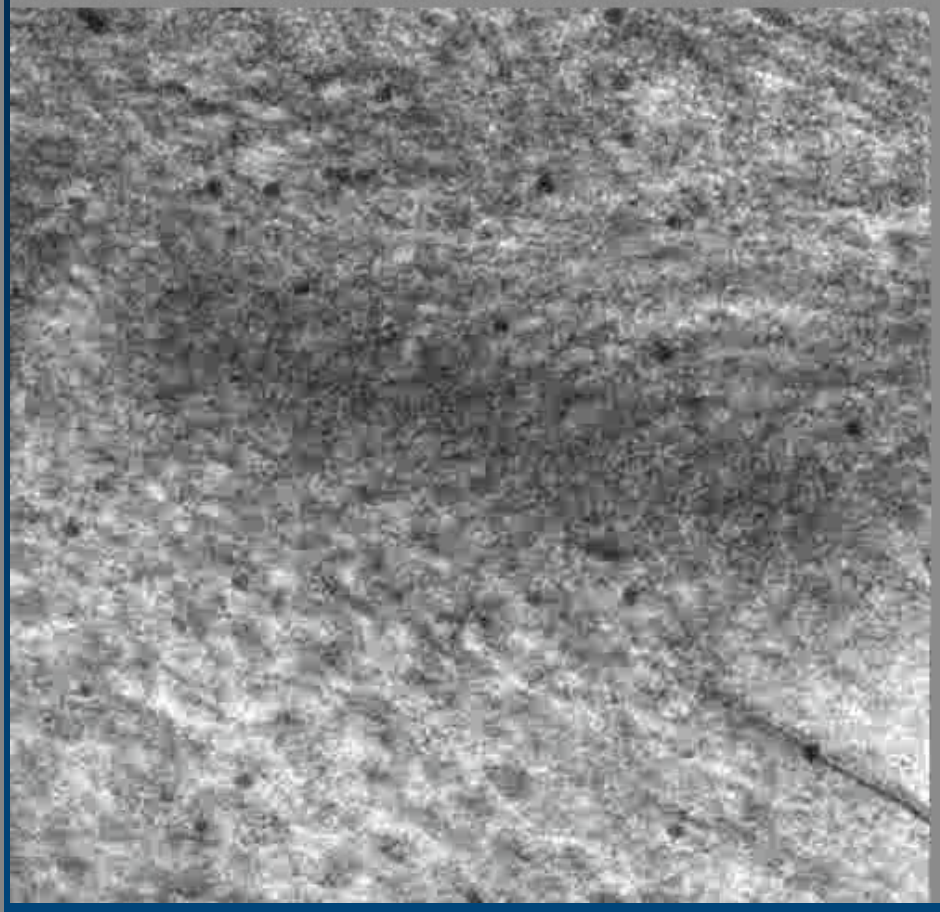

Mouse embryonic cardiac myocyte mitochondrion

G. Porter (URochester), D. Mankus (Wadsworth)

Single Axis ±45º

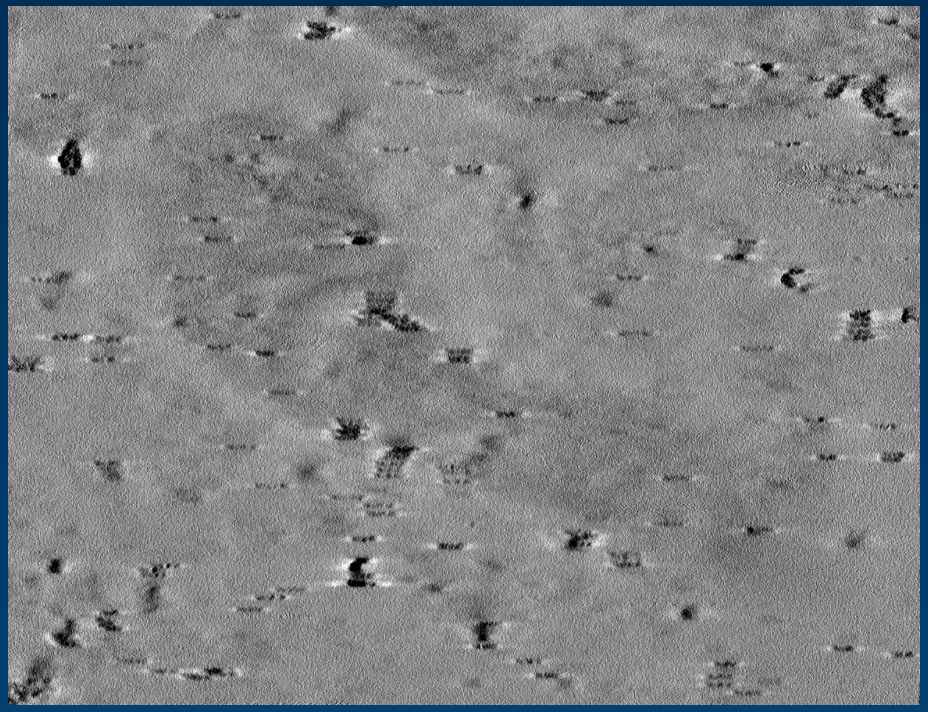

Dual Axis ±70º

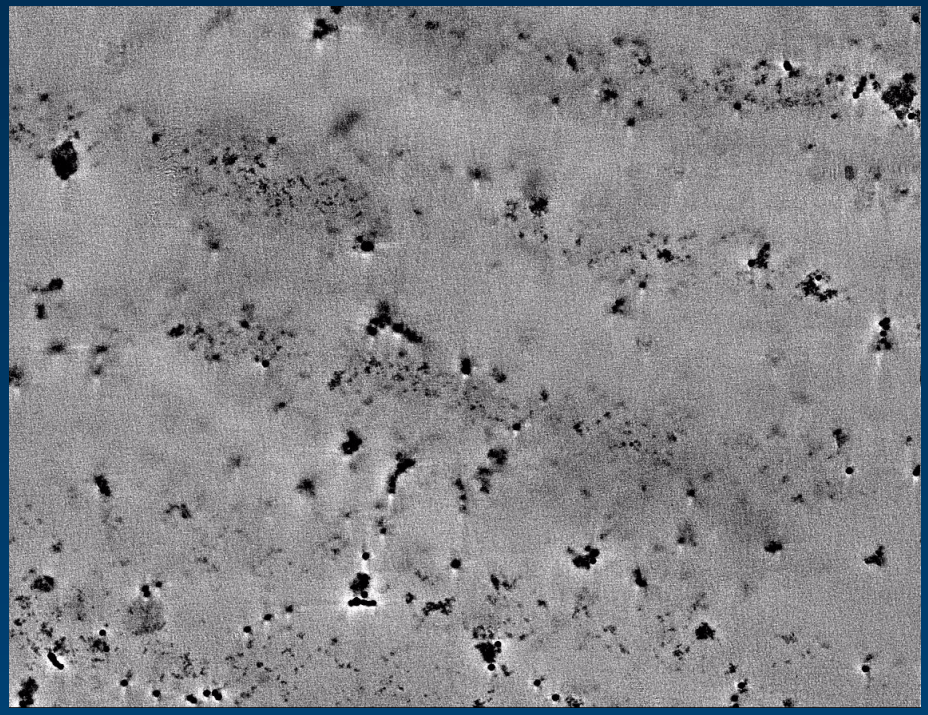

In principal, most efficient way to collect data for slab geometry is not even-angular spacing of projections but scheme that decreases spacing as tilt angle increases:

$$\Delta\theta(\theta) = (180^{o}d/\pi T)\cos\theta$$

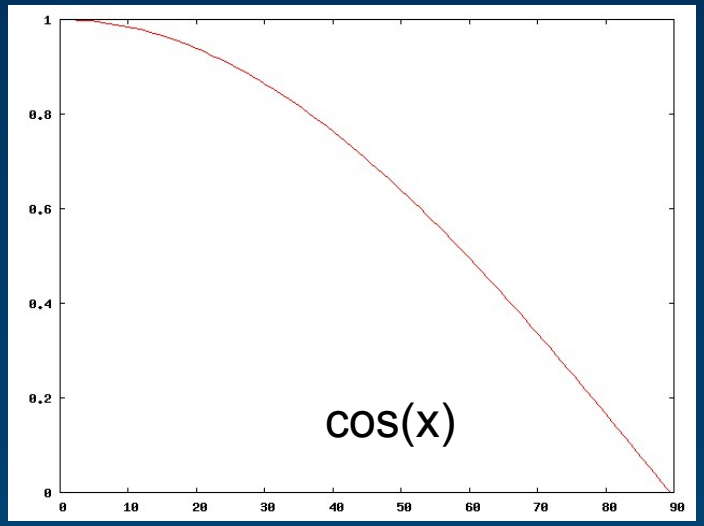

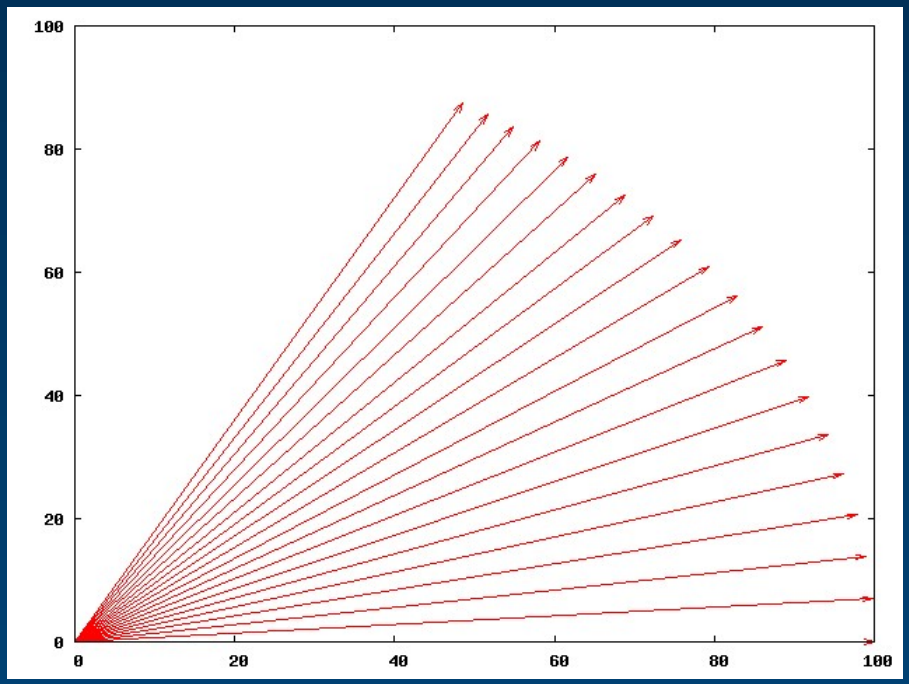

Saxton et al (1984) Ultramicroscopy 13, 57-70

Resolution limits

The above criteria set upper limits on attainable resolution, but there are many other factors that go into determining the quality of a 3D reconstruction.

e.g.

- specimen preservation
- specimen thickness
- radiation damage
- imaging conditions (pixel size, defocus)
- alignment of projections
- algorithm for reconstruction
- averaging

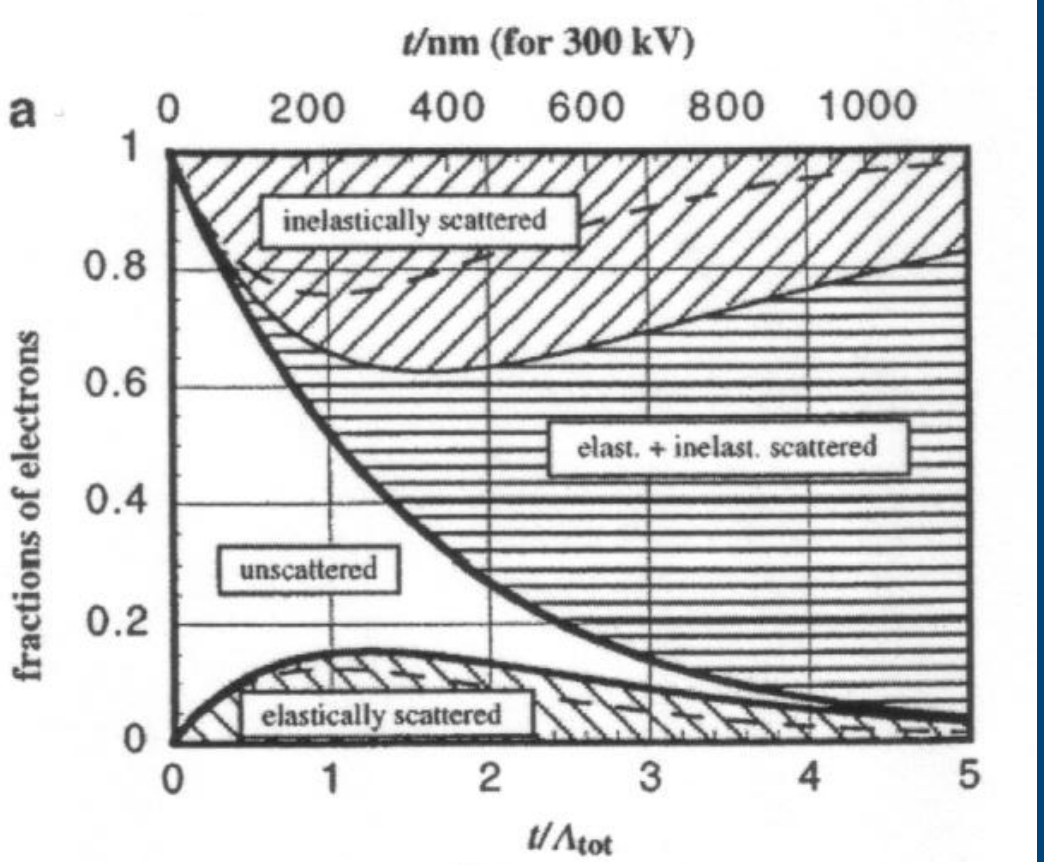

Distribution of scattered electrons for vitreous ice

Fig 4.1 from (Koster, Grimm et al. 1997)). When the electron beam penetrates the specimen, three types of scattering events can take place. When the specimen is thin enough, the majority of the electrons will transfer through the sample as if the sample was not present (*unscattered* electrons). A fraction of electrons that scatter within the specimen experience energy loss (*inelastic scattering*). Another fraction of electrons that scatter will do so with negligible energy loss (*elastically scattered* electrons). (a) Distribution (without an aperture) over the elastic (lower diagonally hatched area), inelastic (upper diagonally hatched area), and mixed (horizontally hatched area) scattering channels for vitreous ice as a function of thickness (in multiples of the total mean free path Λ_{tot} and, for 300 kV, in nm). The dashed lines mark fractions of single (elastic or inelastic) scattering. (b)

Electron energy loss

directly measure energy loss of inelastically scattered electrons

Can either record spectrum or image from selected energy range (e.g. zero loss)

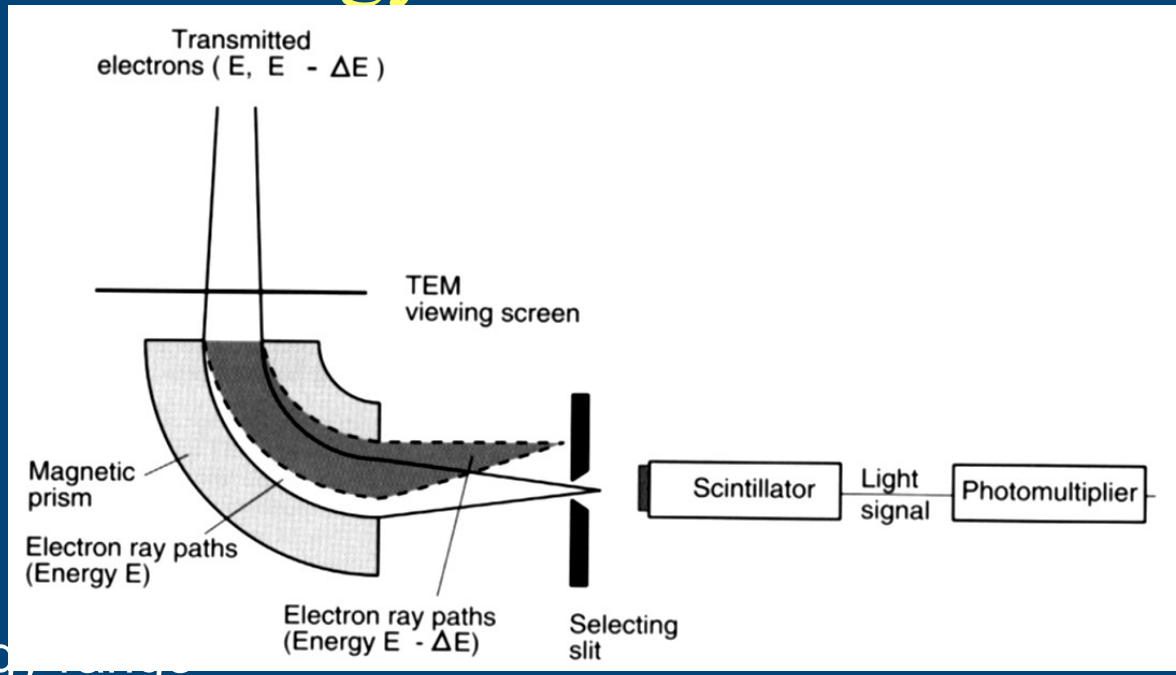

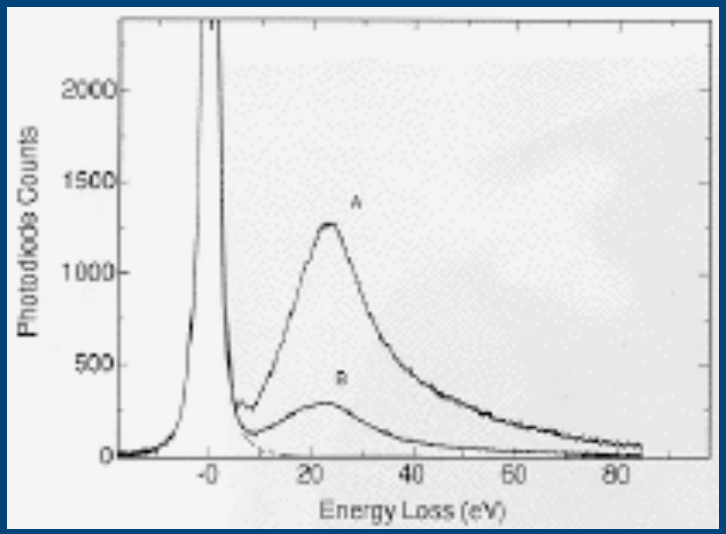

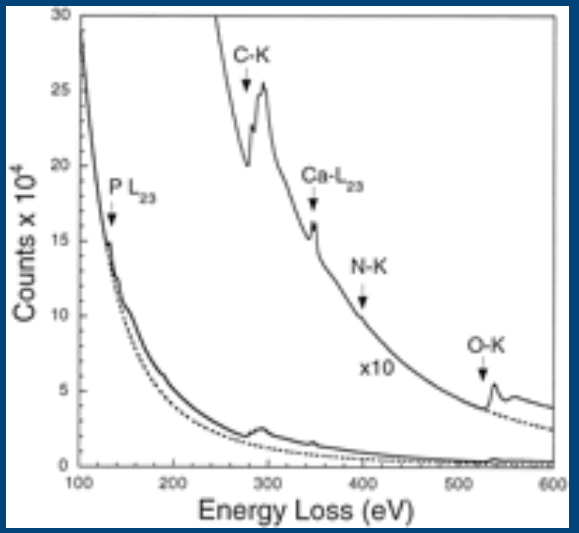

But they can be filtered out (after they damaged the specimen)

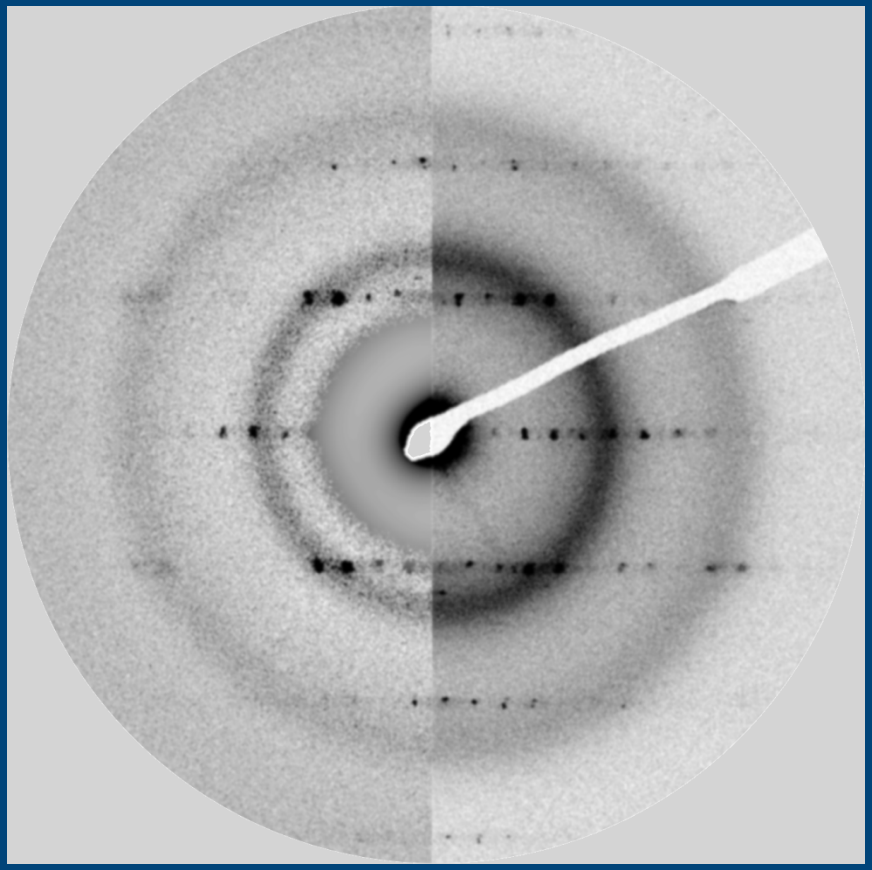

-filter +filter

Energy filters

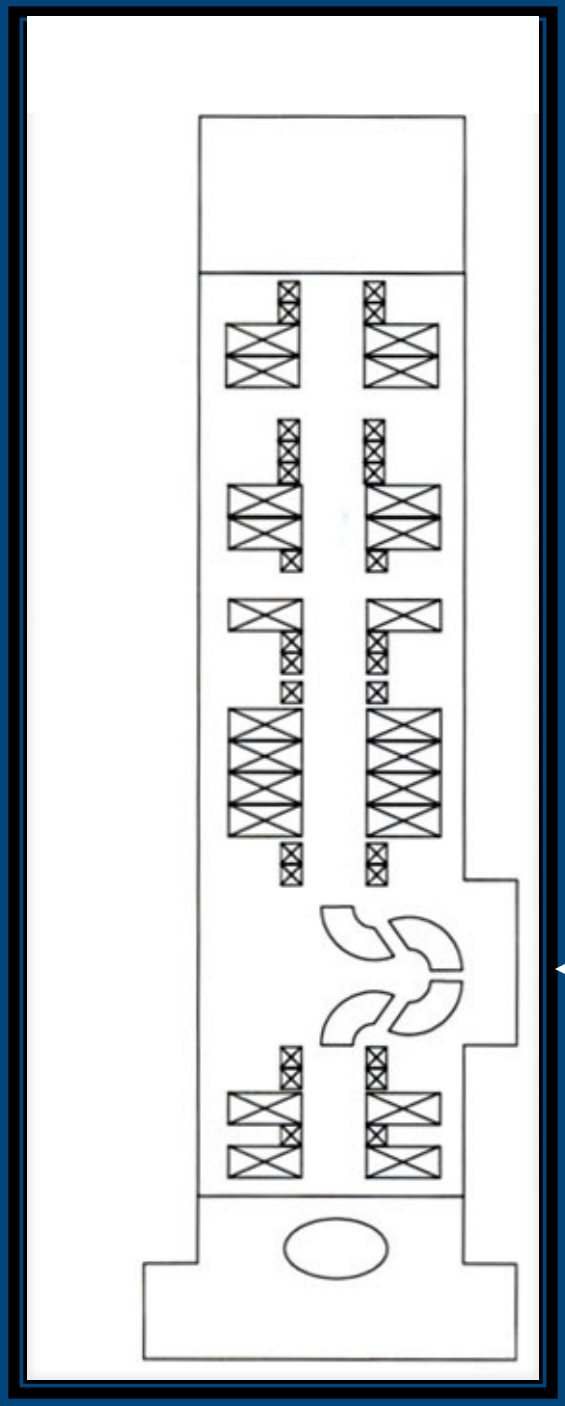

in-column

post-column

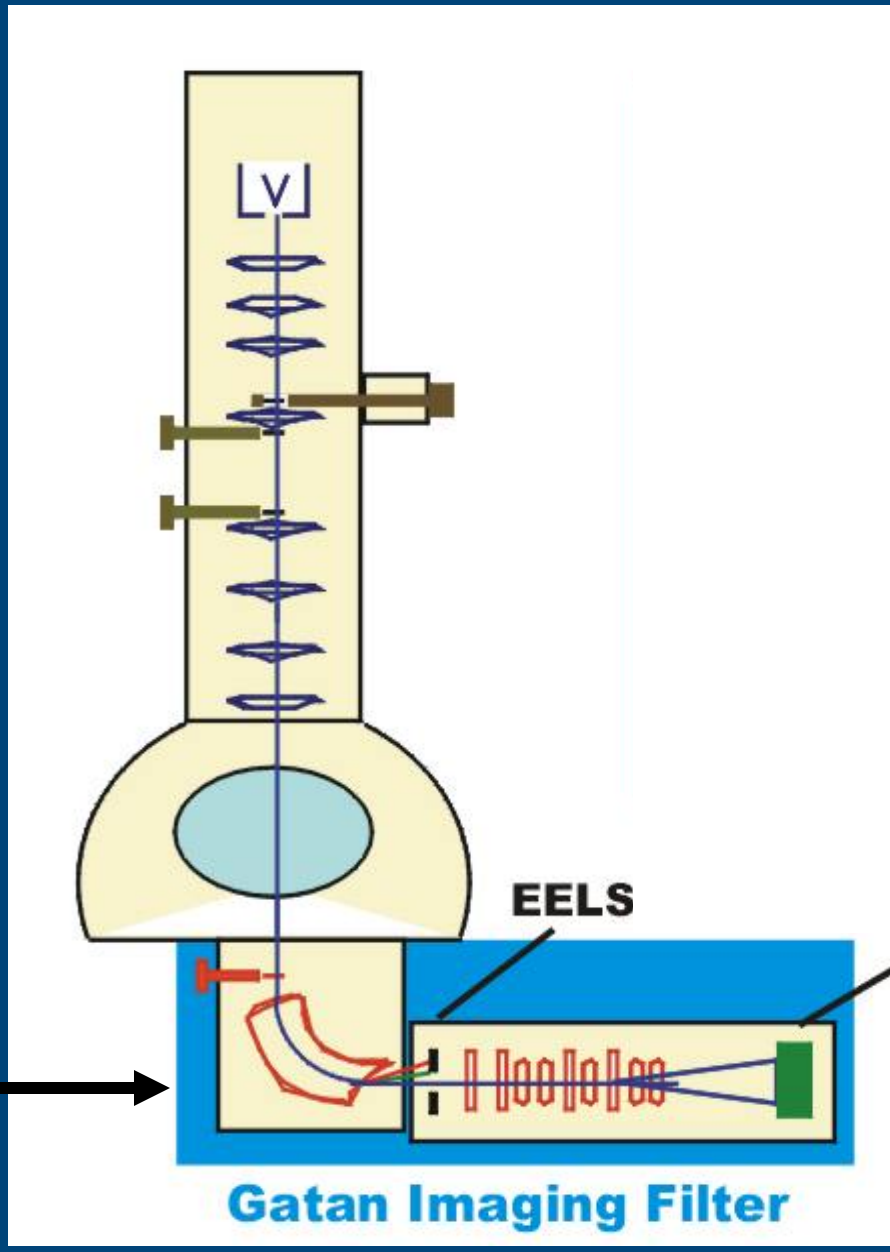

3. Computation

Alignment of projections

- Least-squares method using fiducial markers
- Markerless alignment, e.g. correlation methods

Computation

Projection alignment

- Least-squares method using fiducial markers

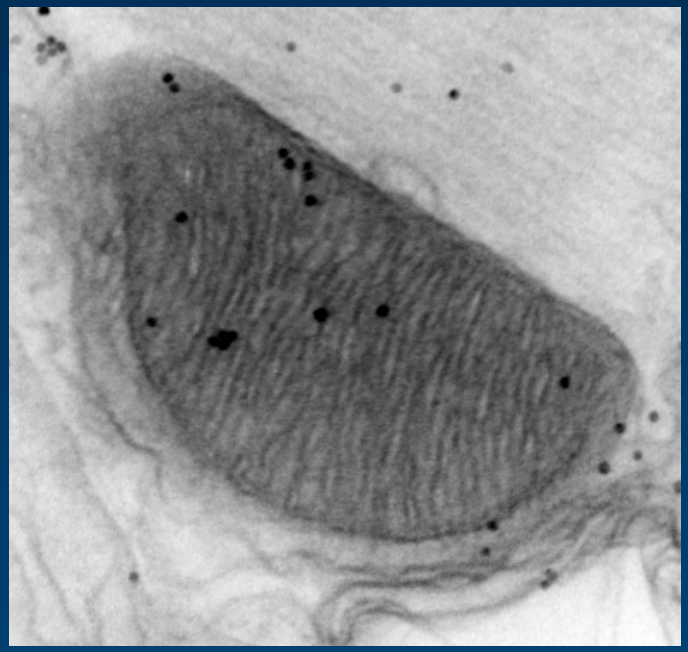

Canary Cardiac Muscle Mitochondria

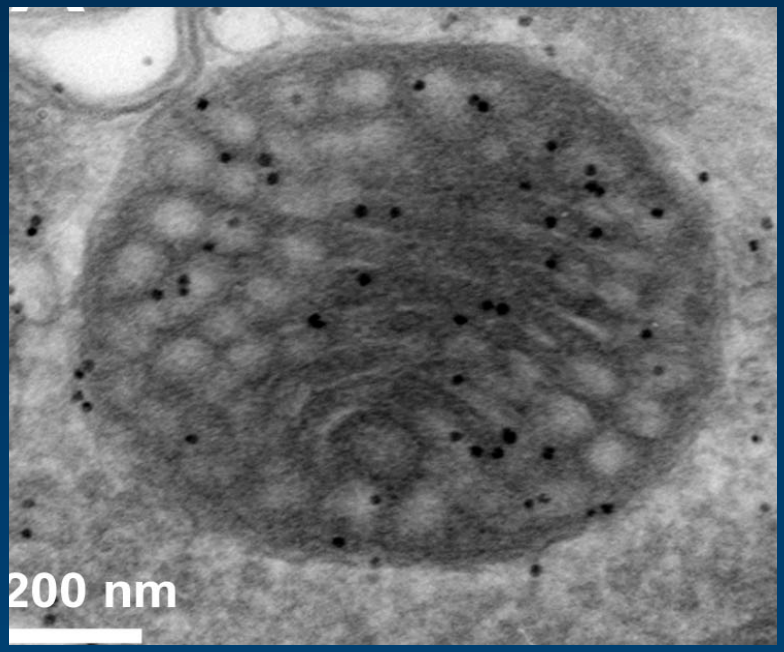

Drosophila Neural Mitochondria (atp6.1)

Computation

Projection alignment

- Least-squares method using fiducial markers

Particle selection rules:

- The more markers the better
- Distribute evenly in field
- Not too close together
- No overlap during tilt series

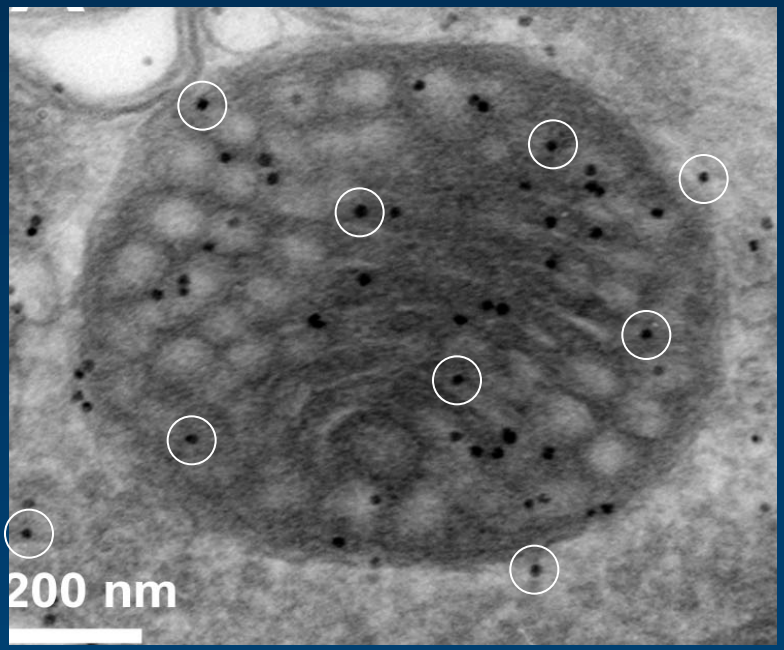

Avoid overlapping fiducial markers

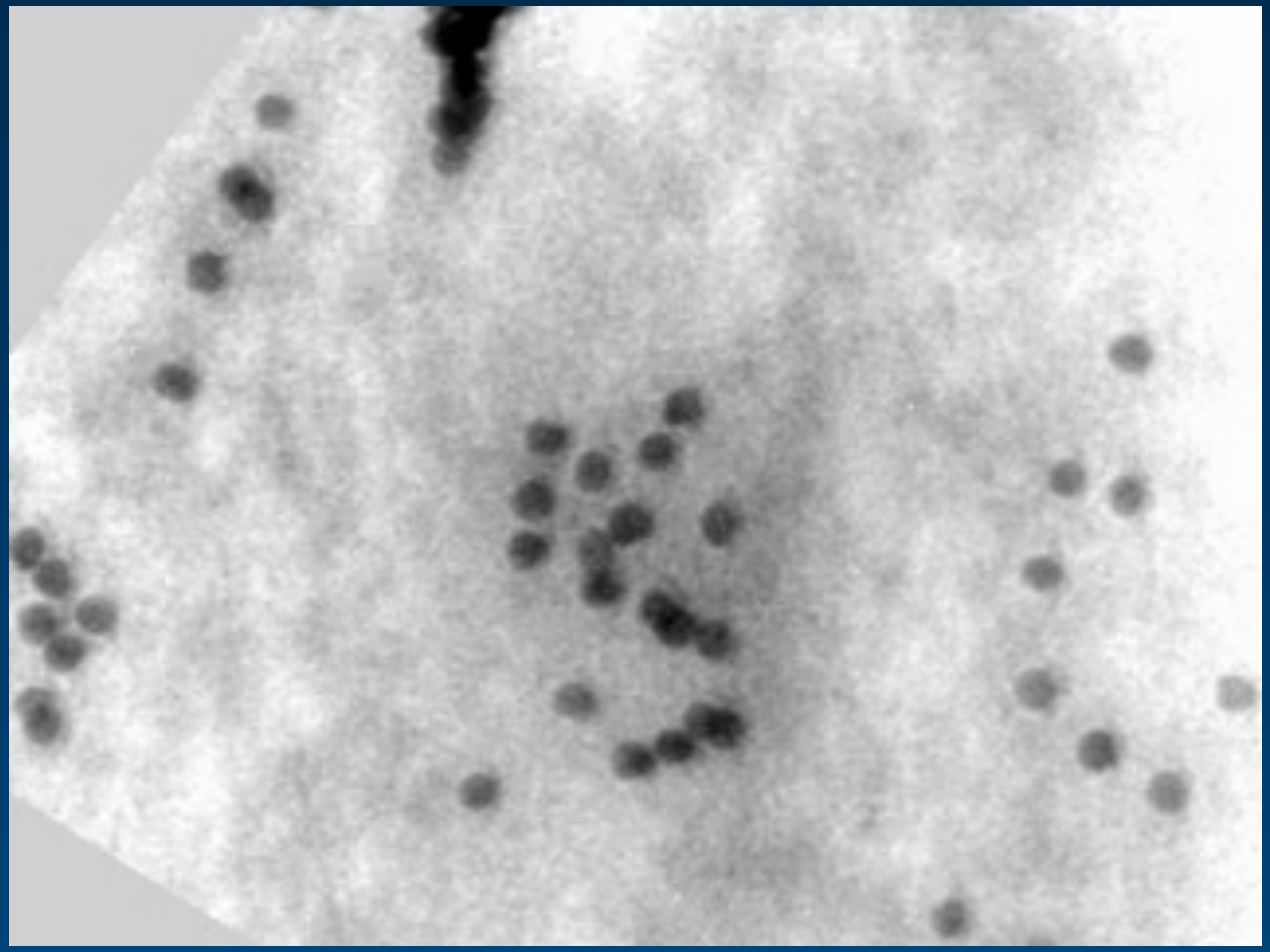

Least Squares Method (Markers)

For images i = 1,….,v
and markers j = 1,….,s

$p_j^i = S^i P A^i M^i y_j + d^i$

Where: p_j^i = marker coordinates in the images
S^i = 2 X 2 rotation matrices about α (in plane rotation)
P = 2 X 3 projection matrix (down the z-axis)
A^i = 3 X 3 rotation matrices – tilt angle
M^i = 3 X 3 matrices – scale change
y_j = 3D marker coordinates in the specimen frame
d^i = translation of specimen and image origins rel. to EM x,y axes

Algorithm iteratively minimizes the error between calculated and observed values of p_j^i .

Lawrence (1992) in Electron Tomography

Fiducial Alignment

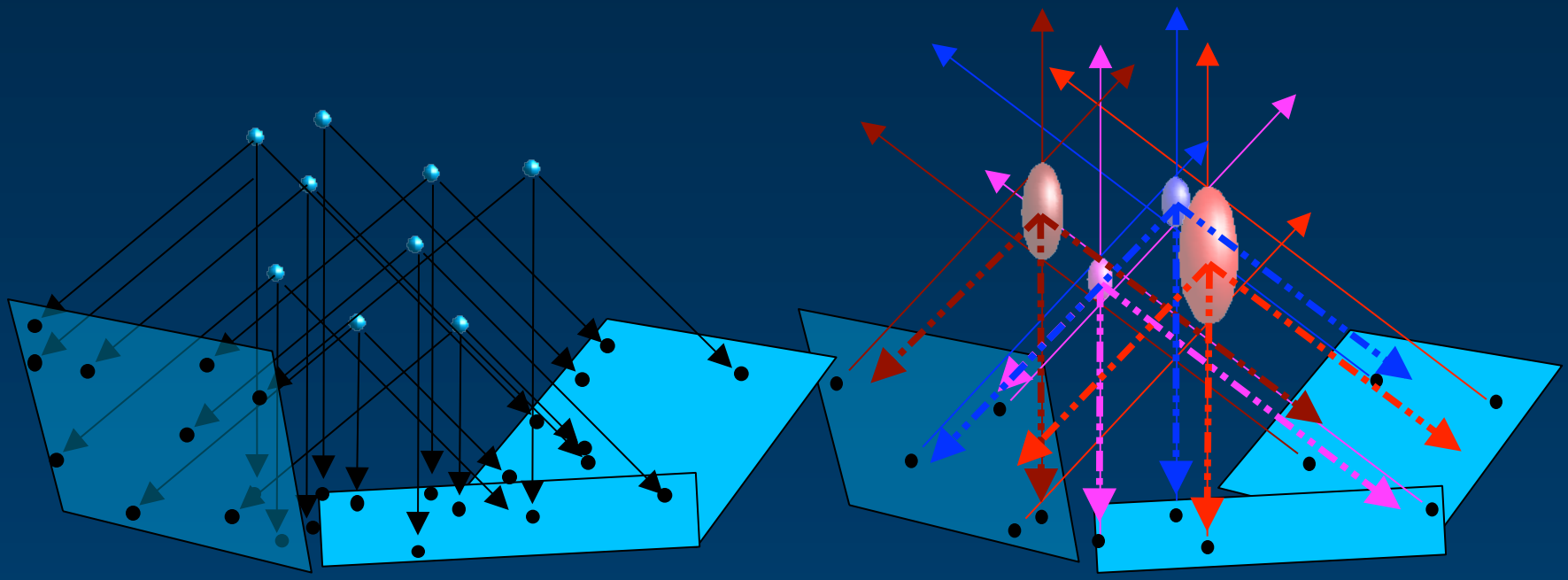

Aligned Images

Un-Aligned Images

Marker alignment of dual-axis tilt series

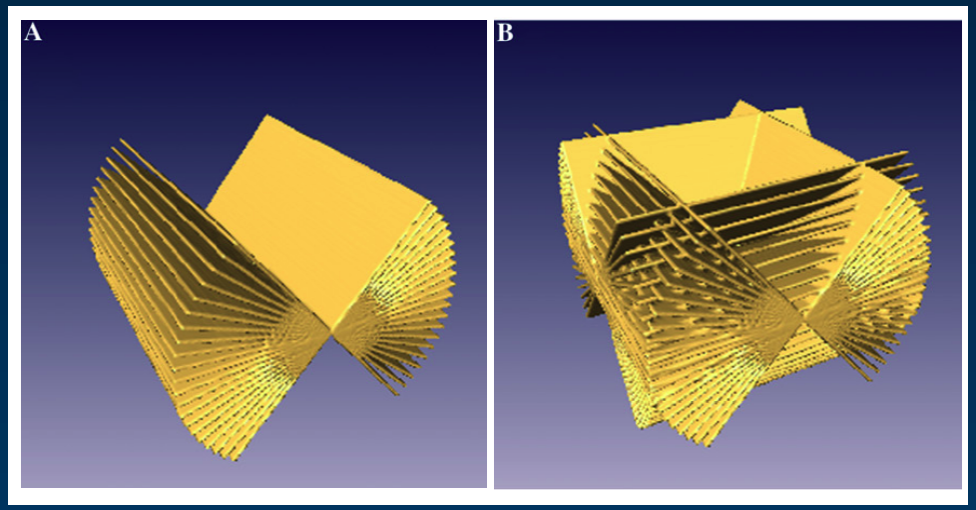

Reduces the missing angular information from a wedge to a pyramid.

- SPIDER: Co-align all projections then reconstruct in one step.
  - Penczek et al. (1995) Ultramicroscopy 60:393
- IMOD: Merge two single-axis reconstructions. Warp second reconstruction to the first.
  - Mastronarde (1997) J. Struct. Biol. 120:343

Computation

Projection alignment

- Markerless Methods:

Computation

Projection alignment

- Markerless Methods - Rationale
  - **Colloidal gold not easily deposited on some samples**
  - **Markers not always where you want them**
    >10 particles evenly distributed around feature of interest
  - **You are aligning the particles not the specimen**
    Distance of particles from center of section reduces accuracy of alignment
    Some sections may move relative to the gold (on carbon film)
  - **Dense particles send streaks (artifacts) into the reconstruction**

Electron Tomography

3. Computation

Projection alignment

- Markerless Methods:

- Cross-correlation methods
  Frank & McEwen in *Electron Tomography* (1992)

Align successive images in tilt series to each other based on overall similarity of the images

Definition of the cross-correlation function (CCF)

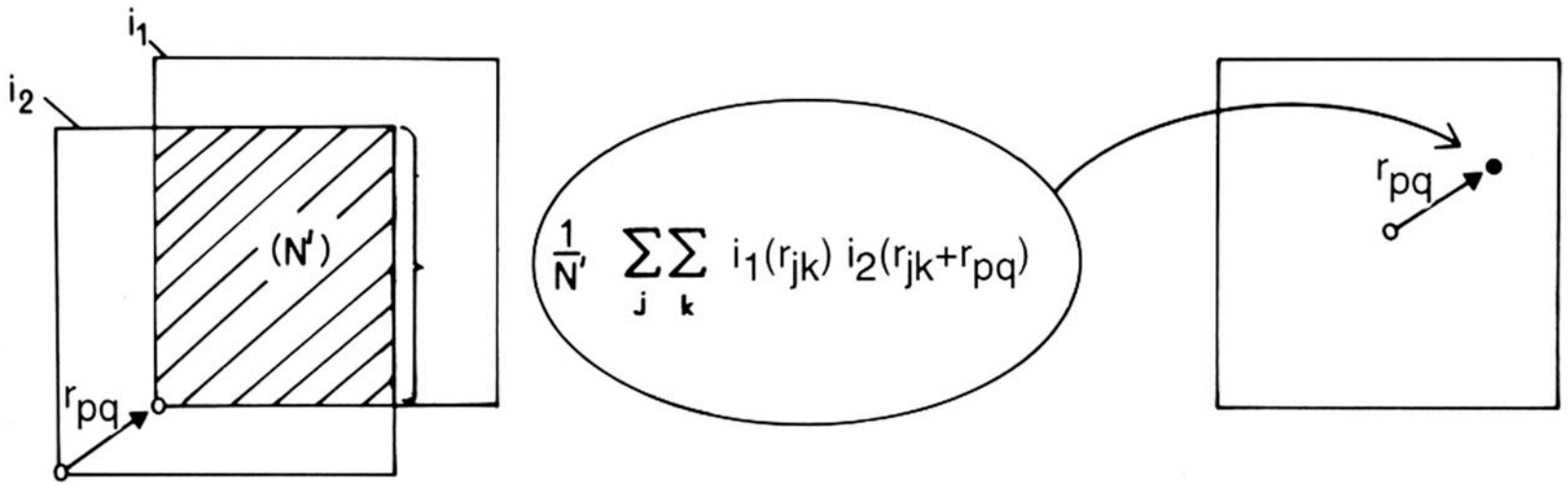

Fig. 3.8. Definition of the cross-correlation function. Image 1 is shifted with respect to image 2 by vector $\mathbf{r}_{pq}$. In this shifted position, the scalar product of the two images arrays is formed and put into the CCF matrix at position (p, q). The vector $\mathbf{r}_{pq}$ is now allowed to assume all positions on the sampling grid. In the end, the CCF matrix has an entry in each position. From Frank (1980). Reproduced with permission of Springer-Verlag, New York.

Think of two transparencies placed on top of a lightbox, containing identical images. The total light transmitted (= the integral of the scalar product) will be maximal when the images on the transparencies are brought in exact overlap.

Cross-correlation

$$f_1 \otimes f_2 = \int_{-\infty}^{\infty} f_1(x+t) f_2{}^*(t) dt = c(x)$$

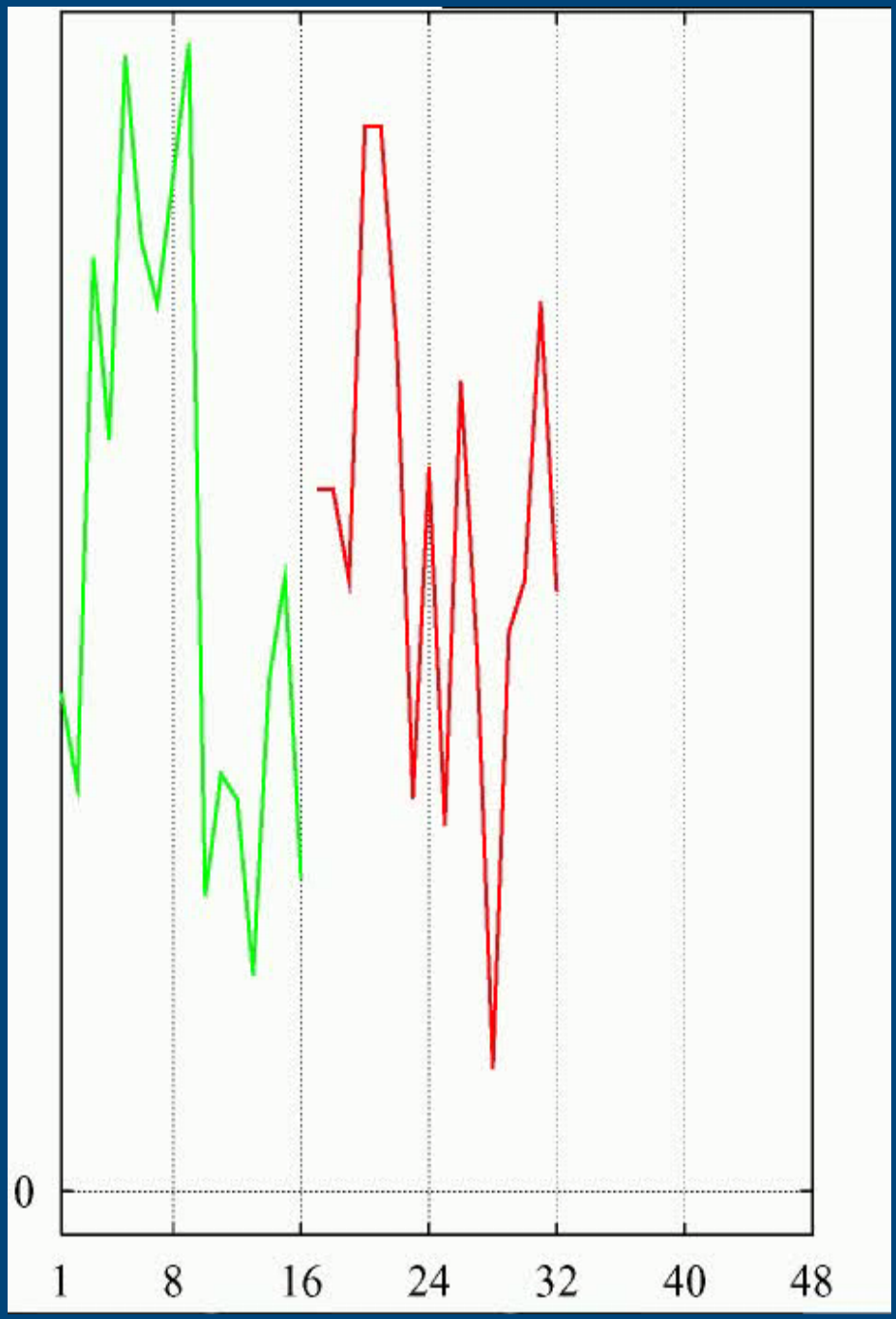

Computation

Projection alignment

- Markerless Methods:

- Cross-correlation methods
  Frank & McEwen in *Electron Tomography* (1992)

Align successive images in tilt series to each other based on overall similarity of the images

PROBLEM: The images are not identical but vary increasingly as tilt angle increases, worse for thicker specimens! Due both to change in angular view and inclusion of new neighboring densities outside untilted field

Problems with markerless alignment

- Works best with strong discrete features in the object
- Without them, alignment in x, ⊥ tilt axis (y), is poorly defined and so it drifts

Original

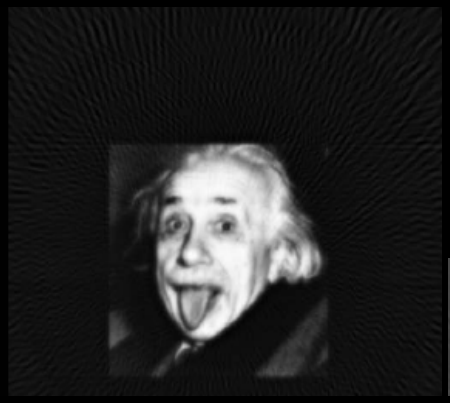

Reconst w/o re-alignment

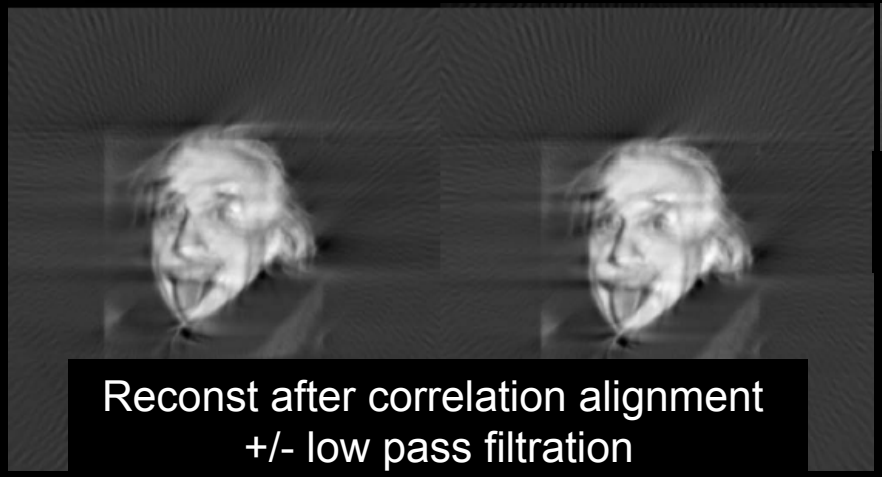

Reconst after correlation alignment
+/- low pass filtration

Reconst after deliberate mis-alignment and correlation alignment, +/- low pass filtration

Jaime_t_cell_avi

Markerless Alignment Scheme
Area Matching

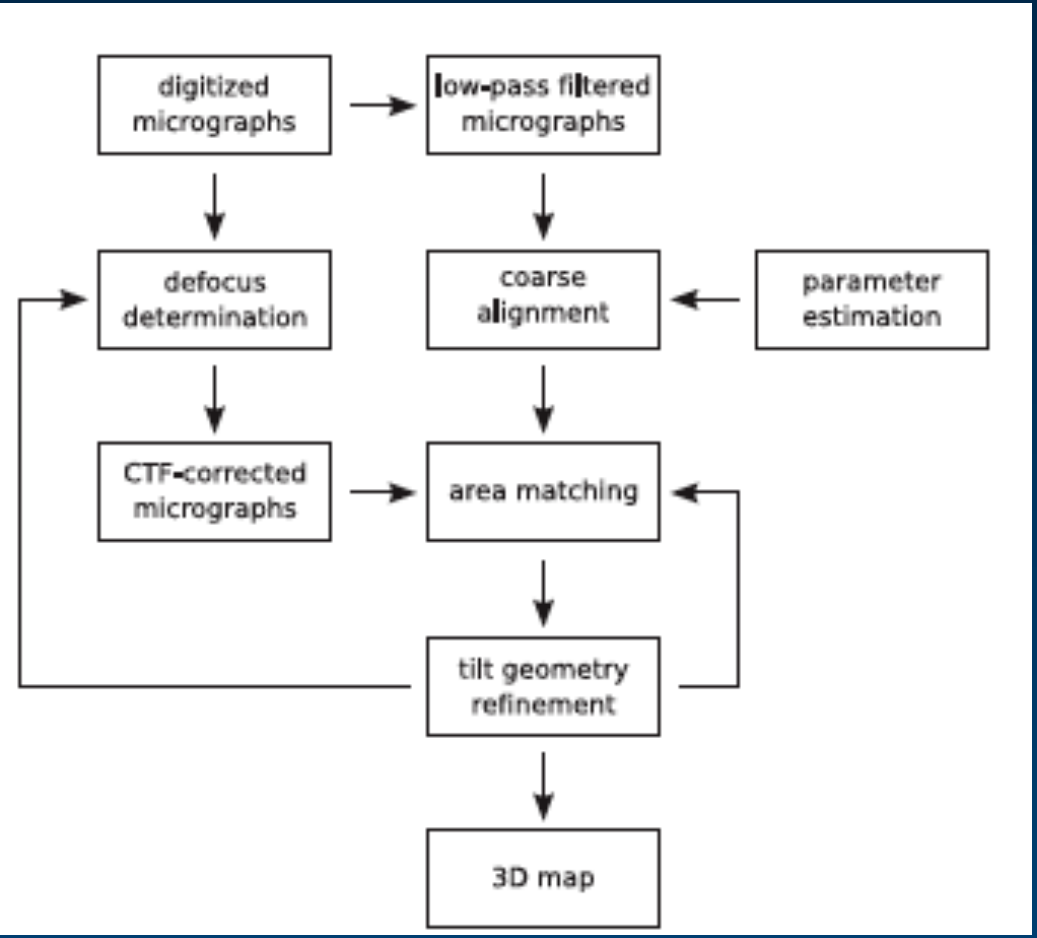

Winkler & Taylor (2006) Ultramicroscopy 106:240

Computation

Reconstruction methods

- Modified (r* weighted) back-projection
- Fourier synthesis
- Simultaneous Iterative Reconstruction Technique (SIRT)
- Algebraic Reconstruction Technique (ART)

Computation

Reconstruction methods

- Modified (r* weighted) back-projection 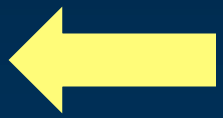
- Fourier synthesis
- Simultaneous Iterative Reconstruction Technique (SIRT)
- Algebraic Reconstruction Technique (ART)

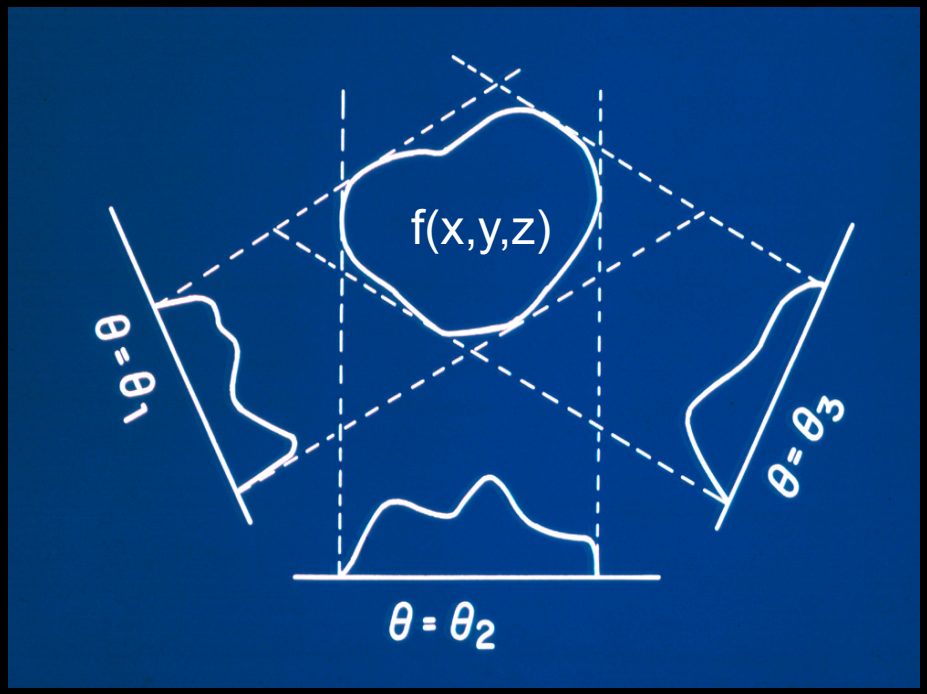

Consider each j (1,2,3..) projection as corresponding to its own coordinate system (z direction defined by the tilt angle)

$$p_j\,(x^j,\, y^j) = \int f(x^j,\, y^j,\, z^j\,)\, dz^j$$

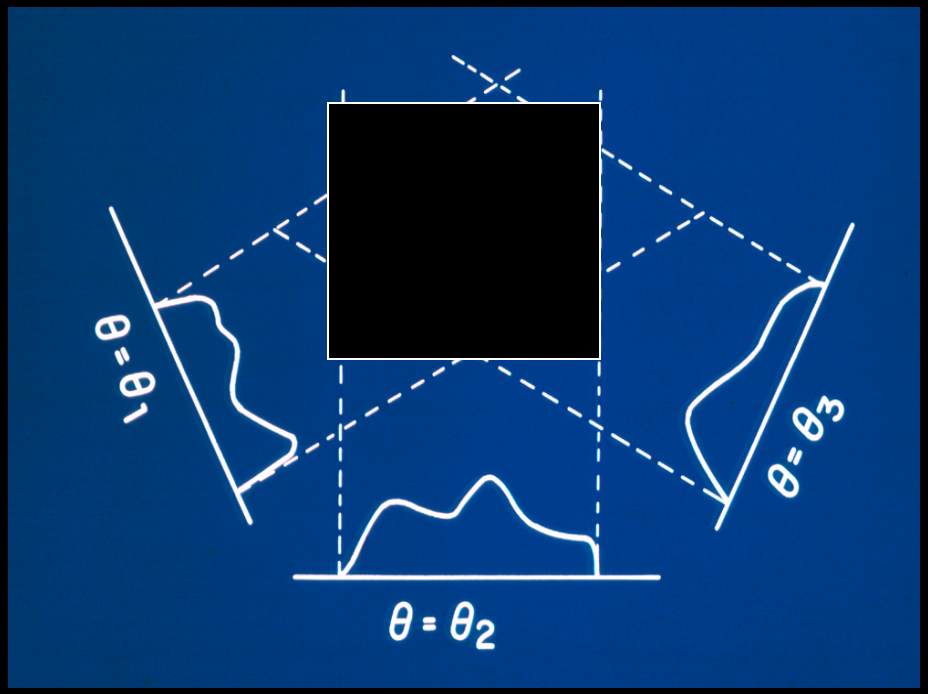

To reverse the process, i.e. recompute f(x,y,z), you need to project the density from each p_j (x,y) back into the volume (cube with sides = D) along its own z direction

$$P_j^b(x^j, y^j, z^j) = p_j(x^j, y^j) * I_j(x^j, y^j, z^j)$$

where:

$$I_j(x^j, y^j, z^j) = \delta(x^j, y^j) \cdot c(z^j)$$

$c(z^j)$ = 1 inside box and 0 outside box ($-D/2 < z^j < D/2$)

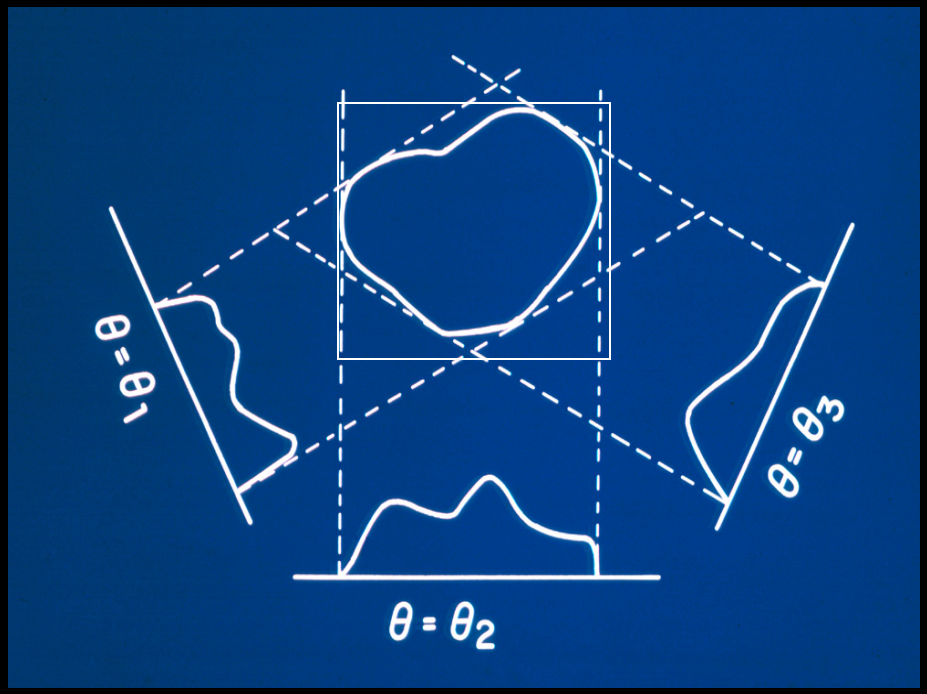

To reverse the process, i.e. recompute f(x,y,z), you need to project the density from each p_j (x,y) back into the volume (cube with sides = D) along its own z direction

Final “back projection body” is sum of the j back projections:

$$b(x^j, y^j, z^j) = \Sigma_j P_j^b(x^j, y^j, z^j)$$

Backprojection

Reconstruction

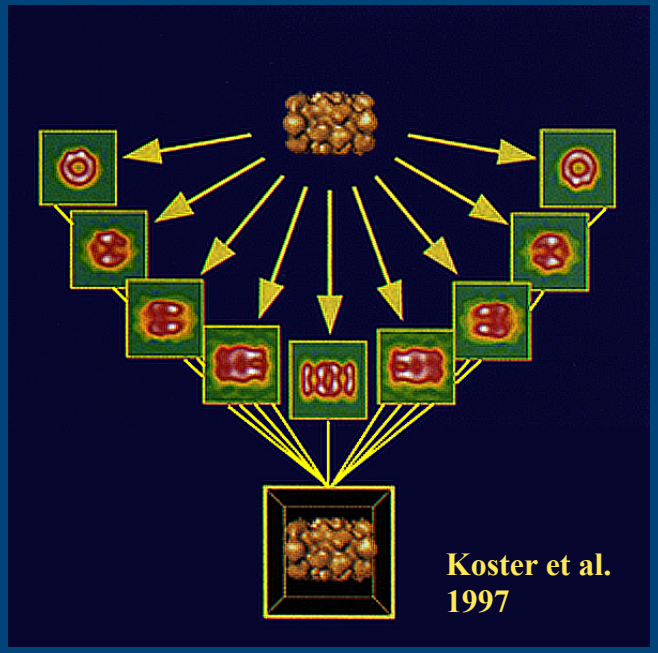

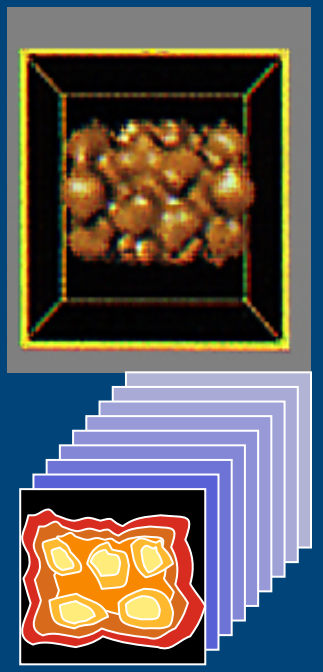

back projection

Tilt series → 3D volume

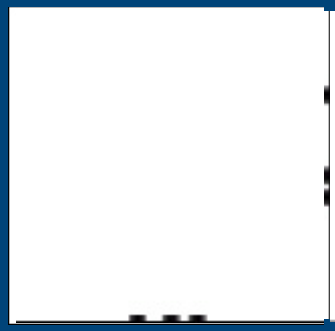

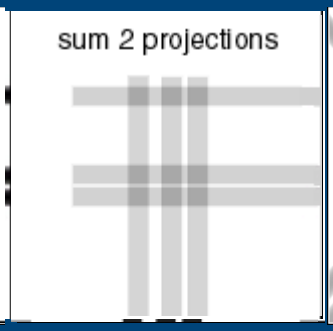

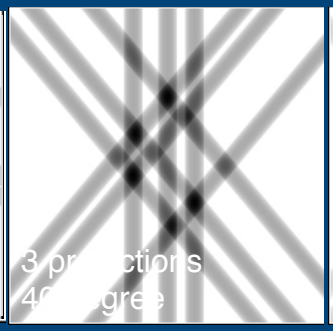

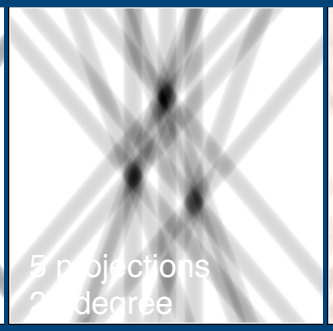

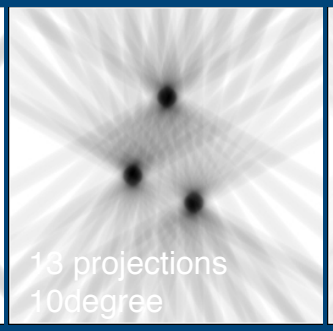

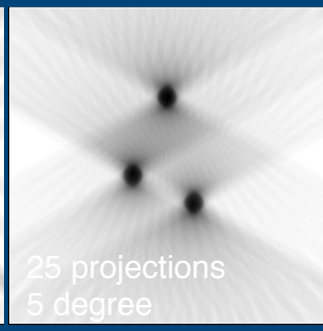

Modified Back Projection

"Back projection body" is the sum of weighted projections

$$b(x^j, y^j, z^j) = \Sigma_j P_j^b(x^j, y^j, z^j)$$

Where $P_j^b(x^j, y^j, z^j) = F^{-1} \{F [P_j^b(x^j, y^j, z^j)] \cdot r^*\}$

Fourier radius in direction ⊥ tilt axis (= x^*)

Needed because higher spatial frequencies are under-represented in simple back projection (In Fourier space, simply summing the amplitudes in each reciprocal pixel)

Fourier Space

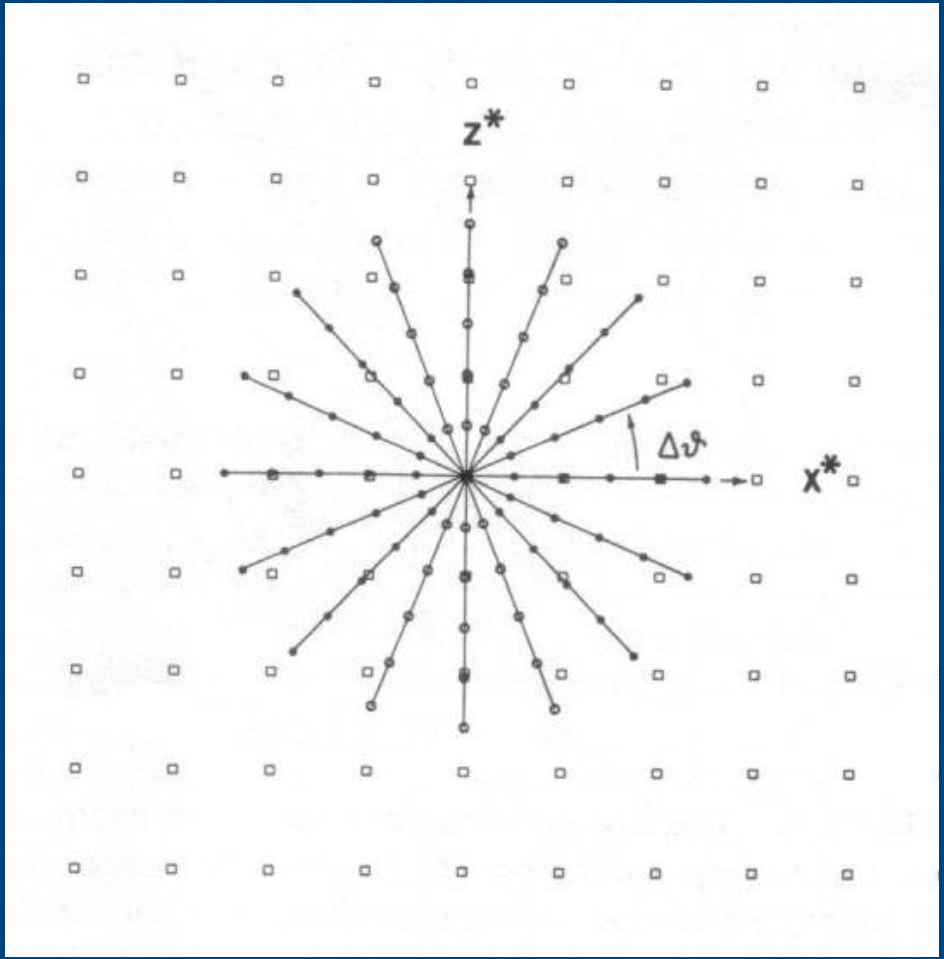

Fourier space

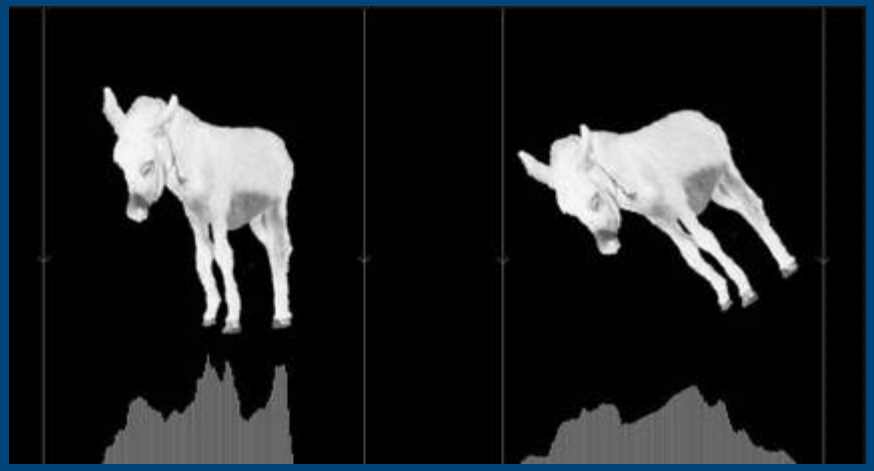

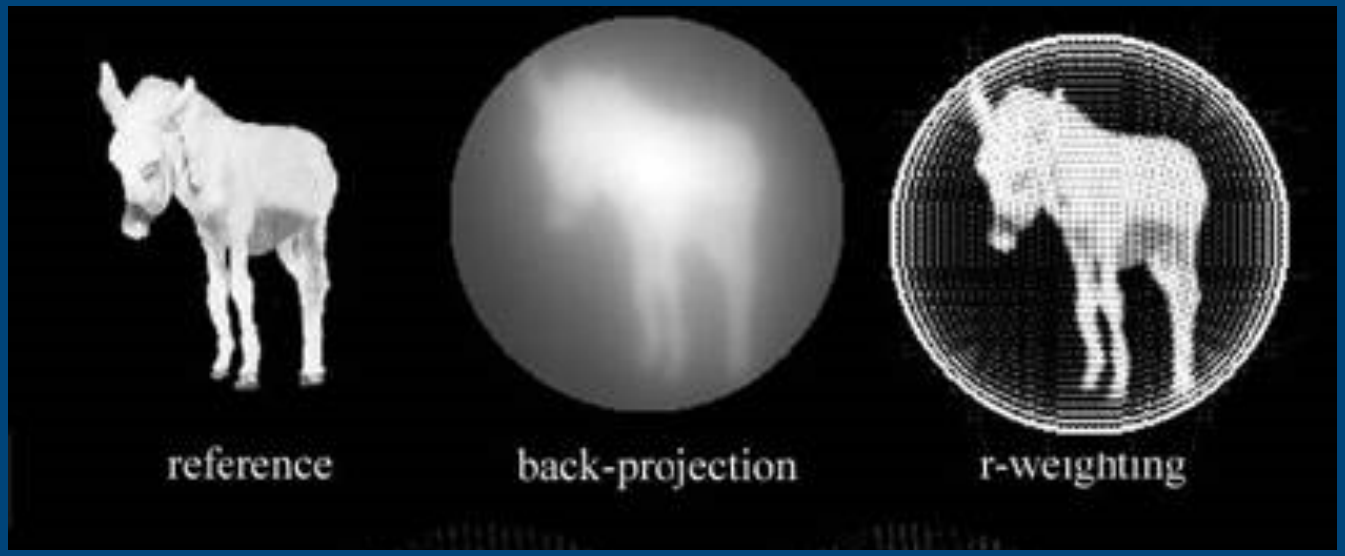

30 Projections at 6° intervals

Computation

Reconstruction methods

- Modified (r* weighted) back-projection
- Fourier synthesis
- Simultaneous Iterative Reconstruction Technique (SIRT)
- Algebraic Reconstruction Technique (ART)

Fourier Synthesis

depends on oversampling and good interpolation scheme

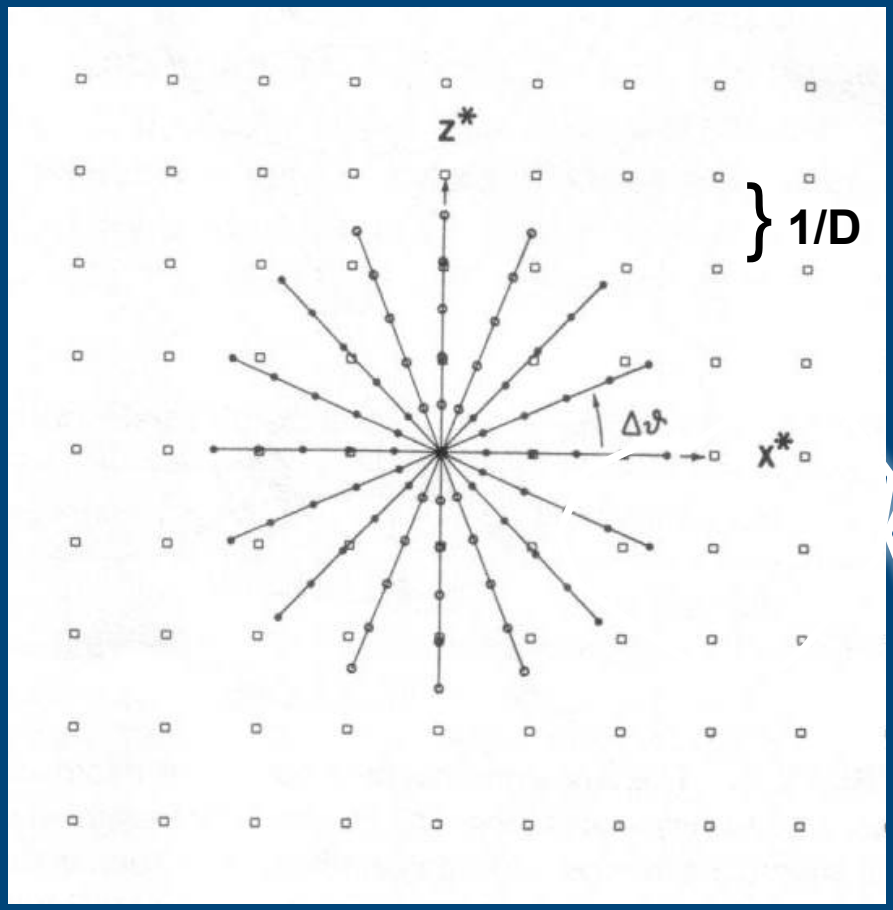

Fourier space

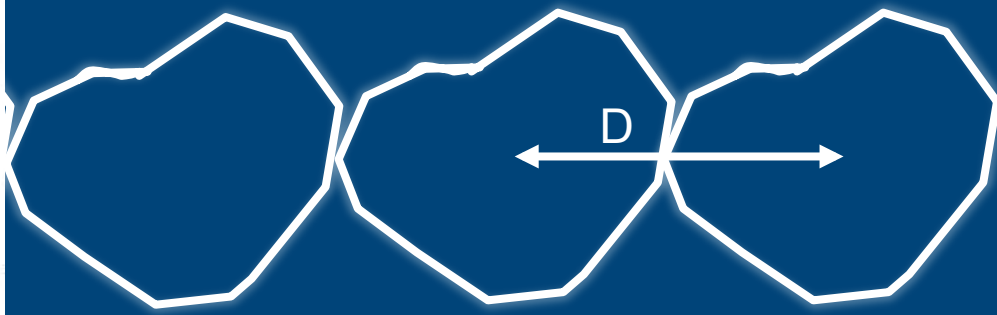

Real space

Electron Tomography

3. Computation

Reconstruction methods

- Modified (r* weighted) back-projection
- Fourier synthesis

- Simultaneous Iterative Reconstruction Technique (SIRT)
- Algebraic Reconstruction Technique (ART)

Computationally intensive but offer advantages (refinement schemes, application of prior constraints…) and are the subject of considerable current interest

SIRT as refinement to dual axis weighted back projection

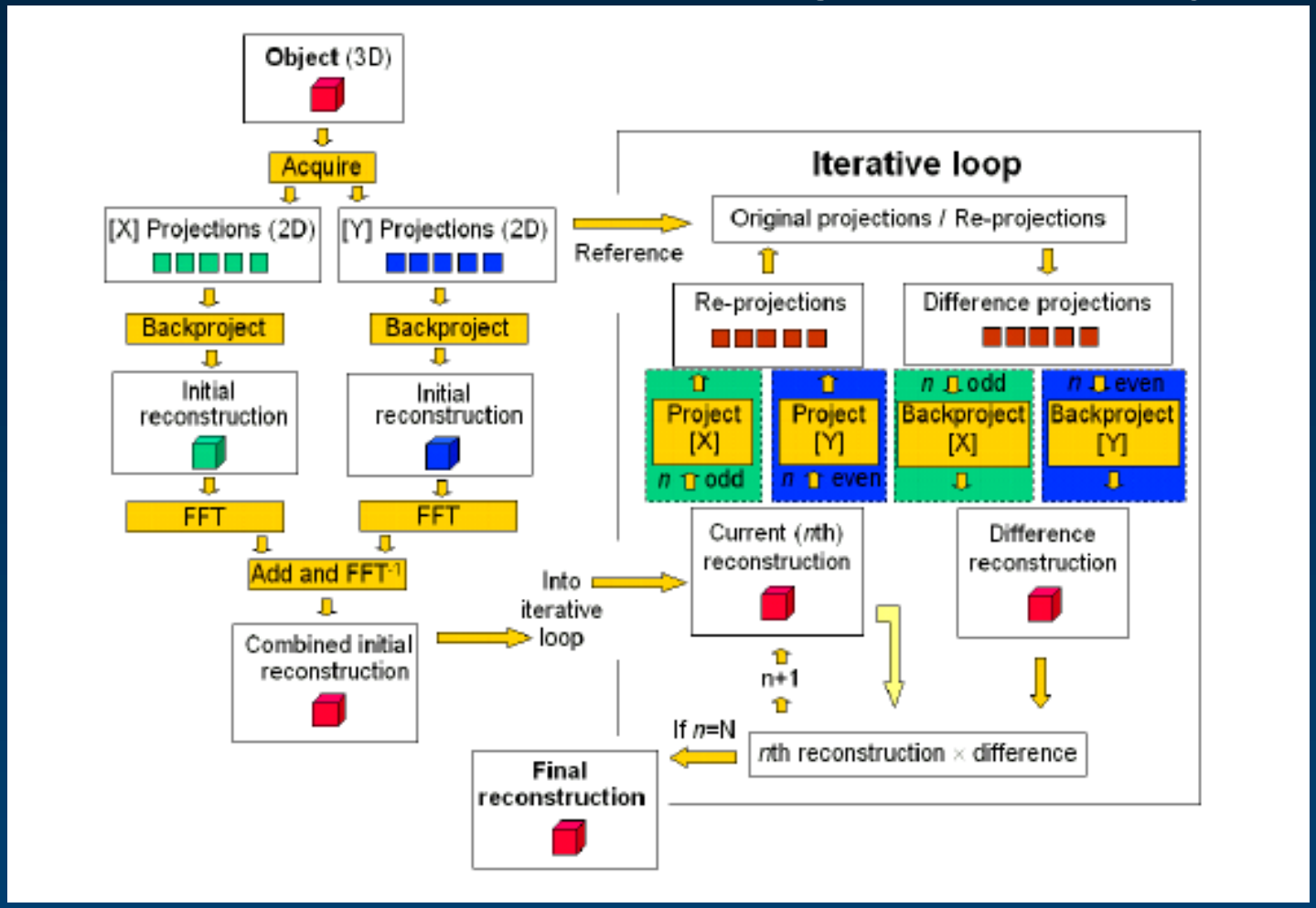

Tong and Midgley

Journal of Physics: Conference Series **26** (2006) 33–36
EMAG–NANO 05: Imaging, Analysis and Fabrication on the Nanoscale

Electron Tomography

3. Computation

Segmentation

- Manual
- Automated

Segmentation

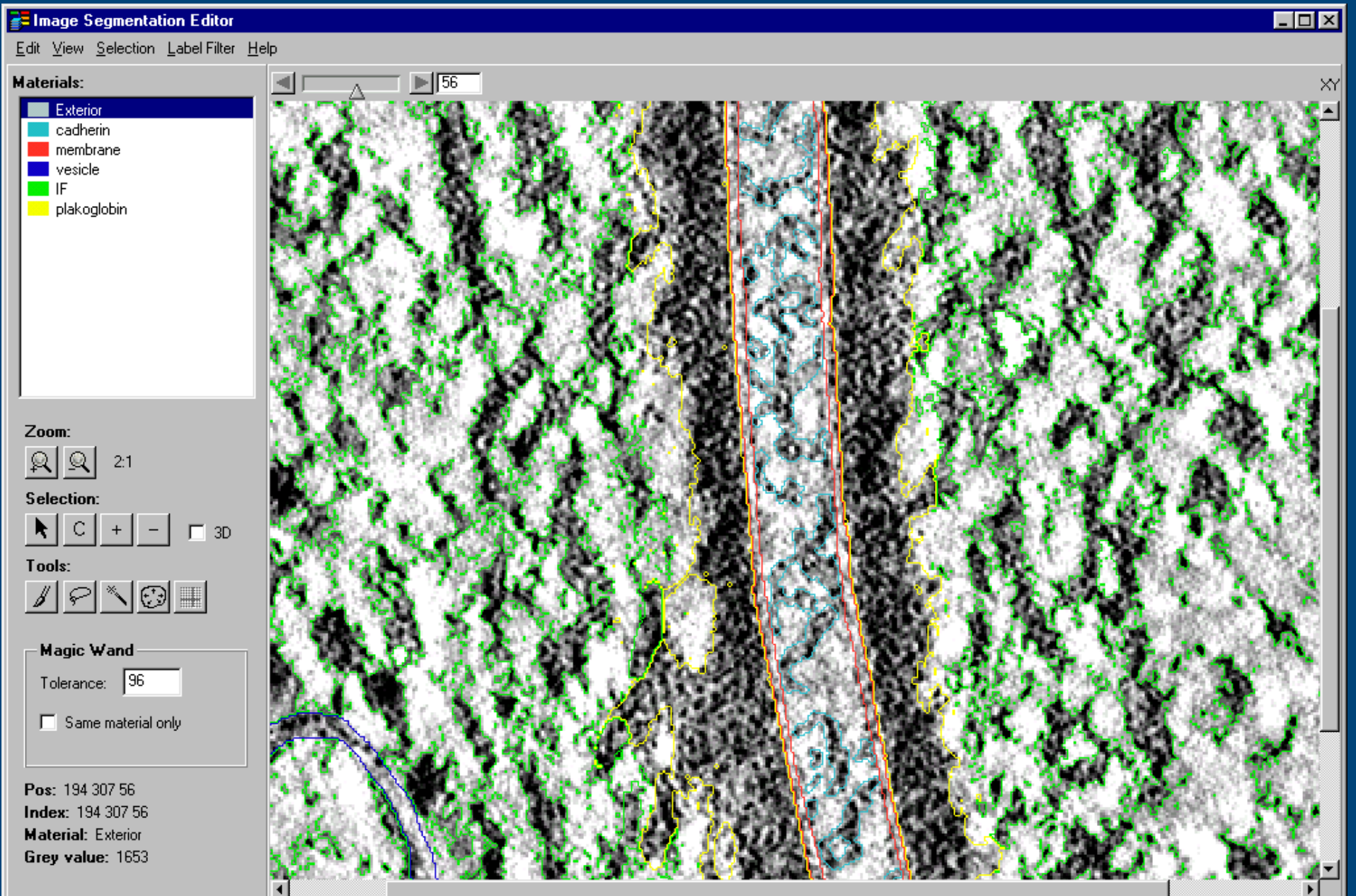

Desmo_c_3d.mpeg

Watershed segmentation

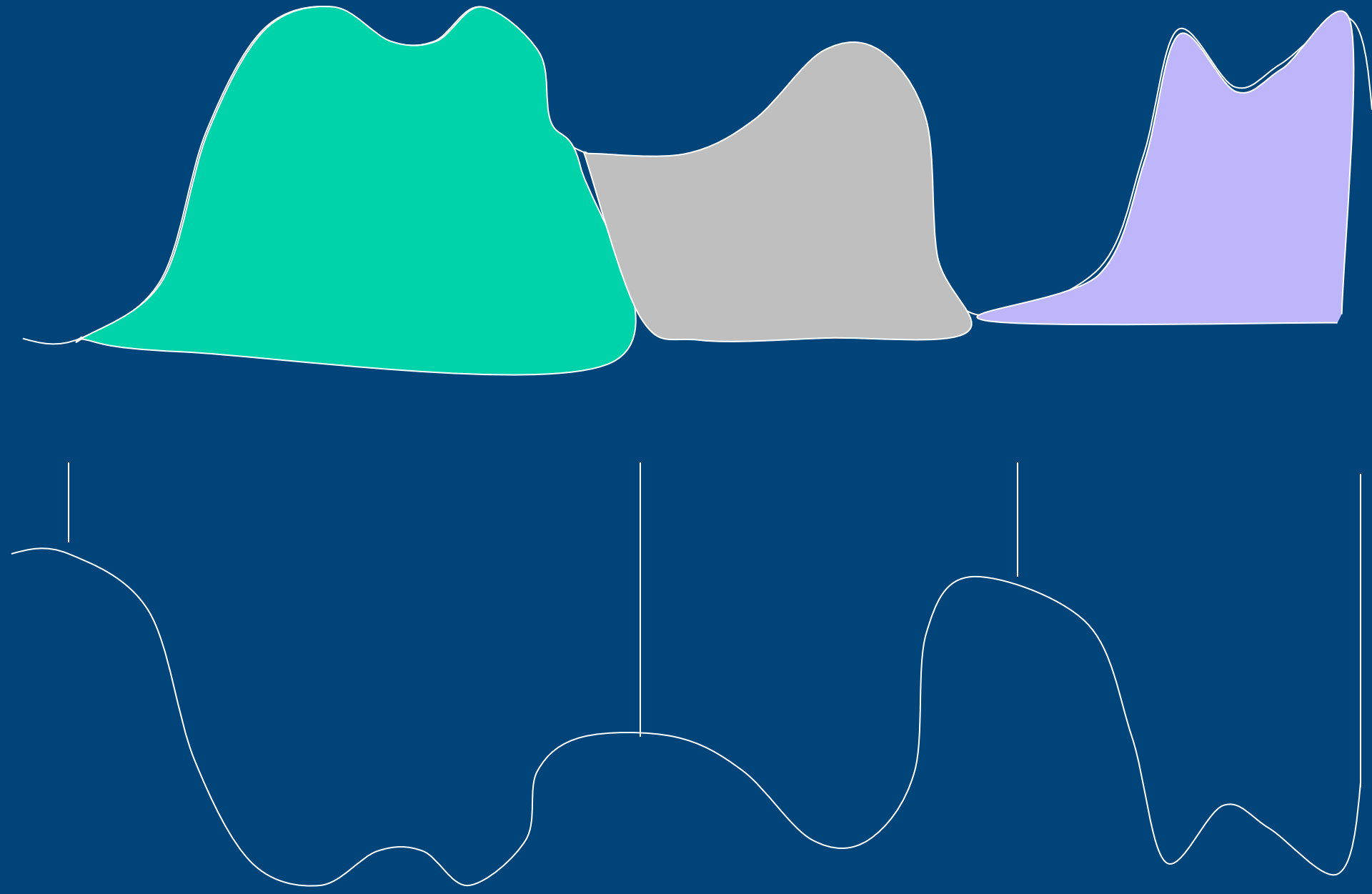

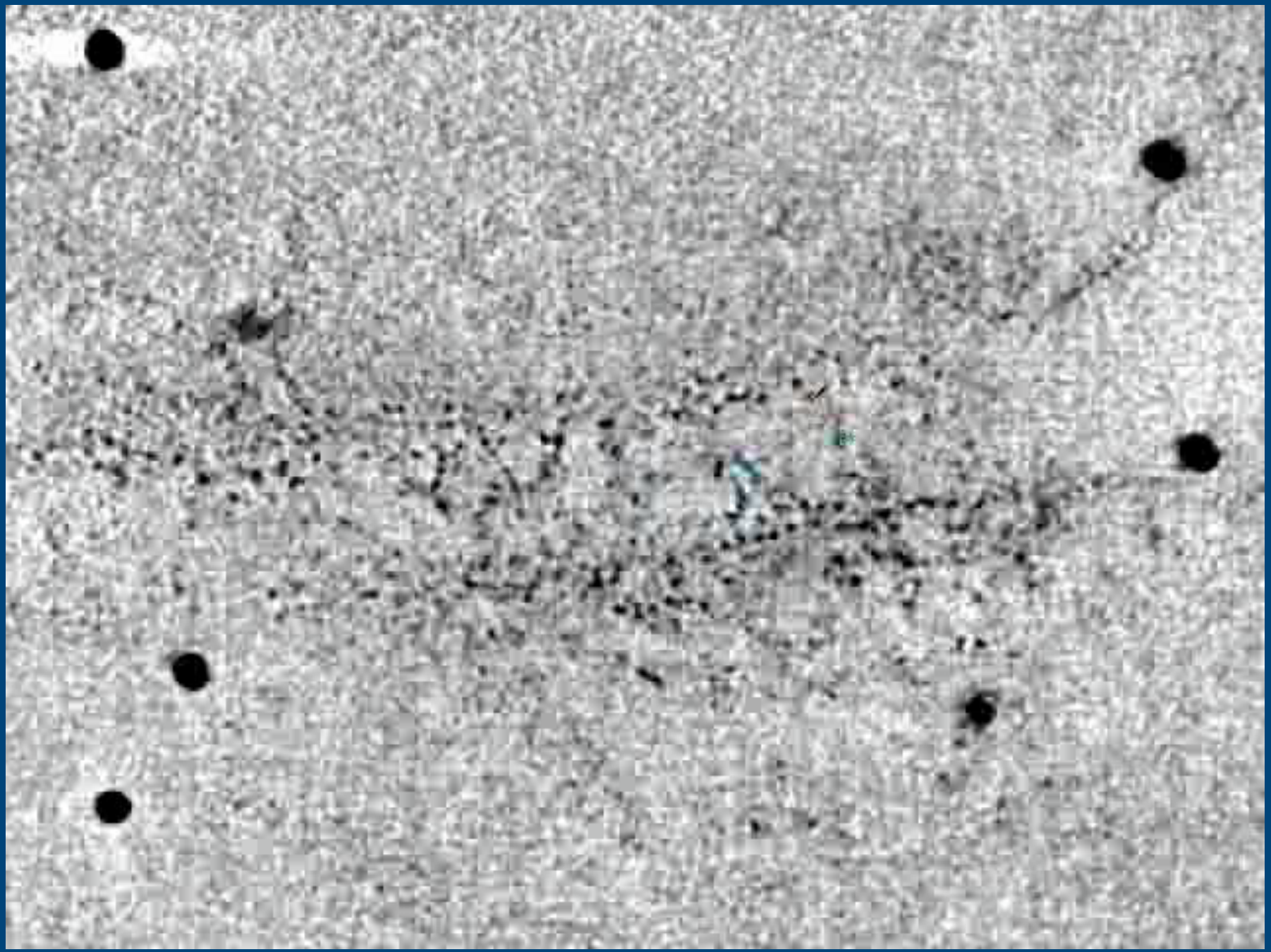

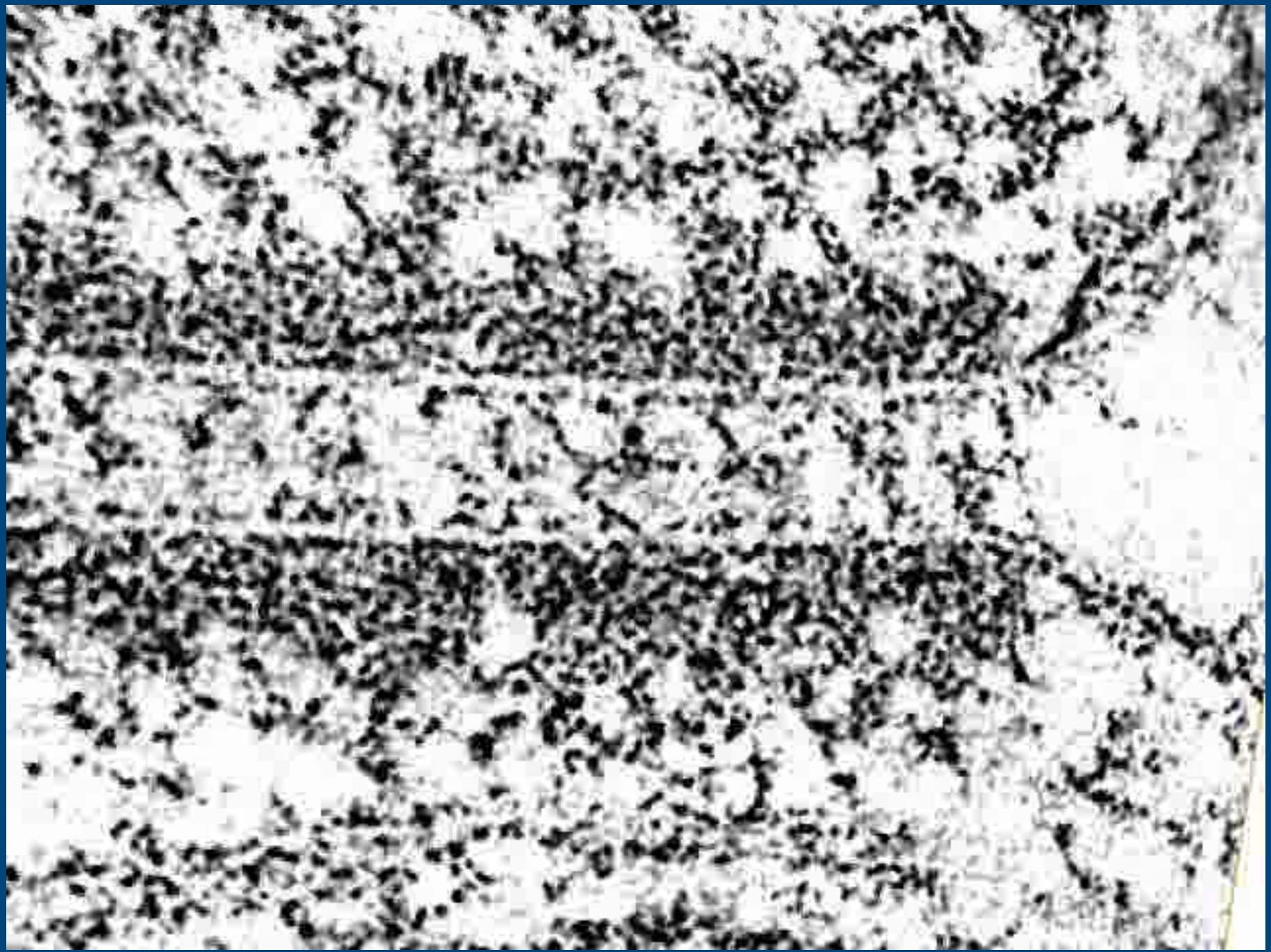

How many projections, N, do you need to achieve a specific "resolution" d?

Cylindrical geometry: $N = \pi D/d$

"Crowther criterion"

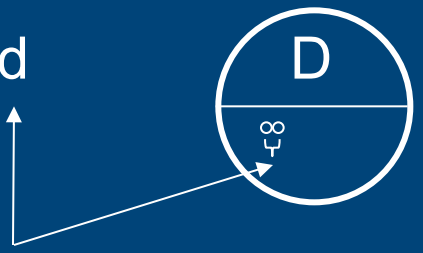

size of smallest feature
or detail of interest

Crowther, DeRosier and Klug (1970)
Proc Royal Soc London A 317: 319-340

How many projections, N, do you need to achieve a specific "resolution" d?

Cylindrical geometry: $N = \pi D/d$

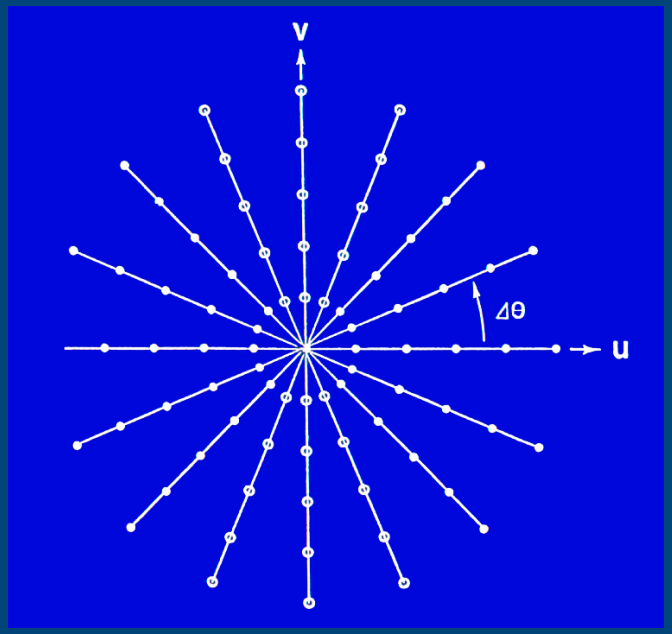

Assumes complete angular sampling

$\Delta\theta = 180^o/N = 180^o d/\pi D$

← Recall "central slice" theorem

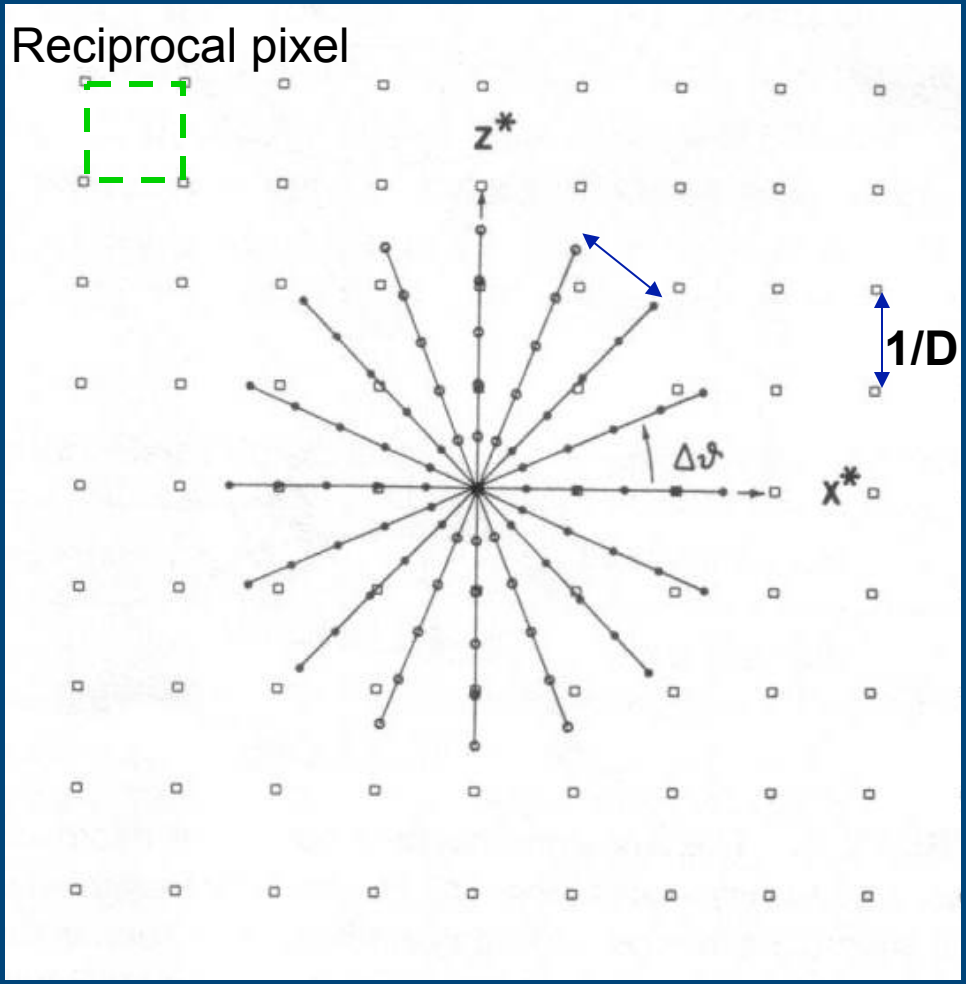

J. Frank (1992) Electron Tomography

Meaning of the criterion:

1/d = the spatial frequency at which each reciprocal pixel has at least one data point

Note: Fourier space at high spatial frequencies is increasingly sparsely populated

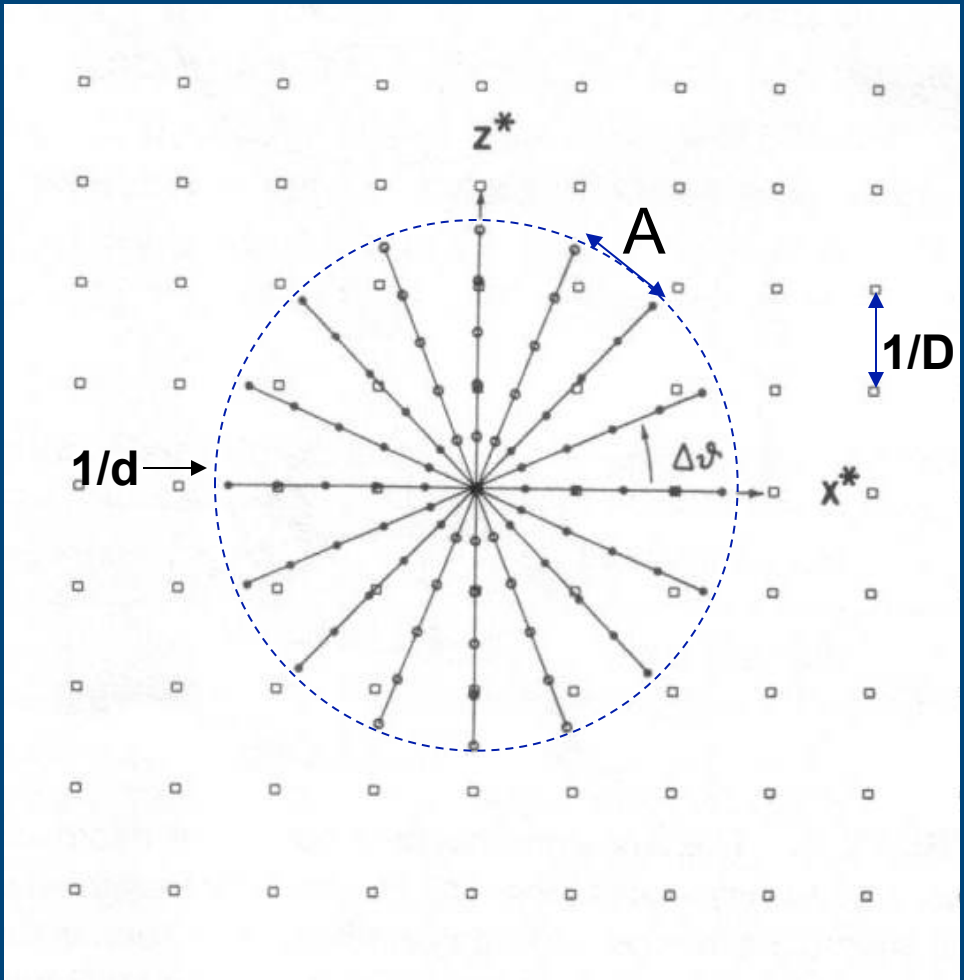

Meaning of the criterion:

1/d = the spatial frequency at which each reciprocal pixel has at least one data point

$C = \pi \text{ diam} = \pi \cdot 2(1/d)$
$C \sim 2N \cdot A = 2N\,(1/D)$

$2N/D = 2\pi/d$

$d = \pi D/N$

Why is reciprocal pixel have dimension of 1/D?

Reciprocal pixel

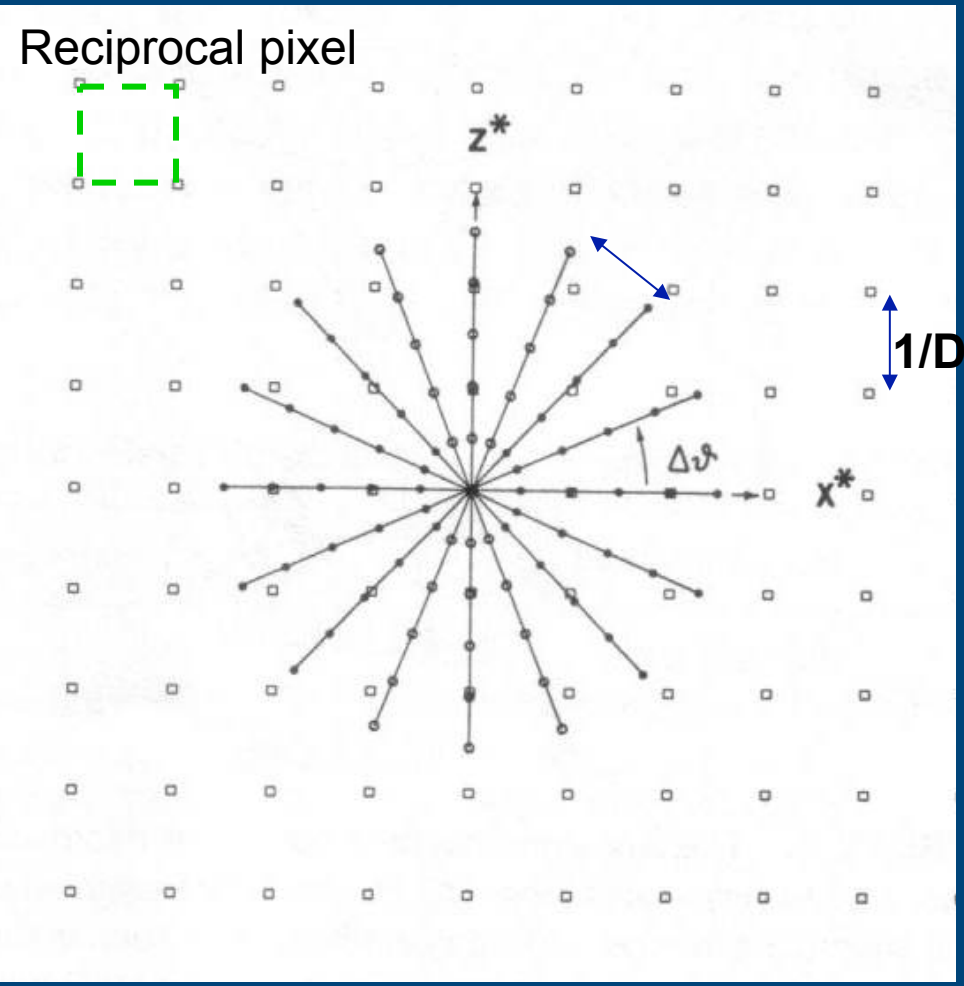

2D crystal

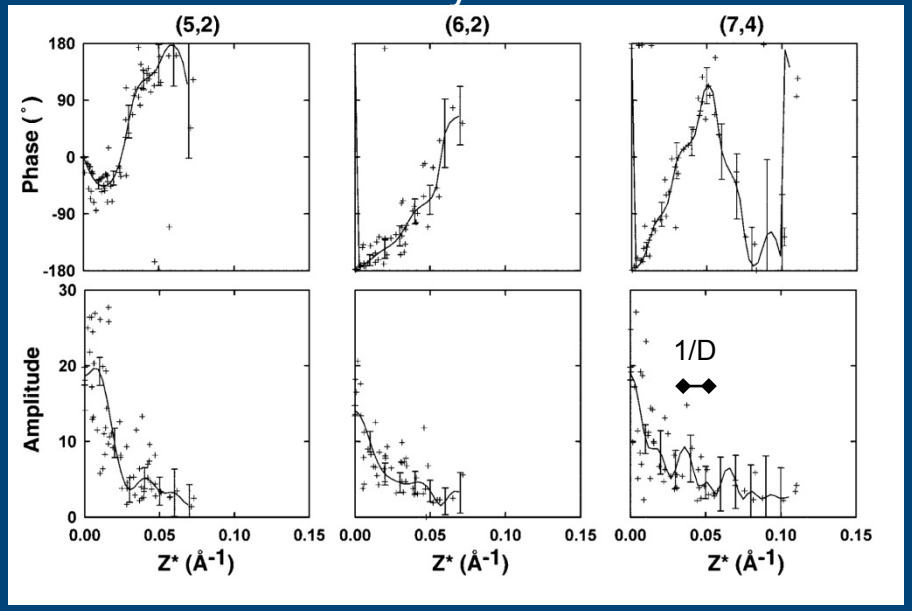

helical crystal

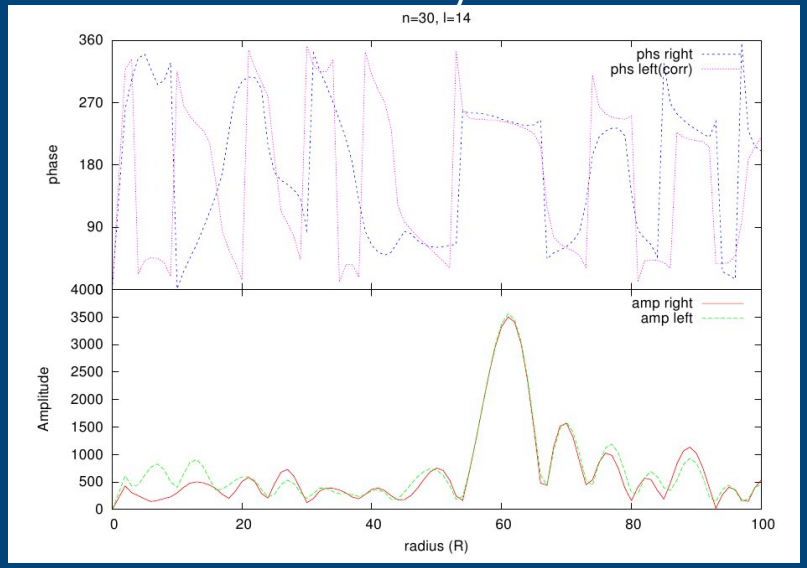

Convolution

Convolution: $$f_1 * f_2 = \int_{-\infty}^{\infty} f_1(x-t) f_2(t) dt = c(x)$$

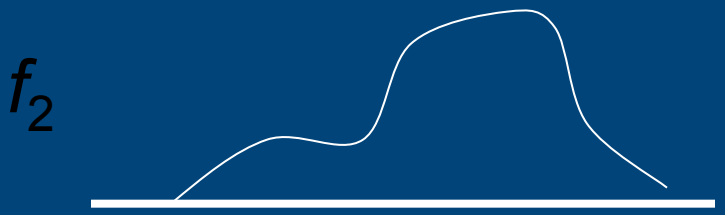

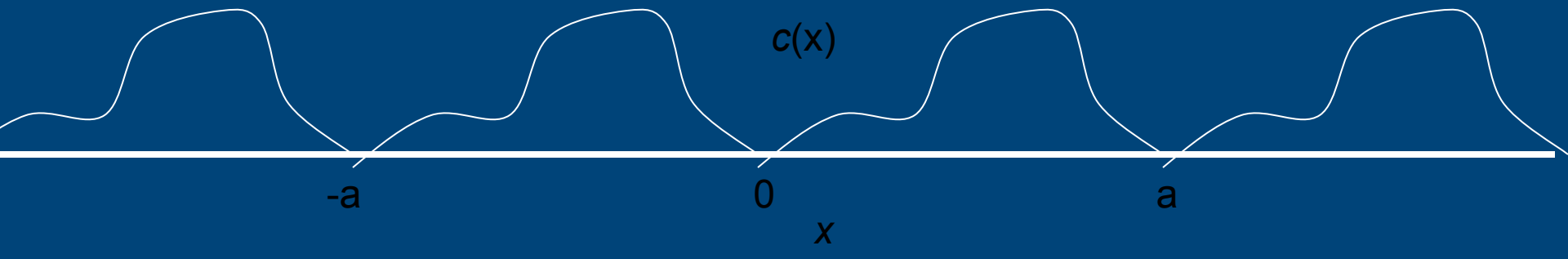

Convolution Theorem

$$\Im[f_1 * f_2] = F_1 \cdot F_2$$

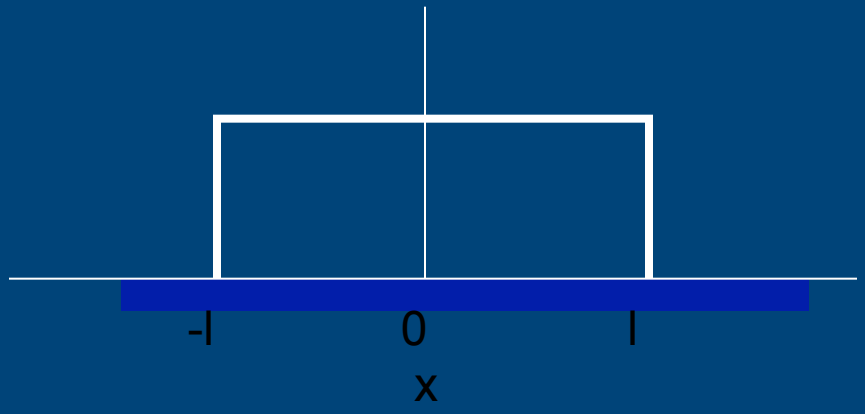

$\Im$

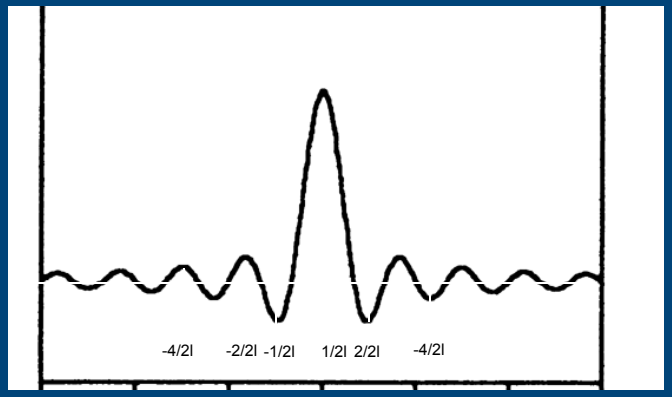

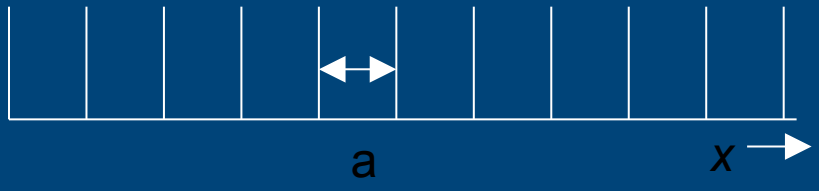

$\Im$

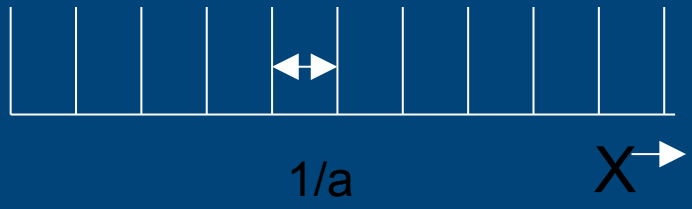

$b(x) * s(x)$

1D crystal

l < a then 1/l > 1/a

$F_1 \cdot F_2$

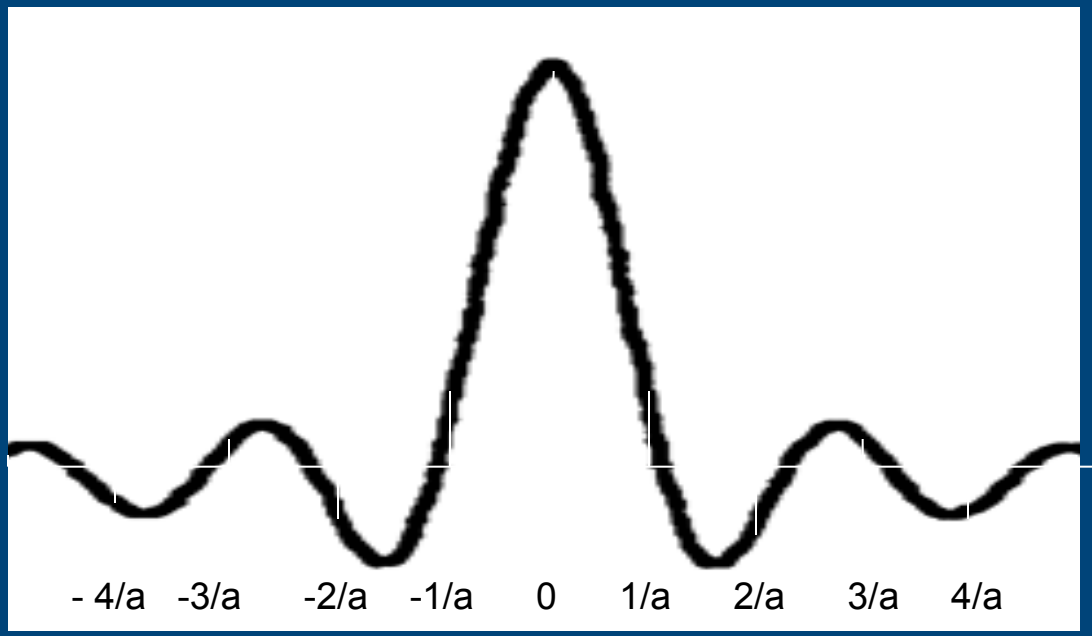

Convolution Theorem:
Fourier-space sampling of 1/D produces Real-space periodicity of D
(would be better off with sampling of 1/2D)